AVOIDTRONICS

Autonomous Collision Avoidance

Final Design Report

Cal Poly San Luis Obispo

Thomas Stevens
Elliot Carlson
Ian Painter

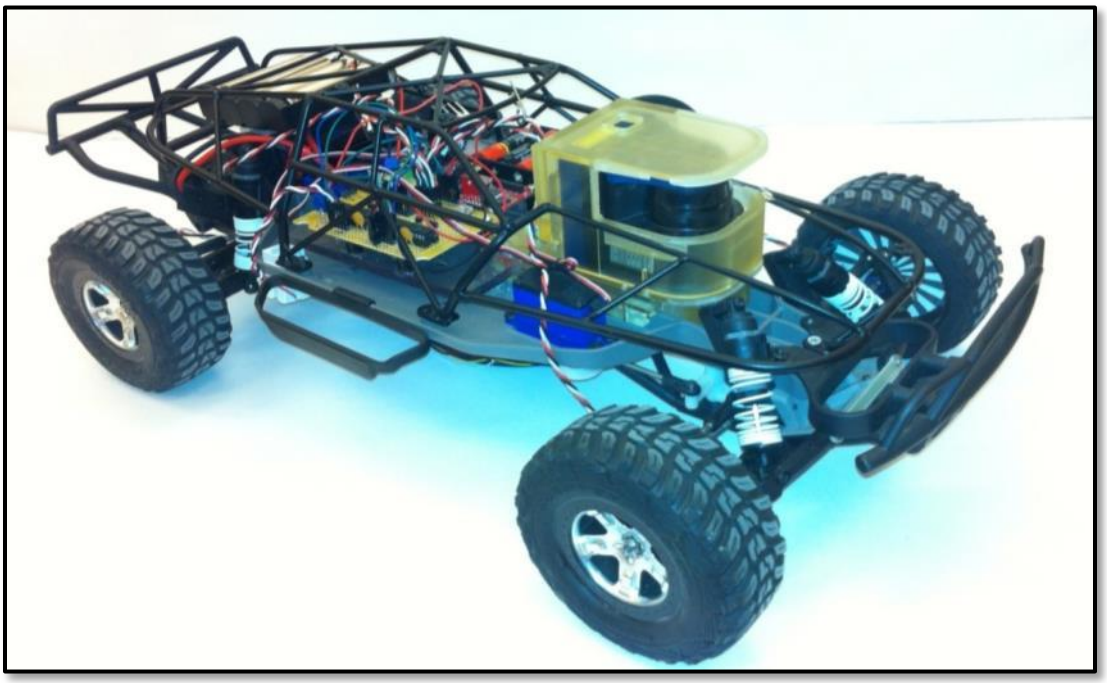

June 14, 2013
Project Sponsor: Dr. Charles Birdsong
Project Advisor: Dr. Charles Birdsong

Table of Contents

Table of Contents

Table of Tables

ABSTRACT

A steering controlled, autonomous collision avoidance system has been developed by California Polytechnic State University. This system represents a step in the direction of fully autonomous driving, while allowing the driver to maintain control of the vehicle during normal driving conditions. In the case of an imminent collision, the system removes control of the vehicle from the user and autonomously steers around the obstacles. The final system is able to avoid two static obstacles with a 95% pass rate and one moving obstacle with a 50% pass rate. With full scale, fleet wide, implementation of this system it is expected that each year up to 7,222 lives could be saved and over 60,000 injuries prevented. This decrease in the number of injuries and fatalities would produce a net yearly savings of up to $132 Billion per year.

Chapter 1. Introduction

The purpose of this project is to create a scaled model of an autonomous car crash avoidance system. The project is a continuation of two projects, the 2010 "Autonomous Crash Avoidance System" senior project and the 2012 "A Model Predictive Control Approach to Roll Stability of a Scaled Crash Avoidance Vehicle" master's thesis. The system developed by these teams utilizes a $1/10^{th}$ scale, two-wheel drive remote controlled car. It uses a Rapidly Exploring Random Tree (RRT) path planning algorithm to determine the steering inputs required to maneuver the vehicle away from a collision. Stability is addressed with a non-linear, eight degree of freedom vehicle model-predictive-stability controller.

The scope of the current project is to implement a sensor that will dynamically detect obstacles as well as the boundaries of the road and feed this data into the control system so that it can react to imminent frontal collisions. This includes an in-depth study of existing sensor technologies, development of data processing algorithms, and integration with the existing system. The vehicle will be controlled by a human driver, using realistic driving controls, until emergency avoidance is required, at which point, the avoidance software will be automatically activated. The transition from driver to computer control will be implemented similarly to modern dynamic stability control, such that for small maneuvers the driver should not be aware of any intervention.

This type of technology has the potential to significantly reduce injury and fatalities from auto accidents. The National Highway Traffic Safety Administration reports that in the United States in 2010 there were 1,542,000 automotive crashes, which resulted in injury, and 30,196 that resulted in fatalities. Nearly 70% of all fatal accidents in 2010 involved frontal collisions and over 10% of all fatal crashes involved distracted drivers. With a computer, which can react hundreds of times faster than the driver and is never distracted, constantly monitoring ahead of the vehicle to avoid to imminent collisions, over 7000 lives could be saved each year and significantly more injuries mitigated.

The project was undertaken with the intention of competing at the 5^{th} annual Enhanced Safety of Vehicles (ESV) student design competition in Seoul, South Korea. Due to the nature of the competition, much of the to design involve development of an interactive and informative presentation to demonstrate the technology.

1.1. Objectives

This project aimed to select and implement sensors for the purpose of object detection and avoidance on an existing $1/10^{th}$ scale RC car. The sensor data is collected and passed into a computer running an RRT algorithm in real time. The data processing code will be modularly developed such that it could easily be ported to another system requiring similar inputs. Tangential to the development and implementation of the sensor system a presentation demonstrating the capabilities of the system was developed for the ESV Student Design Competition. The interactive presentation offers the audience firsthand experience with what this technology may feel like when scaled to a full size vehicle. The formal engineering specifications listed in Table 1 reflect the customer requirements as well as those of the ESV Design Competition. These requirements were obtained by completion of the Quality Functional Deployment (QFD) found in Appendix A. The QFD was used to generate, compare, and evaluate formal engineering specifications and their corresponding metrics. The QFD helped to develop, refine, and evaluate different specifications by comparing how each specification related to customers concerns. Multiple specifications were determined by the existing system or project constraints. The operating frequency of the sensor was determined by the existing 20 Hz system frequency which is limited by the MPC controller. When possible, such as with the viewing angle, specific target quantities were calculated. The viewing angle was determined from geometric relations after selecting target horizontal ranges, see 6.2.Appendix B for calculations. A specification table can be found below and is followed by a justification for each parameter and its assigned value.

1.2. Specifications

The specifications presented in Table 1 represent a baseline for project success. The specifications were determined using the QFD presented in Appendix A or based on the previous system's performance.

Table 1 Engineering Specifications

Spec. #	Parameter Description	Requirements (units)	Tolerance	Risk	Compliance
	System				
	Cost				
1	Cost	$2,500	Max.	H	I, S
2	Number of Sensors (#)	1	Min.	L	A, T, I, S
3	Cost of Repairs	$350	Max.	M	T, I
	Geometry				
4	Sensor Size (LxWxH)	6in. X 5in. X 4in. = 120 in.^3	Max.	H	A, T, I, S
5	Total Car Weight (Car+Sensor+Components)	8.1 lbf	Max.	M	S
6	Sensor Weight	1.6 lbf	Max.	M	A, I, S
	Operation				
7	Operating Temperature	32 - 120 °F	Range	L	I, S
8	Max Speed	6.82 mph	Min.	H	A, T, I, S
9	Repeatability	95%	Min.	H	A, T, I
10	Time to Collision Threshold	0.6 s	Min.	M	A, T, I, S
11	System Engage Speed	2 mph	Max.	M	T, I
12	Processing Time	50 ms	Max.	H	T, S
	Quality Control				
13	Driver Satisfaction Index	80%	Min.	M	A, T, I
14	Port sensors/sensor code to other systems	2 day	Max.	L	T
15	Setup Time (Presentation + Control System/Track)	1 Hr.	Max.	M	T, I, S
	Energy				
16	Battery Lifetime	50 mins.	Min.	M	A, T
17	Battery Swap Time	10 mins.	Max.	L	T, I
	Safety				
18	Emergency shut-down time	50 ms	Max.	L	T, I
19	Successful Test Scenarios	3 Scenarios	Min.	M	T
	Sensor				
20	Horizontal Range	1 - 10 ft.	Range	H	A, T, I, S
21	Sensor Sampling Frequency	20 Hz.	Min.	M	S
22	Horizontal Sensor Viewing Angle	54°	Min.	M	A, T, I, S
General Notes					
1) All exposed wiring shall be wrapped with heat shrink tubing and all loose wires shall be fastened to the RC car with zip ties.					
2) Avoidance system must remain modular and integrate seemlessly into existing system, including but not limited to sensors and sensor data processing.					

- **Cost:** The cost represents the total project budget for this senior project. The funds come primarily from previous successful entries into the ESV design competition. The project budget of $2,500 was designated by the project sponsor.

- **Number of Sensors:** The project requires that the vehicle is able to autonomously detect obstacles requiring a minimum of 1 sensor to be mounted on the vehicle. With the maximum limit set by computational power and space requirements, this criterion allows for systems including multiple sensor types or arrays of a single sensor type.

- **Cost of repairs:** This specification allows for the measurement of system durability. Cost of Repairs includes the replacement of damaged boards or RC car components. This does not cover the replacement of the primary sensors. Steps shall be taken to mitigate this cost such as providing a protective enclosure for the boards and implementing an emergency system shutdown. Based on the repairs in previous phases of this project a $350 maximum was selected for a tolerable cost of repairs.

- **Sensor Size/Dimensions:** The size was selected to ensure that the sensor would be able to fit into the space currently available on the RC car. The aesthetics of the system were also considered as this project will ultimately be judged on the overall system. A size of 6" x 5" x 4" was determined to be the maximum acceptable size.

- **Total Car Weight:** This specifies the total allowable vehicle weight. This specification includes the existing system, the sensor(s), and all additional hardware. The weight of the system affects the vehicle handling; a car that is too heavy may not be able to execute the maneuvers demanded by the code. If the additional weight is added over the front or rear axle, rather than at the cg of the vehicle, it is possible to bottom out the suspension with less weight than if added at the cg. To obtain the maximum vehicle weight the weight needed to bottom out the suspension, when placed over the front axle, was added to the existing vehicle weight. A weight of 8.1 pounds was selected as a maximum value that cannot be exceeded.

- **Sensor Weight:** Since the sensor is located directly above the front axle, the location most likely to cause the suspension to bottom out,, a limit was place on its weight. This value was determined by placing known weights over the front axle and observing when the front suspension bottomed out. This value was selected as the maximum value that could be tolerated to maintain existing RC car performance. It should also be noted that stiffer springs can be purchased for the RC car, thus allowing a larger sensor weight.

- **Operating Temperature:** The sensor and system must be able to tolerate operation in varied conditions to allow for international as well as domestic use and shipping conditions.

- **Max Speed:** The max speed at which the system can reliably execute collision avoidance maneuvers was determined by previous projects to be 1/10th the speed of a full size vehicle traveling at freeway speeds. This resulted in a maximum avoidance maneuver speed of 6.83 mph. This speed is limited by the top speed of the vehicle and the processing power of available.

- **Repeatability:** Successfully repeating collision avoidance is one of the main goals of this project. A value of 95% was selected as a target value instead of 99.9% due to limited project resources. This represents the target reliability for the 3 avoidance scenarios specified in "Successful Test Scenarios"

- **Time to Collision Threshold:** The system shall not react to detected objects unless the vehicle is determined to be within 0.6 seconds of a collision. This benchmark value came directly from the Mercedes Benz PreSafe Automatic Braking System, which engages full sbraking 0.6 seconds from a collision. This value takes into account the fact that not all detected objects pose an

immediate risk of collision. A common example is an obstacle traveling towards the vehicle but in the other lane.

- **System Engage Speed:** The system will not engage at speeds below 2 mph. This speed was chosen to prevent the system from engaging at residential driving speeds or below. At these speeds a collision is extremely unlikely to be fatal and an autonomous maneuver could cause more harm than the collision.

- **Processing Time:** The total processing time for one iteration of the system must be less than 50 milliseconds. The total processing time includes data transmission, data parsing, and RRT & MPC processing. The selected value, 50 milliseconds, is the predetermined simulation frequency of the MPC algorithm. Failure to meet this specification may leave the system blind to obstacles or without crucial steering commands for multiple iterations.

- **Driver Satisfaction Index:** The driver satisfaction index was created to obtain feedback from drivers using the system and their reaction to the technology taking control of the vehicle, temporarily, to avoid obstacles. This value will attempt to quantify the driver experience of the transitions from user to computer control and vice-versa. A value of 80% was chosen as the target because many people have a negative reaction to the idea as well as different driving styles, which the computer may interfere with (most-likely for the good of the driver). Our system will do its best to please the drivers, but not every driver can be satisfied simultaneously. The index quantity for the system will be obtained thru survey and first-hand experience of operating the crash avoidance system, specifically relating to handling, reaction to losing control during collision avoidance, and the regain of control.

- **Sensor System Porting:** The code developed for this system must be able to be ported into another system within 2 days. This assumes that the dynamic modeling for the MPC controller has been previously completed and that the system inputs are the same as the inputs found in this system. This specification allows for the code to be easily implemented on another vehicle as this project progresses.

- **Setup Time (Presentation and Track):** The presentation material and driving track must be able to be set up in less than one hour. The setup time includes, but is not limited to, the driver controls, the video feedback system, the track itself, the computer control system, and the presentation material. This specification is required by the time constraints of the ESV international competition.

- **Battery Lifetime:** The batteries, Li-ion and car battery must last a minimum of 50 minutes. This specification represents the target lifetime to power sensors, control boards, communication modules, and the vehicle itself. This specification was determined to allow near continuous presentation of the system at the ESV international competition and during the driver perception survey.
- **Battery Swap Time:** The batteries, Li-ion and car battery, must be able to be swapped in less than 10 minutes. It is essential that system maintenance time be minimized during presentations in order to maintain the audience's attention.

- **Emergency System Shut Down Time:** In an emergency situation the system must be able to be shut down in less than 50 milliseconds. Due to the potential for damage to the system and possible harm to bystanders in the event of a system failure an emergency shutdown is to be implemented. This will allow the operator to shut the system down from the driving controls. The value was selected to assure that the system shuts down prior to executing the subsequent steer command.

- **Successful Test Scenarios:** Three Three different test scenarios involved most often in frontal collisions will be targeted for collision mitigation. These scenarios all involve the target vehicle traveling down a straight roadway having to avoid obstacles in three different scenarios. The scenarios are as follows: a stationary object in the middle of the roadway, a obstacle traveling across the target vehicles path, an obstacle in the vehicle path that moves as the vehicle gets within close proximity.

- **Horizontal Range:** The system must be able to detect obstacles that are more than 1 foot away and less than 10 feet away from the vehicle. The maximum value was selected using the time to collision threshold and the maximum speed previously determined. The value was also compared against similar threshold values set by the Mercedes Benz PreSafe Automatic Braking system and were found to be similar. Due to the limitations of the hardware the vehicle cannot avoid a similarly sized obstacle within 22 inches of the front of the vehicle so a minimum range of 1 foot is acceptable.

- **Sensor Sampling Frequency:** The sensor must be able to sample data at a frequency of at least 20 Hz. This value was selected to assure that there is a new scan for each iteration of the system. At lower frequencies it is possible that two subsequent paths could be planned using the same data which may not accurately represent the environment.

- **Horizontal Sensor Viewing Angle:** The horizontal viewing angle of the sensor must be at least 54 degrees. The horizontal viewing angle is a measure of the minimum angle that the sensor can detect in a 2D plane parallel to the ground. This angle was determined from the minimum horizontal range and the width of the wheelbase of the vehicle. See 6.2.Appendix B for a complete calculation.

1.2.1. Specifications updates

Throughout the design process additional specifications were determined that would allow the team to internally measure the success of the design. Additionally some specifications were updated to more accurately represent the project goals. In cases where the specification was changed, the system will be tested against both the original and the final metric.

- **Driver Satisfaction Survey:** It was determined that rather than measuring the success of the survey by the 80% acceptance rate originally stated it would be more appropriate to measure success by the number of participants surveyed (minimum of 30). By not seeking to achieve a certain approval rating the results of the survey are expected to be less biased by the team's goal.

- **Detected Obstacle State:** The frontal area and position of the detected obstacle must be within 10% of actual position and frontal area of the obstacle. The Detected Obstacle state seeks to evaluate the accuracy of the data from the LiDAR as well as the accuracy of the data parsing algorithms. It was determined that frontal are was a more acceptable measure than obstacle volume due to the 2D scanning.

- **Avoid Two Static Obstacles:** The test vehicle must be able to avoid two static obstacles 8 out of 10 times. This specification seeks to test the system's ability to handle situations with multiple obstacles. 80% was selected as the acceptable minimum due to its relative complexity in comparison to the one obstacle test

Chapter 2. Background

The following section describes existing sensor technologies as well as their implementation in various collision avoidance technologies.

2.1. ESV Student Design Competition

The Enhanced Safety of Vehicles (ESV) student design competition is a three tiered, international design competition. Student design teams submit a project proposal declaring their intent to develop a vehicle system in one of 15 different categories. The categories include but are not limited to: collision avoidance, electric vehicle safety, and distraction mitigation. Upon review of the project proposals teams are selected to compete at a regional level. At the regional level the designs are presented to a panel of judges and are critiqued on the basis of technological advancements, scalability, and vehicle safety improvements. The top three teams from the North American, European, and Asian regions are selected to present at the ESV international conference in Seoul, South Korea in May 2013. The top team at the conference, as judged by the international panel of judges, is named the winner of the 2013 student design competition.

2.2. Sensors

A brief description of existing sensor technologies is presented below.

2.2.1. Radio Detection and Ranging (Radar):

Radar sensors transmit high frequency radio pulses and record the time required for the signal to reflect off of an object and return to the receiver. The Doppler frequency shift of the returned signal is also recorded. The recorded data is used to calculate the position and velocity of the object. Figure 1 depicts a radar system emitting a series of radio pulses, which are then reflected off of the metallic surface of an airplane and returned to the sensor. This data would then allow the sensor to determine the position and velocity of the airplane.

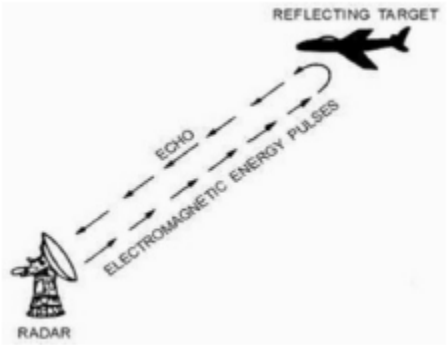

Figure 1 Radar System Detecting an Airplane

There are two main types of radar detectors with applications in vehicle collision avoidance. Pulsed Doppler (PD) Radar is the most common and operates on the Doppler principle, which states that all objects will exhibit a frequency shift from the transmitted signal to the received signal. This frequency shift is what

allows the radar to detect the velocity of an object. Frequency Modulated Continuous Wave (FMCW) radar operates similarly to the image processing discussed in section 2.2.4. The FMCW radar breaks the detection area into small sections and uses background subtraction, the process of overlaying two consecutive frames and removing what is the same, to detect changes or moving objects.

2.2.2. Light detection and Ranging (LiDAR)

LiDAR operates on the same basic principles as radar. High frequency light waves, often produced by a laser, are emitted and the time required for the signal to reflect back as well as the Doppler shift are recorded. The emitted light usually has an extremely short wavelength in the ultraviolet or infrared region. The high frequency waves of the LiDAR sensor are focused in a smaller beam than a radar sensor. This results in a detection area that is orders of magnitude smaller, but with a less scattered, stronger reflected signal. In order to overcome the small beam width of the laser, LiDAR detectors usually involve a rotating mirror that directs the beam through a horizon and vertical viewing angle allowing the sensor to scan over a greater area.

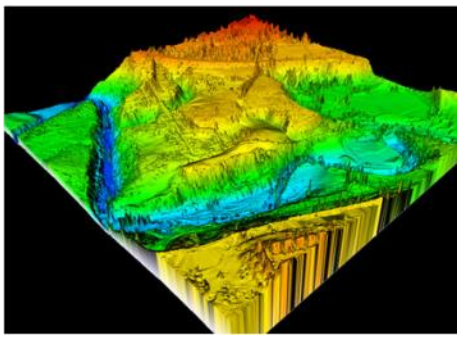

Figure 2 Terrain Mapping using a 3-D LiDAR Sensor

Figure 2 above shows a large terrain area which was mapped using a three dimensional LiDAR sensor. The sensor capturs the contours of the terrain and the resulting map could be used for aircraft navigation or topographic map generation.

2.2.3. Ultrasonic

Ultrasonic sensors use the same principles as radar and LiDAR, but emit ultrasonic sound waves, which are reflected off of the object. The reflected waves are received and the time delay is used to determine the position of the object.

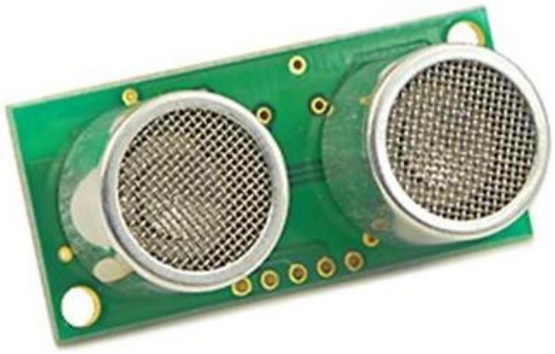

Figure 3 Ultrasonic Sensor

Figure 3 shows a simple ultrasonic sensor. The metallic, cylindrical protrusions are the emitter and receiver for the sensor, while the printed circuit board provides the electronics to convert the ultrasonic wave into an electrical signal.

2.2.4. Image processing

Image processing involves taking a video of the surrounding and using pixel data and image processing software to extract information from the video. The software can be developed to extract various objects from the video such as moving objects, obstacles, or roads. The angular position of these objects can then be determined, however, the distance from the camera cannot be accurately determined without further sensor input.

Figure 4 Path Planning using Image Processing

Figure 4 shows the use of a still frame image for path planning. The image was first processed such that only the brightly colored objects were visible. A boundary was then constructed around each object and a path-planning algorithm was used to determine a path between the obstacles. The path and the initial photo were then overlaid to determine the final path.

It is also possible to use a stereo camera as the input for image processing. A stereo camera takes two simultaneous videos from slightly different angles and using the same principles as the human eye, overlaying the images, to create a 3D image. Using the know distance between the cameras and the

difference in angle between the two images it is possible to detect both distance and angular position of an object.

Figure 5 Stereo Cameras taking Two Pictures Simultaneously

Figure 5 shows the output of a stereo camera system. The two photos in the Figure 5 are slightly offset allowing the dog's paw to be seen in the image on the left, but not in the image on the right. This difference in the images would be used to determine the position of the dog's paw and its distance from the cameras.

2.2.5. Magnetic

Magnetic sensors use magnetic fields to detect proximity. The magnetic sensor detects if there is a magnetic field, and if so returns a binary high/low signal to indicate that there is an object in the magnetic field of the sensor. There are many types of magnetic sensors; however all require that the object being sensed is magnetic, meaning that a magnetic sensor would not be able to detect a pedestrian.

Figure 6 Hall-effect Magnetic Sensor

2.2.6. Infrared Imaging

Infrared imaging uses the same principles as a camera, where the intensity and wavelength of light is captured, however, the light captured is outside of the range of human vision. The wavelength for infrared can be as long as 14,000 nanometers (450-750 nanometers for visible light). This allows infrared cameras to be used at night as well as during the day and to capture thermal gradients in the subjects being photographed.

Figure 7 Traditional Camera Imaging on the Left Compared to Infrared Imaging on the Right

Figure 7 shows the difference between an image seen by a traditional camera and by an infrared camera. In the infrared image the temperature gradient of the person produces different wavelengths of radiation, producing the image seen. It is also possible to detect the radiation given off by the person's hands even though they may not be visible to the human eye.

2.3. Existing Systems

The following section presents a brief review of existing collision avoidance systems. The sensors used for each system are also presented.

2.3.1. Mercedes-Benz Brake Assist PLUS and PRE-SAFE®

High end Mercedes come equipped with Brake Assist PLUS and PRE-SAFE® which implement audio cues and automatic braking, respectively, if a collision is detected. Brake Assist PLUS makes auditory and visual cues to the driver if a potential collision is detected. It simultaneously calculates the braking force necessary to stop the vehicle in time and makes that force available as soon as the driver touches the brake pedal. If the driver does not respond to the cues, the PRE-SAFE® system initiates 40% braking 1.6 seconds from a detected impact and full braking .6 seconds from impact. All environment data is collected using one long range radar detector with a range of 600 ft and 2 short range radar detectors with an 80° viewing angle and 90 ft range.

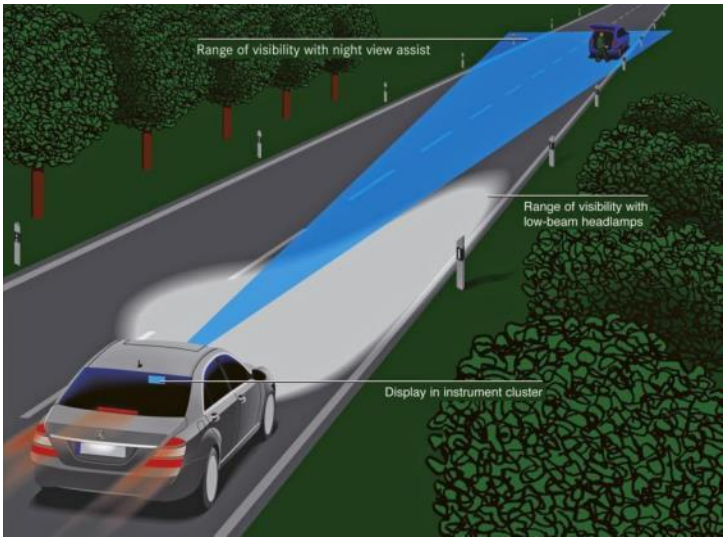

Figure 8 Mercedes Braking System

2.3.2. Google Autonomous car

Google is currently developing a car that is able to autonomously navigate all roads. While the full details of the autonomous car are beyond the scope of this project, how the car detects and responds to obstacles is relevant. The Google car uses a combination of a Velodyne 64 beam LiDAR detector, GPS, 4 radar detectors, and image processing in order to create a 3D map of the environment. This map is then processed by a computer to determine which objects are permanent, i.e. lamp posts and mailboxes, and which objects are transient, i.e. pedestrians and cars. This information is then used by the vehicle software to determine the ideal path to avoid colliding with any of the obstacles.

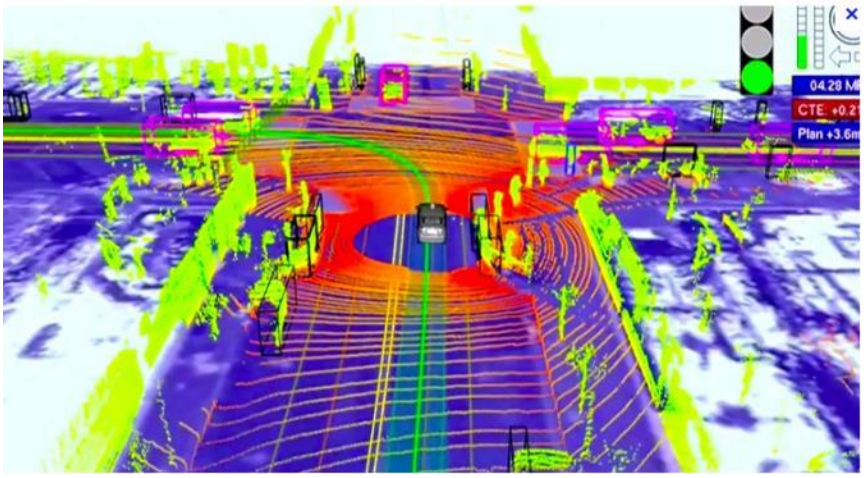

Figure 9 Image obtained by Google Car's Multiple Sensors

2.3.3. MIT Autonomous RC plane

MIT has recently developed an RC plane that is capable of autonomous flight over a pre-programmed route. The plane uses an onboard LiDAR sensor to map the environment and uses the mapped environment to identify obstacles and react accordingly. The RC plane uses the RRT path-planning algorithm described in section 2.4.1 to avoid obstacles at speeds up to 25 miles per hour.

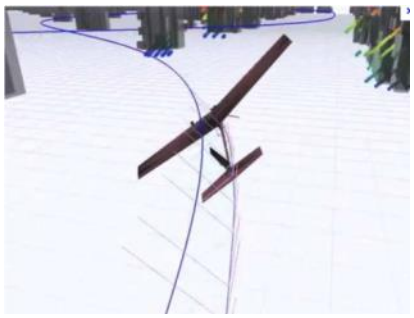

Figure 10 MIT's Autonomous Plane Following RRT generated Path

2.4. Path Planning Algorithm

2.4.1. Rapidly Exploring Random Tree Algorithm

The Rapidly Exploring Random Tree (RRT) Algorithm is an algorithm used for finding a solution to high dimension search spaces. In this example a 2D space with arbitrarily placed physical obstacles will be discussed. In a 2D space the algorithm starts with an initial search node and places a second node that is then connected to the first with a straight line. A third point is then added and is connected by a straight line to the nearest point along the previous line. Subsequent points are added and connected to the tree, causing it to grow. If a node or line intersects a boundary condition, in this case an obstacle, that branch of the tree is terminated and the tree explores other possible solutions.

Figure 11 Random Trees Generated by RRT

2.4.2. Model Predictive Controller

Model Predictive Control (MPC) is a method of control for complex multivariable systems. The concepts presented here will be developed using the example of a vehicle executing collision avoidance maneuvers with velocity and steering control. At each processing step the state of the system is sampled, in this system reading in steer angle and velocity, and the cost function given by Equation 1 is minimized for a future timestep [t,t+T].

$$J = \sum_{i=1}^{N} w_{x_i}(r_i - x_i)^2 + \sum_{i=1}^{N} w_{u_i}\Delta u_i{}^2 \quad (1)$$

With:

x_i = i^{th} controlled variable (e.g. measured position)

r_i = i^{th} reference variable (e.g. required position)

u_i = i^{th} manipulated variable (e.g. steer angle)

w_{x_i} = weighting coefficient reflecting the relative importance of x_i

w_{u_i} = weighting coefficient penalizing relative big changes in u_i

The resulting system inputs are executed – in the example case a small change in steer angle or velocity- and the state of the system is once again sampled. The calculations are repeated for the now current time step.

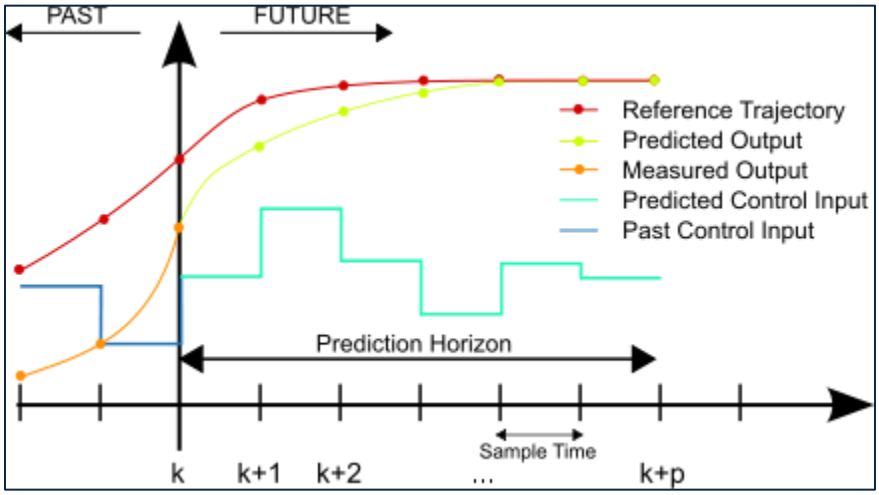

Figure 12 Graphic illustration of the MPC control theory

Chapter 3. Design Development

The main design decision of the project is the sensor selection. This section outlines the procedure undergone to select a sensor with each section highlighting a different sensor technology.

3.1. Design Flowchart

The flow chart shown in Figure 13 is the process that was used in choosing a sensor system. The analysis begins with five feasible sensor types: ultrasonic, infrared, LiDAR, radar, and image processing. The ultrasonic, infrared, and image processing were subjected to testing. The other sensors, being more expensive, could not be tested. However these sensor types were either modeled or researched. Then the systems were compared in a series of decision matrices. The flowchart acts as a guide to our design process, which is outlined in more detail in the following sections.

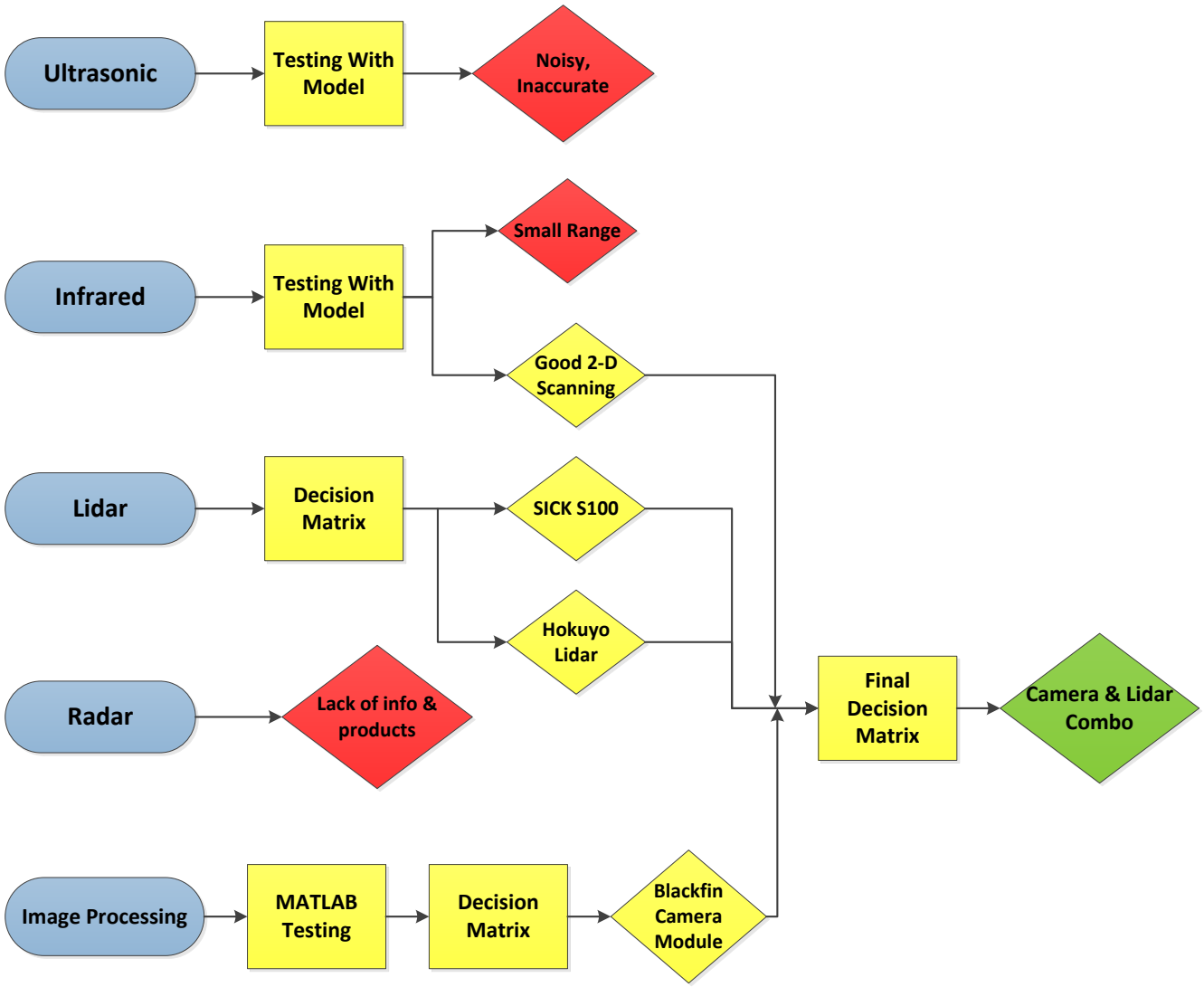

Figure 13 Sensor Selection Flowchart

3.2. Sensor Technologies Testing

The following section describes the testing conducted for each sensor technology considered. The results of the testing are also presented. Based upon the test results a series of products were selected for both image processing and LiDAR sensors and were compared in decision matrices.

3.2.1. Ultrasonic

The following section details the testing conducted with an ultrasonic sensor.

3.2.1.1. Experimental Concept

In order to evaluate ultrasonic sensor's ability to detect an obstacle, a prototype platform was setup on a small RC car by attaching a microcontroller and reading data from an ultrasonic sensor. The influence of environmental conditions such as operating the sensor inside and outside was also observed to evaluate how well this sensor technology will perform in a crowded presentation environment. Mounting locations were also systematically changed to determine any interferences or any noise that may be exist when placed at various points on the vehicle.

3.2.1.2. Testing Procedure

The car was tested in multiple different scenarios. First, different mounting locations were explored. The ultrasonic was mounted to the front bumper of the car, see Figure 14, and on two different heights above the car. Second, the sensor was tested in indoor and outdoor conditions. Lastly, two driving scenarios were performed. Sensor output was recorded with the car moving towards a stationary object, then with an object moving towards a stationary car.

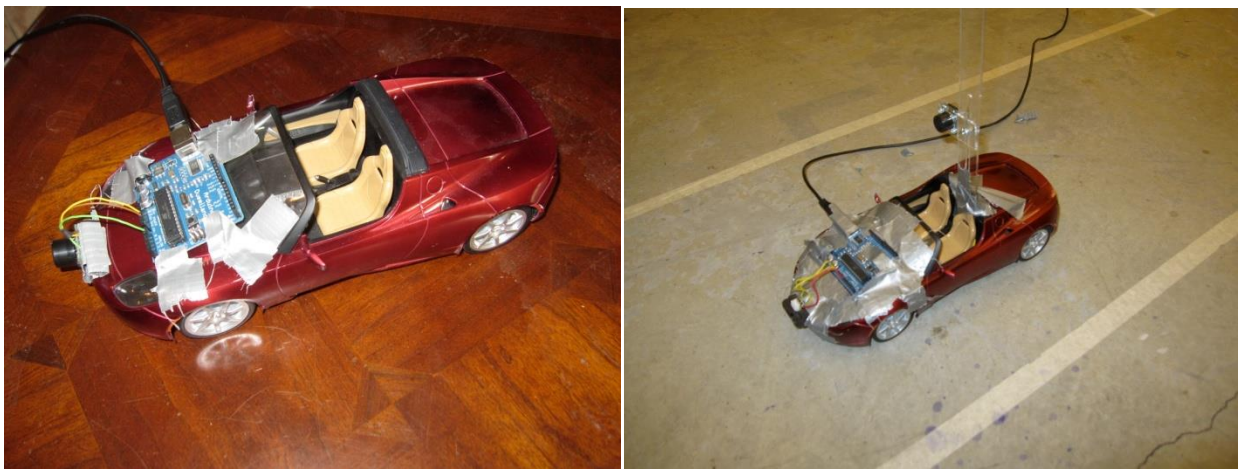

Figure 14 Prototype with Sensor Mounted on Front Bumper (left) and Sensor Stand (right)

3.2.1.3. Results

The effects of mounting location on the car are very important with the ultrasonic sensor. If mounted too low, as in the case with the sensor mounted on the front bumper, the sensor will detect the ground in front of the car. This diminishes the range drastically of the sensor. By mounting the sensor higher above the car, see Figure 14, much better data is received from the sensor. Another consideration when using ultrasonic sensors is the effects of indoor versus outdoor use. In an outdoor setting the sensor is fairly good at picking out at accurately detecting a single object. However in a crowded room the sensor will detect only the closest object in its range, which may not be the object that is desired to detect. The ultrasonic consistently output data with excessive noise. This was partially due to vibrations of the sensor. When the sensor was mounted higher on the mount it vibrated more causing larger spikes in the output. Due to the noise, output filtering would be required with the system to eliminate false data. From these tests it became evident that one ultrasonic would not be sufficient in determining the state of the obstacle. Additionally, the ultrasonic can only detect the obstacle's distance and not the angle it is at from the car. For these reasons the ultrasonic is not a good choice for the project.

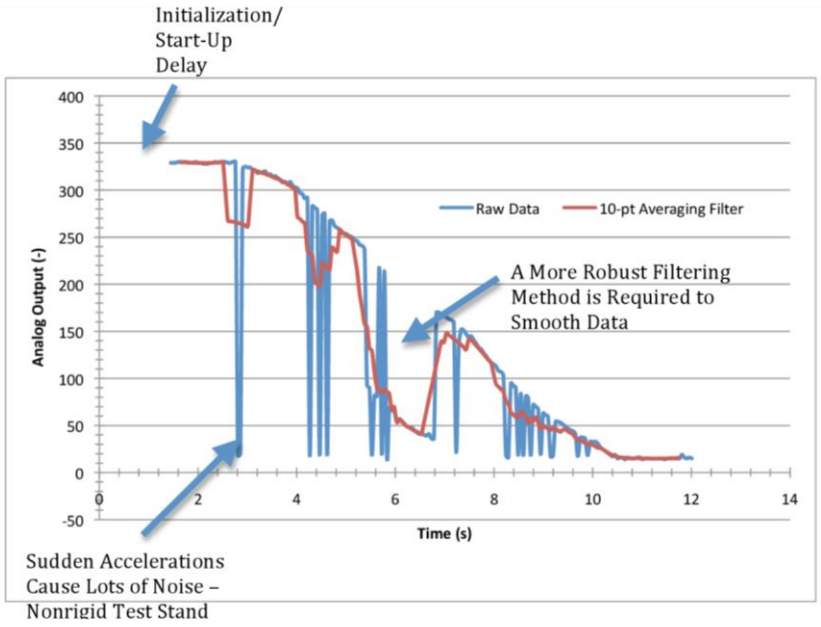

Figure 15 Ultrasonic Mounted on Upper Location of Elevated Stand Outside

Figure 15 shows the output when the model was driven straight towards a stationary object. The noise shows that vibrations are a noteworthy issue when considering mounting the sensor(s). This was caused by sudden accelerations and the wobble of the sensor mount. The red line shows the data after being filtered with a ten point average.

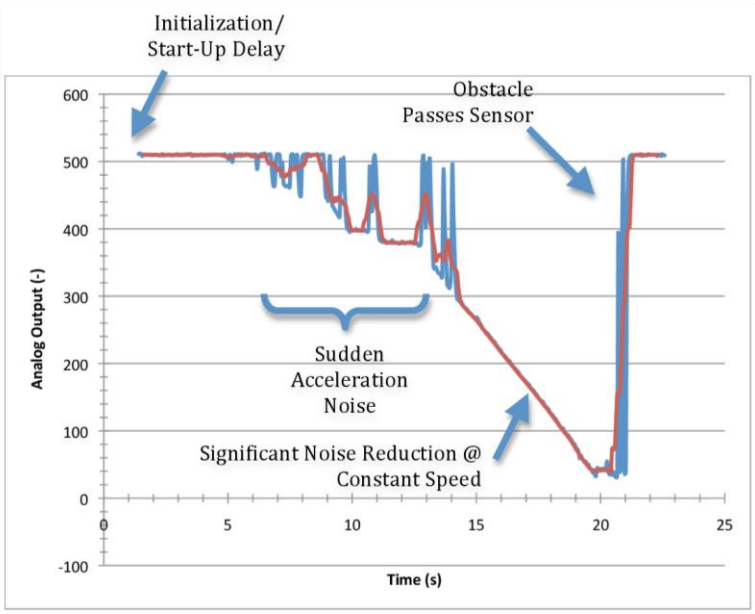

Figure 16 Ultrasonic Mounted at a Lower Position on the Elevated Stand Outside

Figure 16 shows the output of an ultrasonic sensor with a 2ft obstacle moving straight towards it. The sensor begins detecting the object at about 5s. The object was moved not at a constant velocity from 5 to 13 seconds causing the variation in output. From 14 to 20 the object was moved towards the sensor at a constant velocity and causing a fairly smooth curve until at 20 seconds the object moved passed the sensor. This test was conducted outside to ensure no detections other than the obstacle.

3.2.1.4. Product Tested

LV-Max Sonar EZ0

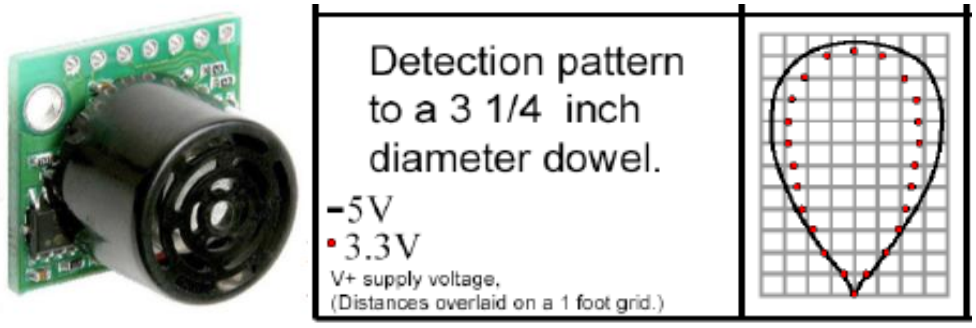

Figure 17 Ultrasonic Sensor and Sensing Area

Pros

- Cheap ($40)
- 3-D beam
- Small
- Analog/Serial

Cons

- Multiple sensors required for azimuth angle
- Noise (filtering required)
- Firing Offset may be required
- Effected by acceleration
- Requires high mounting to not detect ground
- Works better outside

3.2.2. LiDAR/Infrared

The following section details the experiments and conclusions relating to the LiDAR and Infrared sensors.

3.2.2.1. Experimental Concepts

In order to evaluate LiDAR and infrared (IR) sensor technology without testing an expensive unit an experimental setup consisting of an IR sensor was mounted to a slowly rotating platform to emulate a scanning LiDAR sensor. This test was performed for both qualitative and quantitative information regarding the effectiveness of scanning range finding technologies. This was considered a valid approach because both sensor technologies are subject to most of the same pitfalls, such as how the surface color and reflectivity of the obstacle influence the sensor output. The color dependence of the IR sensor was investigated by reading values from the sensor at a fixed distance from a cardboard presentation board from spots colored different colors. The amount of power reflected from the emitted beam is how this particular sensor detects range. In order to verify this expected power relationship, which we can expect to drop off as distance to some power. A power curve was fit to data taken from the sensor at various distances from an obstacle. This particular IR outputs an analog value representing the power of the reflected beam. Numerous values were taken at fixed distances from the sensor in 1in. increments. This data was then fit to a power curve to observe and verify the power and range relationship.

3.2.2.2. IR Approach and Recede Test Procedure

In this test a Sharp IR sensor was mounted to the front bumper of the test vehicle shown in Figure 14. The vehicle was driven towards an object until the front bumper made contact with the object and then backed away from the object until the sensor could no longer detect the object.

3.2.2.3. IR Approach and Recede Results

A power curve was fit to the relation between distance and sensor output to verify the power law nature of intensity to drop off as a function of distance to some power (the inverse square law). The results agreed very well with a power relationship and the non-linear distance relationship was verified successfully, as can be seen in Figure 18.

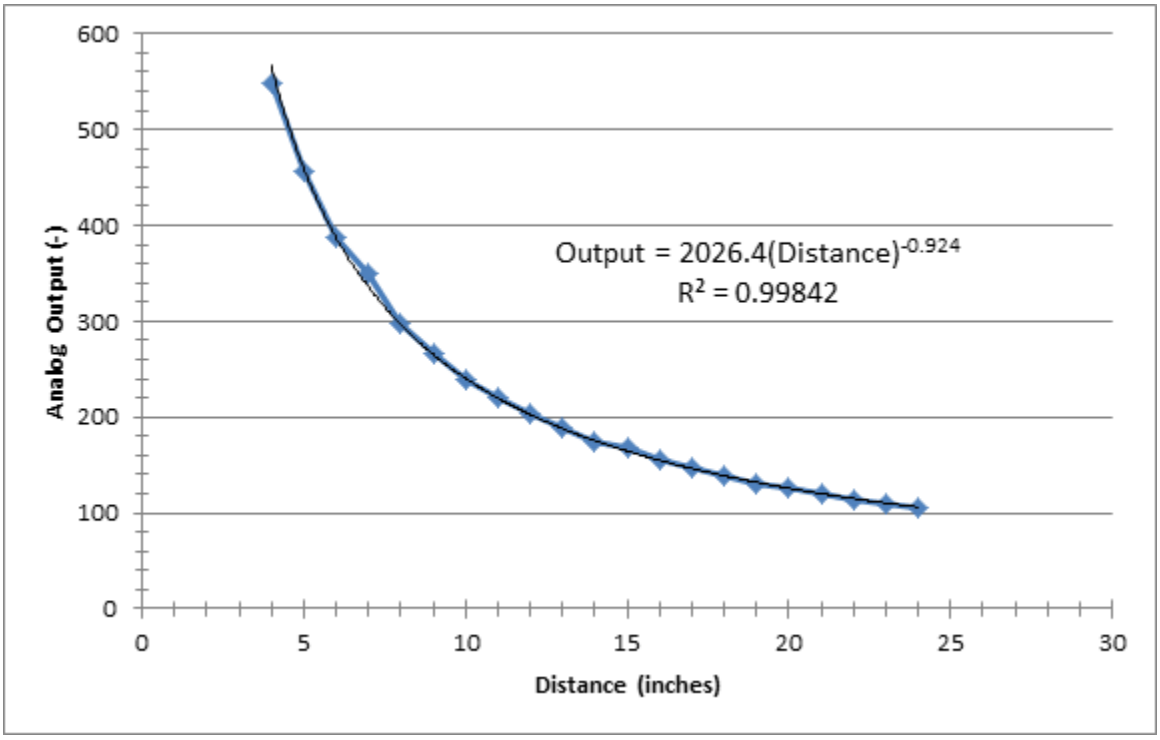

Figure 18 Sharp IR sensor analog output as a function of distance

Figure 19 shows the output for an IR sensor as a vehicle approaches, reaches a close range, and then recedes. It is apparent that there is a discontinuity between the approach and the recession of the obstacle. This occurs for IR sensors when an obstacle is too close, which gives bad data. This discontinuity could potentially be eliminated through the use of filtering and comparing the output to what is physically possible. A ten-point average is also shown in red, which shows rather good agreement between the raw and filtered data with only a same amount of noise. Another note to make is the non-linear region that exists in the middle of the output region of the sensor.

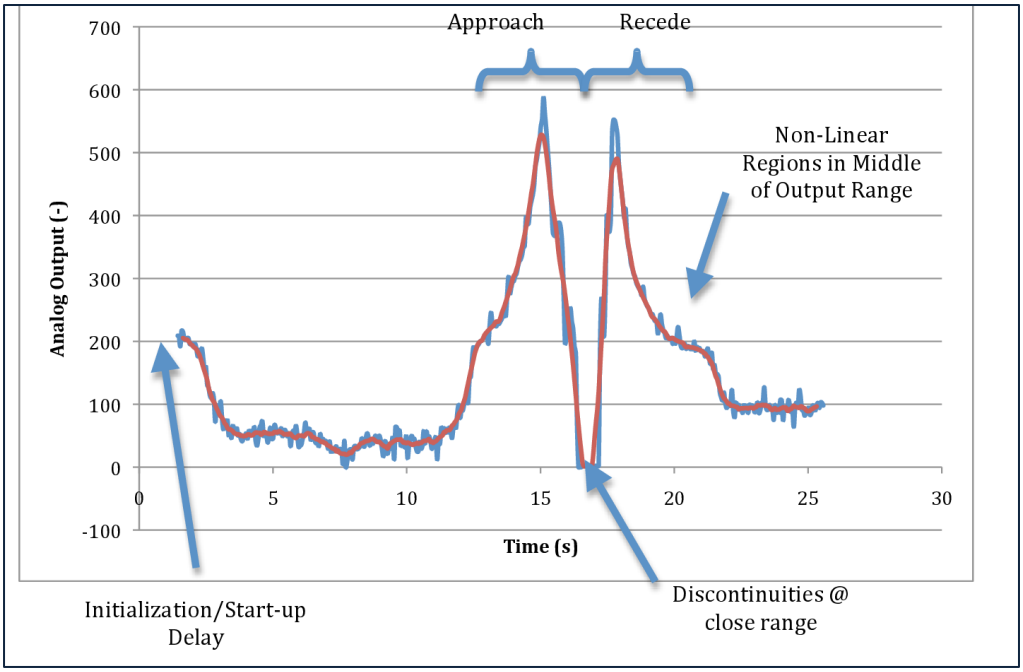

Figure 19 IR Sensor Approach and Recede at 20 Hz

3.2.2.4. Scanning LiDAR Emulation Test Procedure

The setup for this experiment, seen in Figure 20, consisted of an IR sensor affixed to a slowly rotating microwave turntable motor raised on a stationary piece of 2x4. This experiment aims at simulating a scanning laser rangefinder to evaluate how effectively a prepackaged product may perform and what value the concept of scanning laser rangefinder holds for completing the functional requirements of the project. In particular, reliability was investigated by comparing data obtained from stationary objects within the sensors range for multiple revolutions in order to see how repeatable the sensor output was. A polar map was drawn with the data obtained to see how effectively an environmental map can be drawn, while observing how much data processing, if any, will be required to obtain an accurate map that will be passed to the avoidance algorithm.

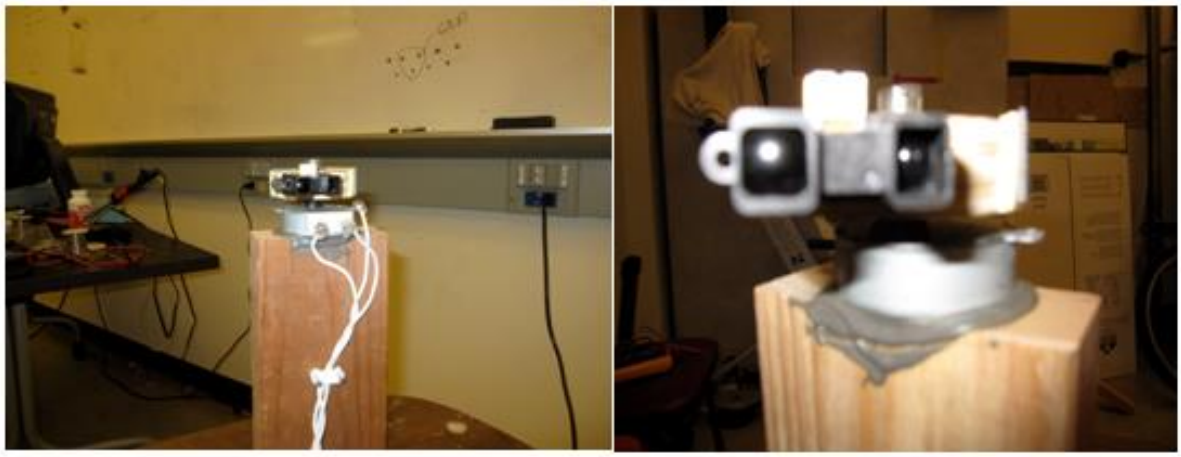

Figure 20 Scanning LiDAR Sensor Experimental Setup

3.2.2.5. Scanning LiDAR Emulation Results

The sensor output for a slowly rotating IR sensor as a function of time for multiple revolutions can be seen in . The sensor was rotated for two continuous rotations for comparison, hence the repeating pattern in the graph. Each bump represents a physical object seen by the sensor during its rotation. Figure 22 shows the polar plot of the experiment.

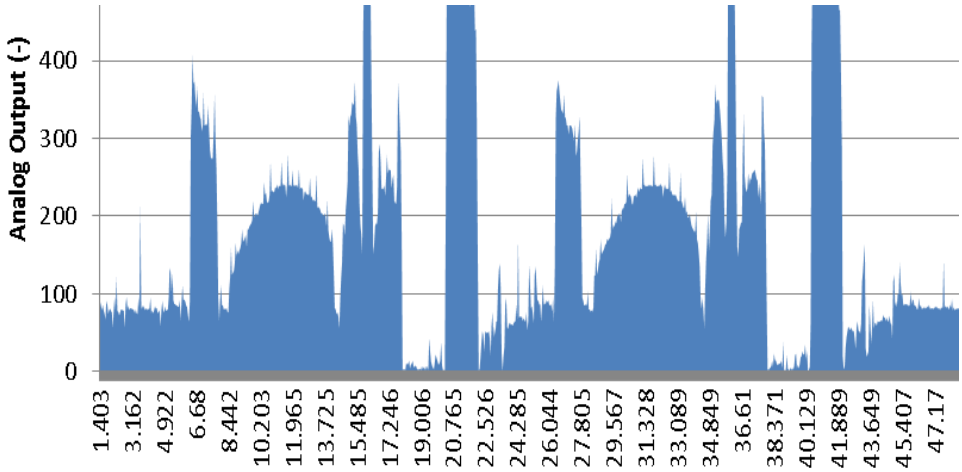

Figure 21 Rotating IR Sensor (6RPM) @ 20 Hz for 2 Revolutions

Error! Reference source not found. shows the consistency of the technology and its ability to affectively draw and environmental map with high accuracy and repeatability without the use of filtering. The sensor also was able to distinguish 3 legs of a chair less than ½" in diameter for both revolutions, which can be seen in the polar plot as the three sharp spikes closely together.

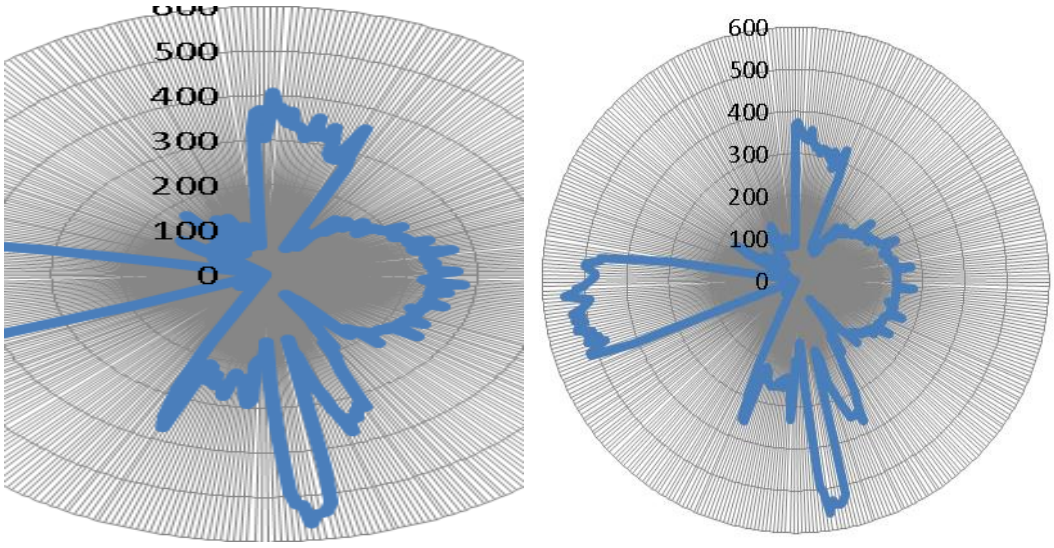

Figure 22 Polar Plots for Rotating IR Sensor (Rotation 1 on left, Rotation 2 on right)

3.2.2.6. Color/Reflectivity Test Procedure

The setup for this experiment, as seen in Figure 23, consisted of placing a Sharp IR sensor a fixed distance of 10 inches from a matte cardboard presentation board. Sensor data was pulled from the sensor using a microcontroller for a period of time. All the data was then average to obtain an average output value for each color.

Figure 23 Color/Reflectivity experimental setup

3.2.2.7. Results Color/Reflectivity

The effect of different colored obstacles on the sensor output can be seen to have a slight difference between colors, especially between black and white colored surfaces. However, this value only deviated by 2% for all tested colors as can be seen in Figure 24, so for the scope of this project reflectivity is not going to be considered a substantial factor affecting performance.

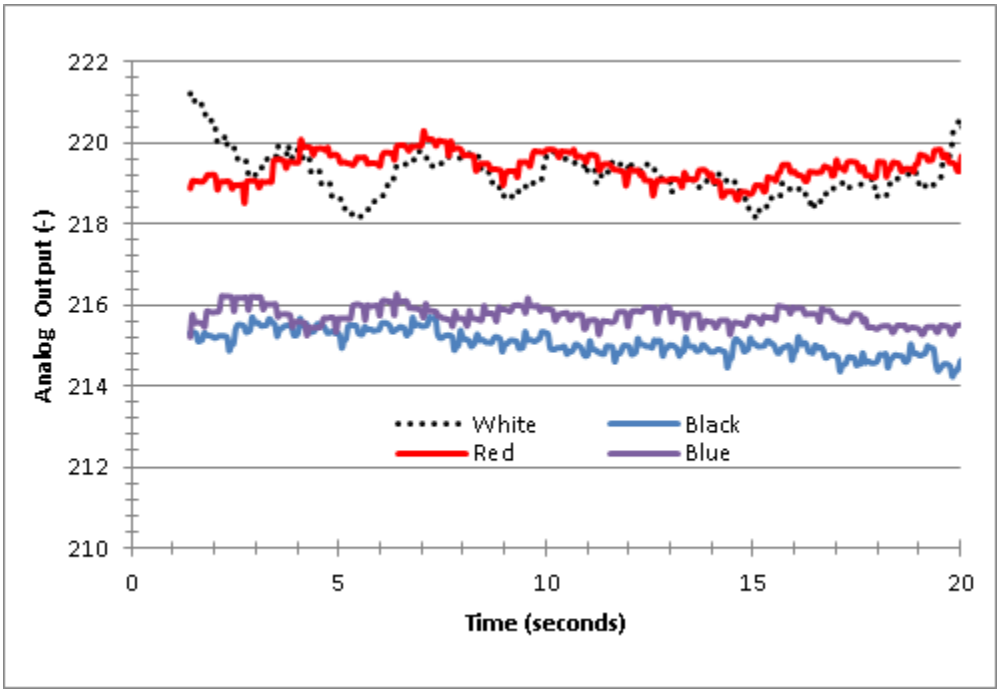

Figure 24 Effect of color on Infrared signal

3.2.2.8. Product Selection

In , five LiDAR sensors that are within the budget are compared in a decision matrix. Each sensor is compared based on six criteria: Cost, Size, Power Source, Range, Viewing Angle, and Scan Frequency. Each of these six criteria is assigned a weight. Scan frequency is the highest with a 30% weight and viewing angle is the lowest at 5%. The weights of each criterion add up to 100%. Each sensor is given an unweighted score between one and zero, one being the highest, zero the lowest. The unweighted score is chosen based on how well that system performs in that category compared to the other sensors. So the best sensor in that category will receive score of 1. The unweighted score is then multiplied by the criteria weight to get the weighted score, seen in the W column. The weighted scores for each sensor are summed and shown in the Total row. A perfect sensor would receive a 100 in this box. The LiDAR with the highest score is the SICK S100 Scanning LiDAR with a score of 67. This sensor has the best scanning frequency at 40Hz. All the other sensors only have a scan frequency of 10Hz. However the SICK S100, does not meet the weight or size specification, at 4" x 4"x 6" and 2.6 lbs. The SICK S100 is also fairly expensive at $2000. The next highest scoring LiDAR is the URG-04LX-UG01, this sensor is substantially cheaper at $1174, but it doesn't meet the scanning frequency spec of 20Hz. With a 10 Hz scan time the sensor will not be able to scan as

fast as the Matlab code runs. So the car will get new sensor data once every two cycles of commands to the car. Meaning the car will be making "blind" decisions every other cycle. The third highest scoring lidar the UBG-04LX-F01 meets all the specifications but the cost. At $2850 dollars the lidar is above the budget by $350. Since all the sensors do not meet our specifications, none can be chosen for our final system unless the specifications are revised.

Table 2 LiDAR Decision Matrix Number

	Criteria	Weight (%)	Sensor									
			URG-04LX (Hokuyo)		UBG-04LX-F01 (Hokuyo)		URG-04LX-UG01 (Hokuyo)		UBG-05LN (Hokuyo)		S100 (SICK)	
			U	W	U	W	U	W	U	W	U	W
1	Cost	25	0.3	7.5	0	0	0.9	22.5	0.7	17.5	0.4	10
2	Size	15	1	15	0.7	10.5	1	15	0.7	10.5	0.2	3
3	Power Source	10	1	10	0.5	5	1	10	0.5	5	0.6	6
4	Range	15	0.5	7.5	1	15	0.5	7.5	0.7	10.5	1	15
5	Viewing Angle	5	1	5	1	5	1	5	0.7	3.5	0.7	3.5
6	Scan Frequency	30	0.2	6	1	30	0.2	6	0.2	6	1	30
Total		100		51		65		66		53		67
Spec. Justification												
1) The Lidar models were chosen based on feasibility of use and price range												
2) Specifications not seen in the Criteria were either not comparably different between sensors or not as relevant as chosen criteria												

3.2.2.9. Product Analysis

The Hokuyo URG-04LX-UG01 Scanning Laser Rangefinder as seen in Figure 25, is presented in the following section.

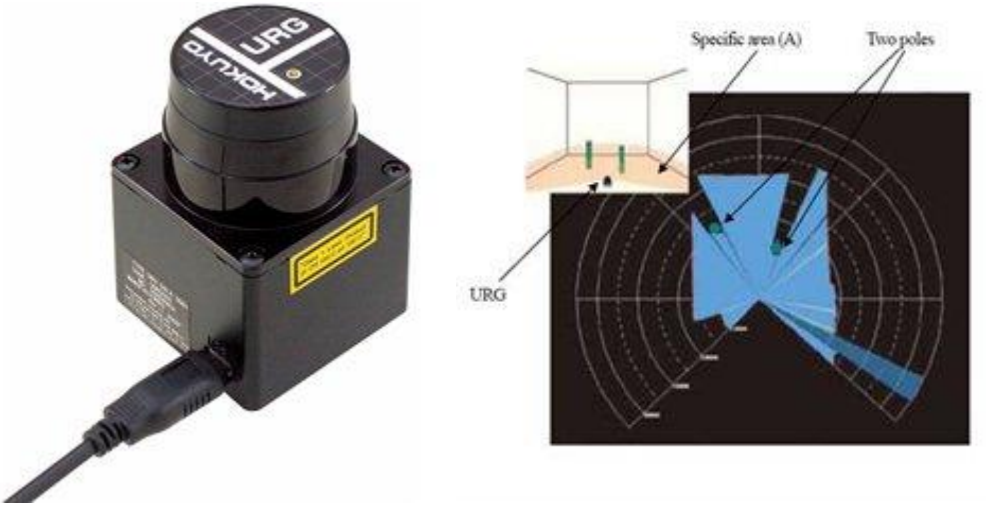

Figure 25 LiDAR Sensor and 2-D map generated by Scanning LiDAR

Pros:

- Range (12ft)
- Viewing Angle (240 degrees)
- Accurate
- Size
- Repeatability

Cons:

- 2-D
- Expensive ($1174)
- Scan time (100ms)
- Non-linear output regions

3.2.3. Radar

Radar sensors seemed to be a promising technology. They are capable of long distance sensing and are commonly used on full scale cars. For example, radar is used in the Mercedes Pre-Safe system. However, after thoroughly researching for radar sensors, none were found that meet the project specifications mainly due to budgetary constraints. Also, the radar sensors the previous teams had used did not have any specification documentation with them and no data sheets could be found on the internet. Due to lack of information on the technology and lack of available products, radar sensors are not a feasible sensor system for the project.

3.2.4. Image Processing

The following section presents analysis of basic image processing as well as a comparison of selected camera modules against project specific metrics.

3.2.4.1. Experimental Concepts

Image processing is a powerful tool that allows the user to extract detailed information from real-time videos. The primary drawbacks of image processing are the high computing overhead required and the complexity of the code. In order to test the computing power needed to run a simple image processing routine a basic image processing code was developed using MatLab.

3.2.4.2. Experimental Procedure

First, code was developed allowing the user to operate the webcam for a windows based platform. The user is able to select the desired frame rate, determining the amount of processing that will be needed. Figure 26 below shows a snapshot of the video output displayed to the user.

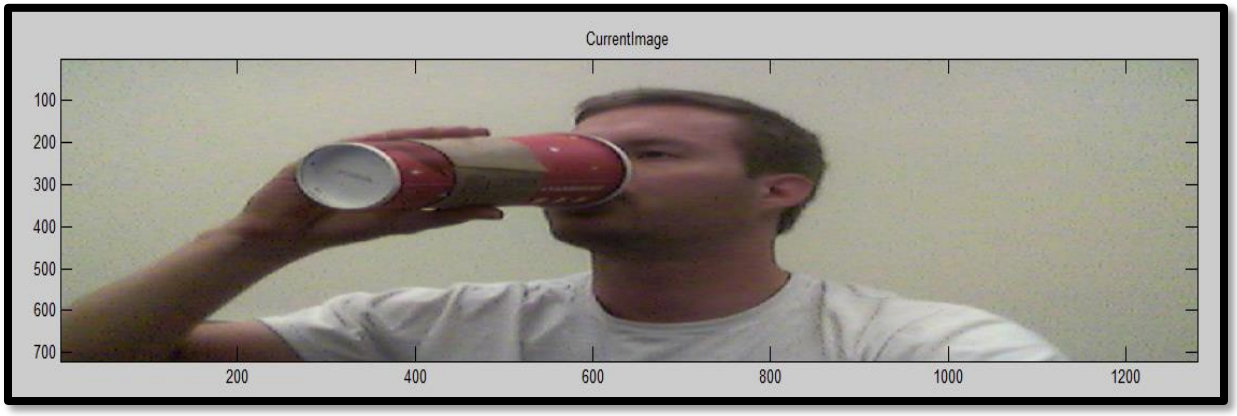

Figure 26 Snapshot of MatLab image processing output

Before beginning the MatLab program a baseline for the physical memory and CPU usage of the computer was recorded. The code was then initialized. As each frame was being displayed the frame was converted to a grayscale image in the background and the average optical density of the frame was calculated. The optical density versus time was then graphed alongside the image. Figure 27 below shows a graph of the average optical density versus frame number.

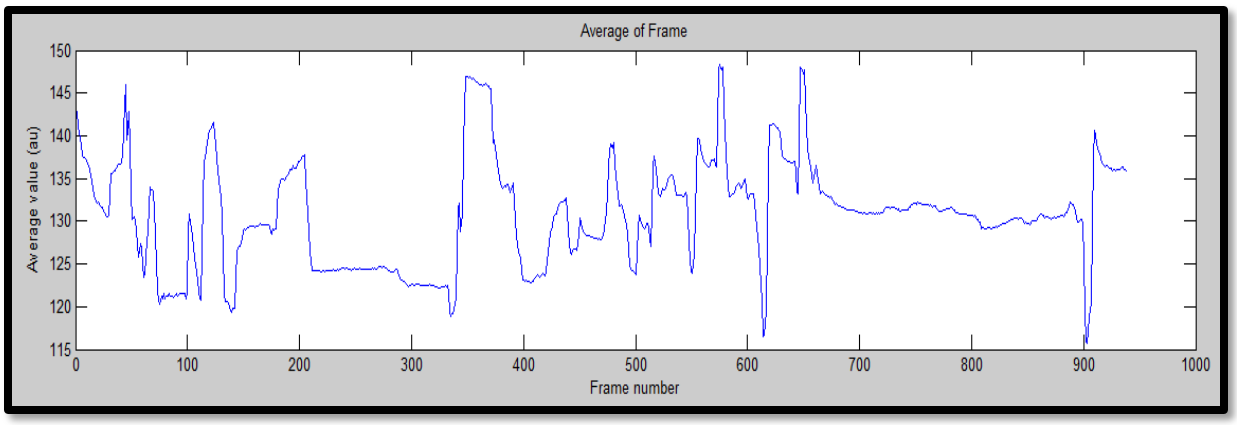

Figure 27 Plot of optical density against frame number for the image stream presented in Figure 26

While the image processing code was running the physical memory and CPU usage was once again recorded. The physical memory and CPU demands with and without the code running were then compared.

3.2.4.3. Results and Conclusions

MatLab contains powerful image processing and machine vision toolboxes which allow the user to easily manipulate images and video frames. The development of the code was based heavily upon MatLab examples and available code, and required only a few hours to develop. Despite the simplicity of the code and corresponding calculations, there was a significant increase in the CPU and physical memory usage while the code was running.

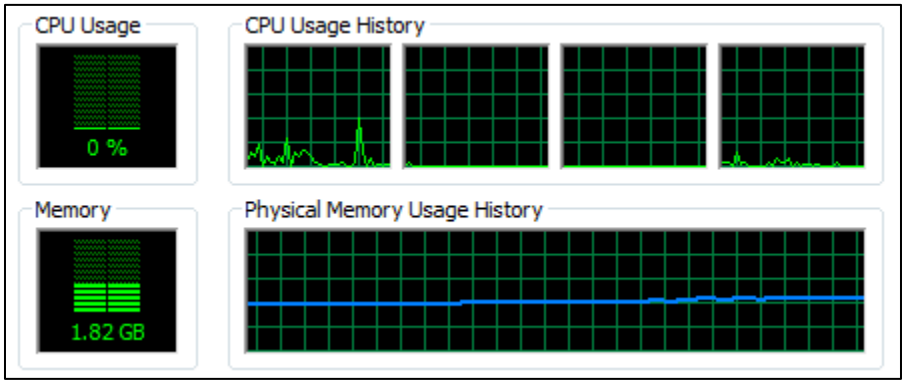

Figure 28 Computer performance with MatLab open but without image processing code running.

Figure 28 above shows the CPU and physical memory with MatLab open but no code running. There is very little CPU usage but 1.82 GB of physical memory are being used.

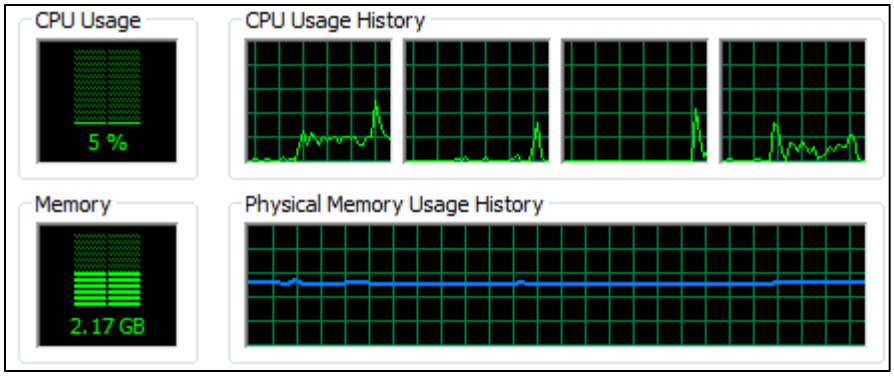

Figure 29 Computer performance with MatLab open and running image processing code.

While the image processing was running the CPU usage rose from 1.82 GB to 2.17 GB, as seen in Figure 29, an increase of over 19% despite the very simple processing that was being carried out. Based on the experimentation conducted it is clear that the processing power required to run complicated image processing could be a concern. In order to limit the amount of processing time needed for each frame it would be advantageous to have onboard image processing at the chip level which can be executed faster than the high level MatLab code. It was also noted that though the camera allows for tracking from side to side it is difficult to track objects moving toward and away from the camera due to the lack of distance detail provided. In order to accurately measure the distance from the car to a moving object that had been detected, non-linear pixel scaling or a secondary sensor would be needed.

3.2.4.4. Product selection

Based upon the experimentation conducted, background research, and previous product experience, the following camera systems were selected for further analysis and comparison.

- Microsoft Windows Kinect
- USB Webcam (multiple versions available)
- Blackfin SRV-1 Camera module
- Surveyor SVS Stereo Vision System
- Android Phone System

After in-depth analysis of the product specifications and definition of project relevant specifications, the afore mentioned products were compared using the decision matrix presented below.

Table 3 Image processing sensor decision matrix

Number	Evaluation Criteria	Weight (%)	Sensor Technology Rank									
			Microsoft Windows Kinect		USB Webcam		SRV-1 Backfin Camera Module		Surveyor SVS (Stereo Vision System)		Android Phone and Mount	
			U	W	U	W	U	W	U	W	U	W
	Cost											
1	Cost	5	0.25	1.25	0.6	3	1	5	0.75	3.75	0.1	0.5
	Geometry											
2	Sensor Size/Aesthetics	20	0.15	3	0.45	9	1	20	0.5	10	0.45	9
	Energy											
3	Power Dissipation	10	0.6	6	0.9	9	1	10	0.9	9	1	10
	Operation											
4	Impact/Damage Resistance	5	1	5	1	5	0.5	2.5	0.5	2.5	1	5
5	Horizontal Range	5	0	0	1	5	1	5	1	5	1	5
6	Resolution	20	0.5	10	1	20	0.75	15	0.75	15	0.75	15
7	Sensor Output/Protocol	15	0.85	12.8	1	15	1	15	1	15	0.75	11.3
8	Sensor Data Processing Time/CPU Overhead	20	1	20	0.6	12	0.95	19	0.95	19	0.4	8
Total		100		58		78		91		79		63

The Blackfin SRV-1 Camera module emerged as the dominant choice from the decision matrix. It outperformed the other sensors in: Cost, Aesthetics, Power Requirements, Horizontal Range, and output protocol. It was outperformed by at least one of the other sensors in: Impact Resistance, Resolution, and CPU overhead.

3.2.4.5. Final Product Analysis

The decision matrix presented in Table 3 led to the selection of the Blackfin SRV-1 Camera Module as the final image processing product.

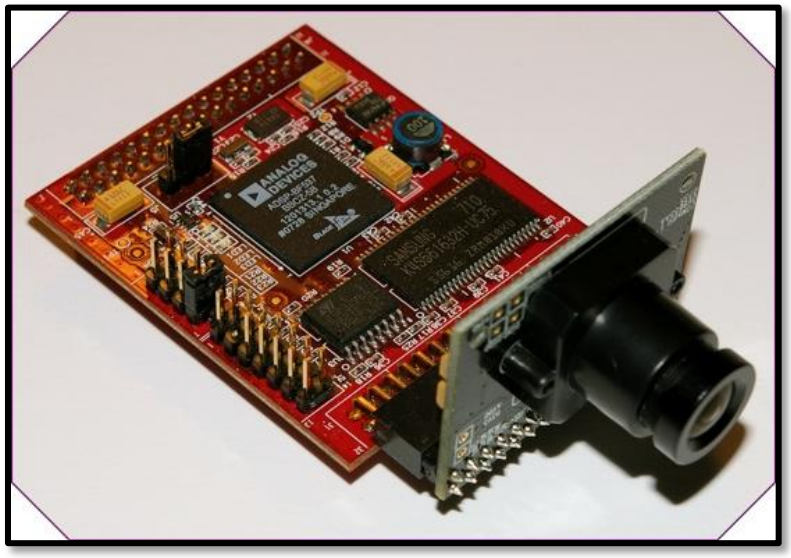

Figure 30 Blackfin SRV-1 camera module

A brief description of the key features is presented below

- Dimensions: 2.0" x 2.6", 1.25 oz
- 3.6 mm lens, 90-deg view angle
- 1280x1024, 640x480, 320x256, or 160x128 pixel resolution
- Onboard image processing
- Built-in C interpreter
- Direct support for 4 Sharp IR range finders

3.2.5. Final Decision Matrix

From the previous analysis there were no sensor systems that met the specifications outlined for the project. The LiDAR sensors have many of the qualities needed, but the sensors within the budget are either too heavy or do not meet the specified scan time. The image processing systems have the required scan time but lack the required distance detection capabilities. The decision matrix below in Table 4**,** pairs multiple sensor types, in hopes of creating a sensor system that meets the project specifications. Four different systems are analyzed. The first is the UBG-04LX-F01 LiDAR (which was previously determined as too expensive at $2850) is used as a reference for comparison. The second option is a Camera (Blackfin SRV-1) and IR sensor. This would be the cheapest of the options but would require the IR to track the object which could be difficult. The third is a Camera and LiDAR (Hokuyo URG-04LX-UG01) combination. The fourth is a dual LiDAR system where the sensors would scan at asynchronous times in order to meet the 20Hz scan rate. As seen in the table the highest scoring combination was the camera and LiDAR system. This system can use the camera to detect obstacles between scans of the LiDAR. Conceivably this would raise the scan frequency from 10Hz to the required 20Hz. This combination meets all of the specifications.

Table 4 Final Decision Matrix with Sensor Pairing

Number	Evaluation Criteria	Weight (%)	Sensor Technology							
			UBG-04LX-F01 (Hokuyo)		Camera and IR Rangefinder		Camera and Lidar (Hokuyo)		Dual Lidar (Hokuyo)	
			U	W	U	W	U	W	U	W
1	Cost	18	0	0	1	18	0.6	10.8	0.2	3.6
2	Sensor Size/Aesthetics	5	1	5	0.5	2.5	0.6	3	0.7	3.5
3	Horizontal Viewing Angle	5	1	5	0.5	2.5	1	5	1	5
4	Vertical Viewing Angle	5	0	0	1	5	1	5	0	0
5	Multiple Object Detection	10	1	10	0.33	3.3	1	10	1	10
6	Horizontal Range	7	1	7	0.75	5.25	1	7	1	7
7	Resolution (Angular/Range)/Detection Accuracy	5	1	5	0.7	3.5	1	5	1	5
9	Ease of Implementation	15	1	15	0.5	7.5	0.6	9	0.8	12
10	Sensor Data Processing Time/CPU Overhead	10	1	10	0.25	2.5	0.25	2.5	0.8	8
11	Scan Frequency	20	1	20	0.9	18	1	20	1	20
Total		100		77		68		77		74

3.3. Conceptual Design Conclusion

In review, the major design decision of the project was to choose a proper sensor for the system. By performing tests and analyzing real products, a preliminary decision as to which sensor will be implemented has been made. A combination LiDAR sensor and camera system is the best choice for the project. This conclusion was made based a variety of analysis. First by performing simple tests on the IR and Ultrasonic sensors, it was apparent that those technologies would not be sufficient. The tests showed problems with these sensor technologies. For the ultrasonic, the output was noisy, giving sporadic and inaccurate data. Also, the ultrasonic can only detect object's distance and not the angle of the object. The IR sensor was less noisy but had a significantly shorter range. However, by rotating an IR sensor with a motor an approximate model of a scanning laser sensor was created, similar to a LiDAR. The results of this test were consistent in mapping a 2-D environment. The success of this test was later used when rating the LiDAR in the decision matrices. Radar sensor technology was a promising alternative, but limited product information and pricing prevented it from being a feasible option. The next technology considered was LiDAR. LiDAR sensors have very good detection angles and ranges. They are capable of detecting multiple objects and mapping a complete 2-D map of the sensors surroundings. Unfortunately no LiDAR sensor within the budget met all of the project specifications. A decision matrix was made to analyze the LiDAR sensors within the projects budget. From the decision matrix three sensors emerged as the best options. The SICK S100 sensor met the frequency scan rate specification however it is quite large at 2.6 lbs and expensive at about $2000. The Hokuyo URG-04X-UG01, was substantially cheaper at $1174 but only had a 10Hz scan rate. The third LiDAR the UBG-04LX-F01 would meet all the specifications but is too costly at $2850. The last sensor option considered was an image processing system. An initial decision matrix was created in choosing the best of the image processing products, from it the SRV-1 Blackfin Camera Module was chosen. However, by itself the Blackfin Camera Module would not meet the specifications. The camera cannot accurately detect how far away obstacles are, thus it needs to be paired with another sensor type. By pairing multiple sensor types a system that meets all of the specifications can be created. In a final decision matrix, these sensor pairings were compared. From this matrix, the combination LiDAR (Hokuyo URG-04X-UG01) and Image Processing system (SRV-1 Blackfin Camera Module) are the best option.

Chapter 4. Final Design

The following diagram shows the high level data flow for the system. The subsystems' logic, software, and hardware will be discussed in detail in the following sections.

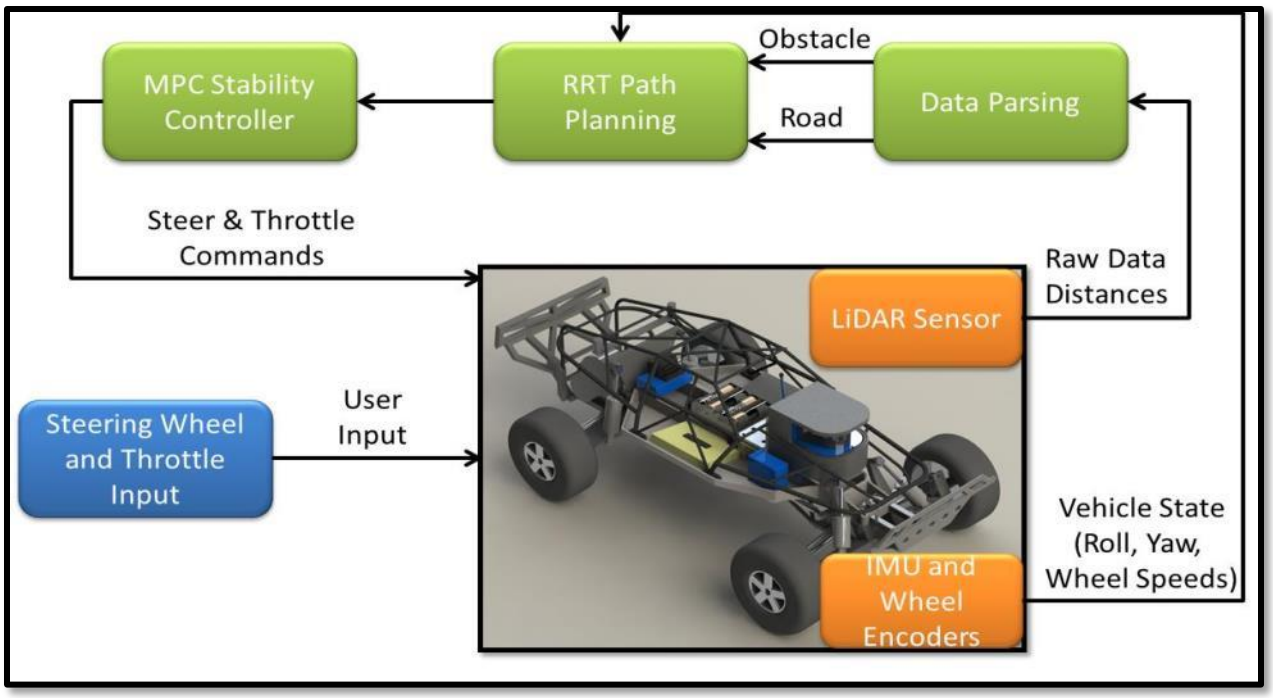

Figure 31. System overview showing the process flow of the system.

The system developed utilizes a $1/10^{th}$ scale, two-wheel drive remote controlled car as the test platform. Environmental data is collected using a Hokuyo UBG-04LX-F01 LiDAR sensor which is capable of producing a scan of the environment 35 times per second. Using the data collected by the LiDAR obstacles in the vicinity of the vehicle are parsed and identified as obstacles. The road cones are parsed separately from the obstacles and are used to locate the boundaries of the road relative to the vehicle. After the road boundaries and obstacles have been determined a threat coefficient is defined for each obstacle using the estimated time to collision between the test vehicle and the obstacle. If the obstacle is outside of the road or the test vehicle is not moving the threat is set to zero. If the threat coefficient for any of the detected obstacles goes outside of the acceptable range the system engages autonomous control. When under autonomous control the system uses the Rapidly Exploring Random Tree (RRT) path planning algorithm to determine a safe path around the collision. The steering inputs needed to follow each segment of the path are calculated with the path and checked against the physical limits of the test vehicle. Once a safe, feasible path has been determined the steer commands are tuned by the non-linear, eight degree of freedom vehicle model-predictive-stability controller to address any steer commands which may have caused rollover

conditions. The tuned steer commands are sent, via a hardwired connection, to the test vehicle, causing it to follow the desired path.

In the final implementation of the code the MPC controller was removed from the loop due to inaccuracies in the developed vehicle model. It is, however, and important part of the project development and will be discussed in the following sections. Stability was achieved by tuning the maximum steer angle that the RRT would allow.

4.1. Hardware Development

The following section details the development of the hardware used in this project

4.1.1. Final Sensor Selection

After the conceptual design review with the project sponsor the project's budget was increased to allow for the purchase of the Hokuyo UBG-04LX-F01 LiDAR sensor, which meets the project specifications. The small, compact sensor has a notably fast scan rate of approximately 35 Hz. A complete specifications sheet can be found in Appendix D. The single LiDAR sensor was selected as the primary sensor as it is much easier to implement than the LiDAR and Camera combination discussed in the design development section of this paper. Figure 32 below shows the LiDAR and some of its key specifications.

Figure 32. Hokuyo UBG-04LX-F01

4.1.2. LiDAR Mounting Bracket Design

In order to secure the LiDAR to the vehicle chassis a mounting bracket was designed. The primary considerations in the design of the mounting bracket were as follows:

- Sensor must not be subjected to any forces, impacts, or accelerations that violate the design specifications of the sensor during normal test operations or foreseeable misuse
- Sensor attitude must be able to adjust ±5 degrees from horizontal

- Sensor must be rigidly secured to the chassis such that there is no detectable relative motion during normal test operation
- Mounting solution must use existing vehicle attach points when possible
- Mounting solution may not interfere with the operation of any existing vehicle components
- Mounting solution must allow access to the LiDAR
- Mounting solution must be removable
- Alterations of existing vehicle design should be minimal

The solution to the above cited design criteria includes the design of a mounting bracket that attaches to existing chassis attach points, a protective casing, and a slight modification of the roll cage to accommodate the mounting bracket.

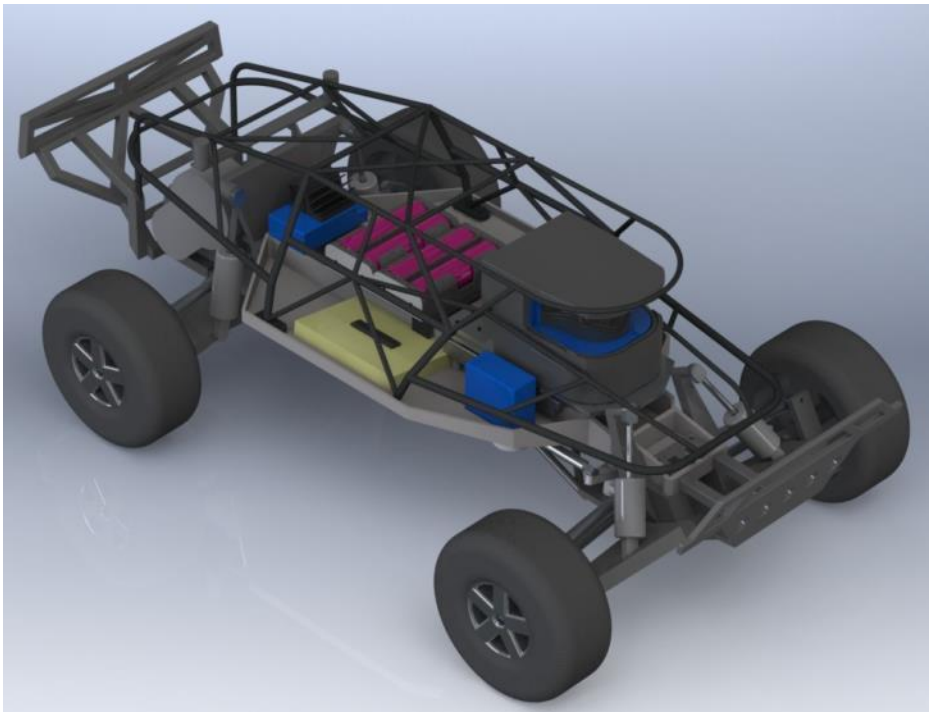

Figure 33. Solid model including updated roll cage and LiDAR mounting bracket

Figure 564 shows a rendered image of the mounting bracket with the re-designed roll cage mounted on the vehicle. The sensor is mounted forward on the vehicle so that there is less interference in the output data from vehicle components.

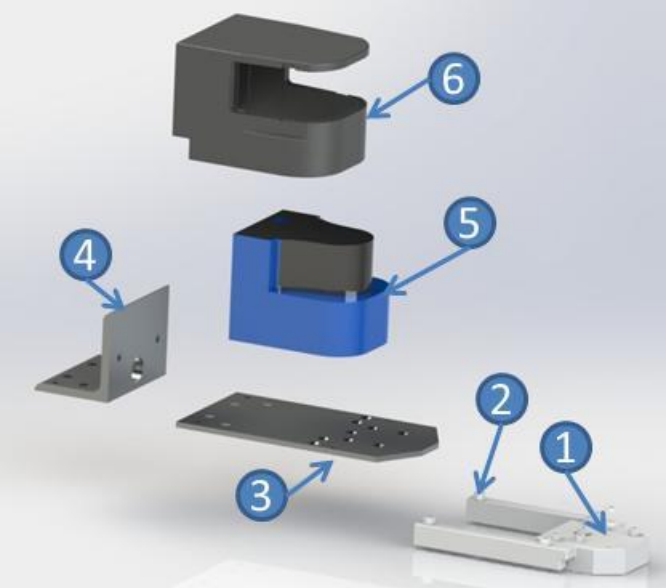

Figure 34. Exploded view of LiDAR Mounting bracket

Figure 345 shows the mounting bracket with the LiDAR attached. The mounting bracket consists of six individual components- including the LiDAR- Technical drawings of which are presented in Appendix O. The standoff (1) uses the existing vehicle features to create a flat mounting surface for the base plate (3). The angle aluminum mounting bracket (4) and the protective case (6) are then attached to the base plate, securing and protecting the sensor. The 22 M3 Jam nuts (2) allow the attitude of the base plate to be adjusted in three dimensions, meeting the requirement for adjustability. The protective case prevents foreign objects from contacting the sensor as well as providing impact and vibration insulation via four 1/16 inch foam inserts. The angle support allows the LiDAR to be rigidly attached to the bracket. All of the mounting bracket components will be created using 3D printing, allowing for the easy manufacturing of complex geometries.

4.1.2.1. Mounting Bracket Analysis

The protective case and the roll cage protect the LiDAR from impact while the foam inserts in the protective case provide vibrational damping for the LiDAR. In a crash scenario it would be possible for the vehicle to experience high accelerations that would then be transmitted to the LiDAR sensor, possibly exceeding the impact resistance rating of the sensor. The LiDAR is rated to withstand a 196 m/s^2 accelerations 3 times each in the x, y, and z directions. In order to assure that the sensor would not experience accelerations greater than this limit the vehicle accelerations were measured in a scaled crash test. All sensitive electronic components were removed from the vehicle and an accelerometer was attached to the chassis of the vehicle. The vehicle was then elevated and allowed to roll down an inclined ramp into a wall.

Figure 35 Chassis Acceleration in frontal collision test setup

The accelerations experienced by the vehicle chassis for multiple runs were measured during the decent and the collision and are presented in Figure 366

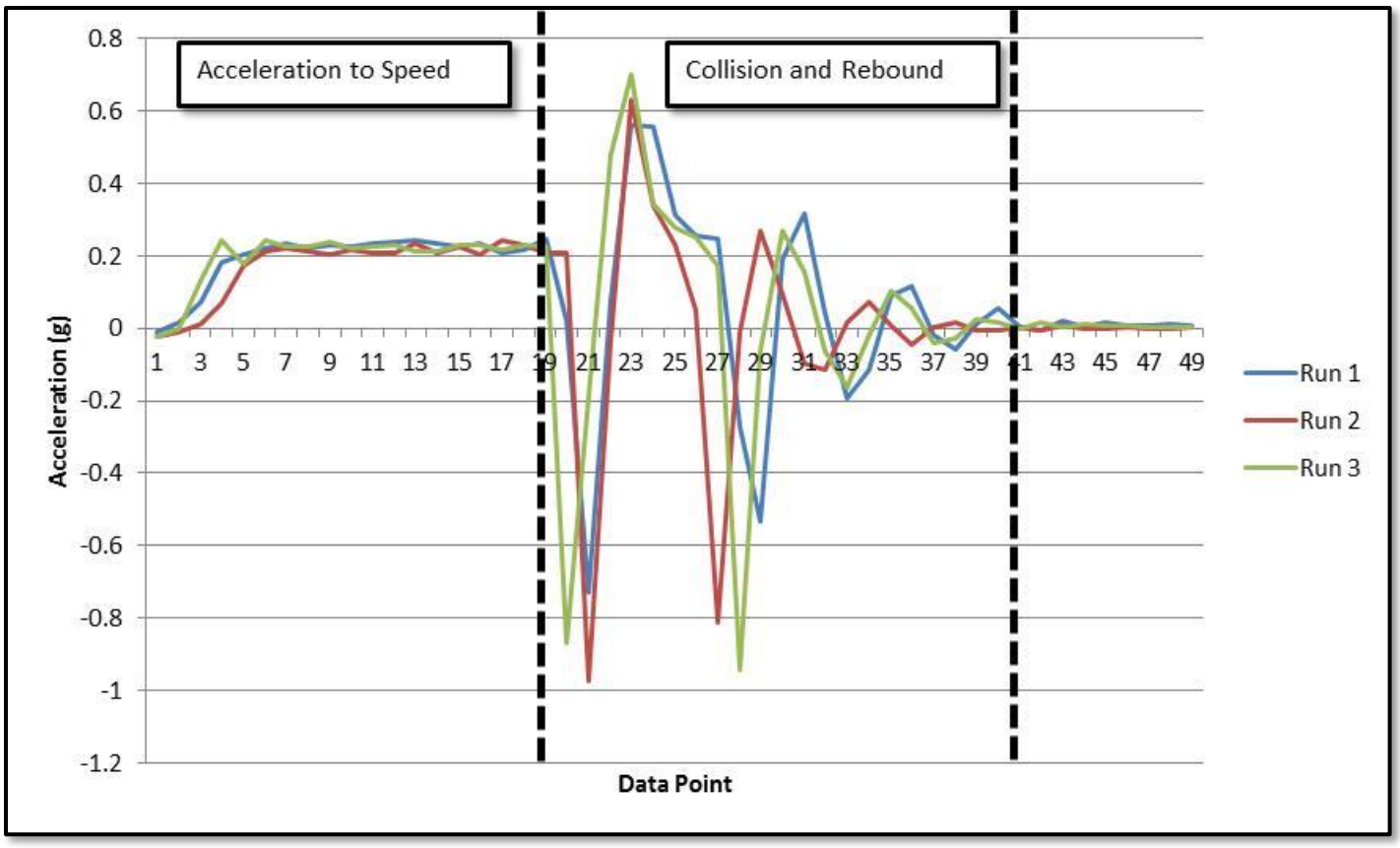

Figure 36 Chassis acceleration as a function of time for the frontal collision setup shown in Figure 34

Using a trapezoidal approximation the vehicle speed was estimated prior to the collision. The average speed of the vehicle prior to the collision was approximately 6.5 ft/s, less than the 10 ft/s test velocity. In order to estimate the vehicle acceleration in a collision at full speed an energy scaling approach was selected. A simplified energy analysis is presented below which shows that the kinetic energy of the vehicle is transferred into spring potential energy of the bumper with some losses due to friction. Using the equations below with the collected data the effective spring rate of the vehicle can be calculated

$$\frac{1}{2}mv^2 = \frac{1}{2}k_{Vehicle}\Delta x^2 + E_{loss\ other}$$

$$V_f{}^2 = V_o{}^2 + 2a\Delta x$$

If it is assumed that $E_{loss\ other}$ represents a constant proportion of the energy lost in a collision with the same vehicle and that the bumper of the car does not reach full compression then a similitude equation can be derived. This equation can be used to calculate the expected accelerations in a collision within a limited velocity range around the test data.

$$\left(\frac{V_{Model}}{V_{Actual}}\right)^2 = \left(\frac{a_{Model}}{a_{Actual}}\right)$$

The maximum acceleration of the vehicle during the three test runs was measured to be .972 g, this resulted in an expected maximum acceleration of 2.27g in a full speed frontal collision. This is a full order of magnitude lower than the acceptable limit for the sensor and therefore requires no further design consideration.

4.1.3. Powering the LiDAR

To power the LiDAR four 3.7V Lithium-Ion batteries will replace the four AA batteries that were used by the previous group. They will mount to the car in a similar and slightly larger four slot battery case. The new batteries will have sufficient voltage to power both the LiDAR and the microcontroller based circuit boards. A proposed schematic for regulating the 14.8-16.5V down to the appropriate voltages of 12V and 3.3V for the LiDAR and the circuit boards, respectively, can be seen in Figure 37. This redesigned power supply utilizes two voltage regulators and a simple voltage divider with filtering capacitors on both the input and output of the regulators to smooth out any sudden current demands. A larger capacitor bank will be used to filter noise and ripple from the battery supply before being regulated. Note that if an appropriate 3.3V regulator is selected, it may not be necessary to use a voltage divider if the 3.3V regulator is specified for such a voltage drop and excess heat dissipation is not a concern. Otherwise, selection of the two resistors making up the voltage divider must be chosen to drop the voltage to a safe level for the regulator. The voltage shall not be dropped below the minimum voltage input for each regulator, according to the component's datasheet.

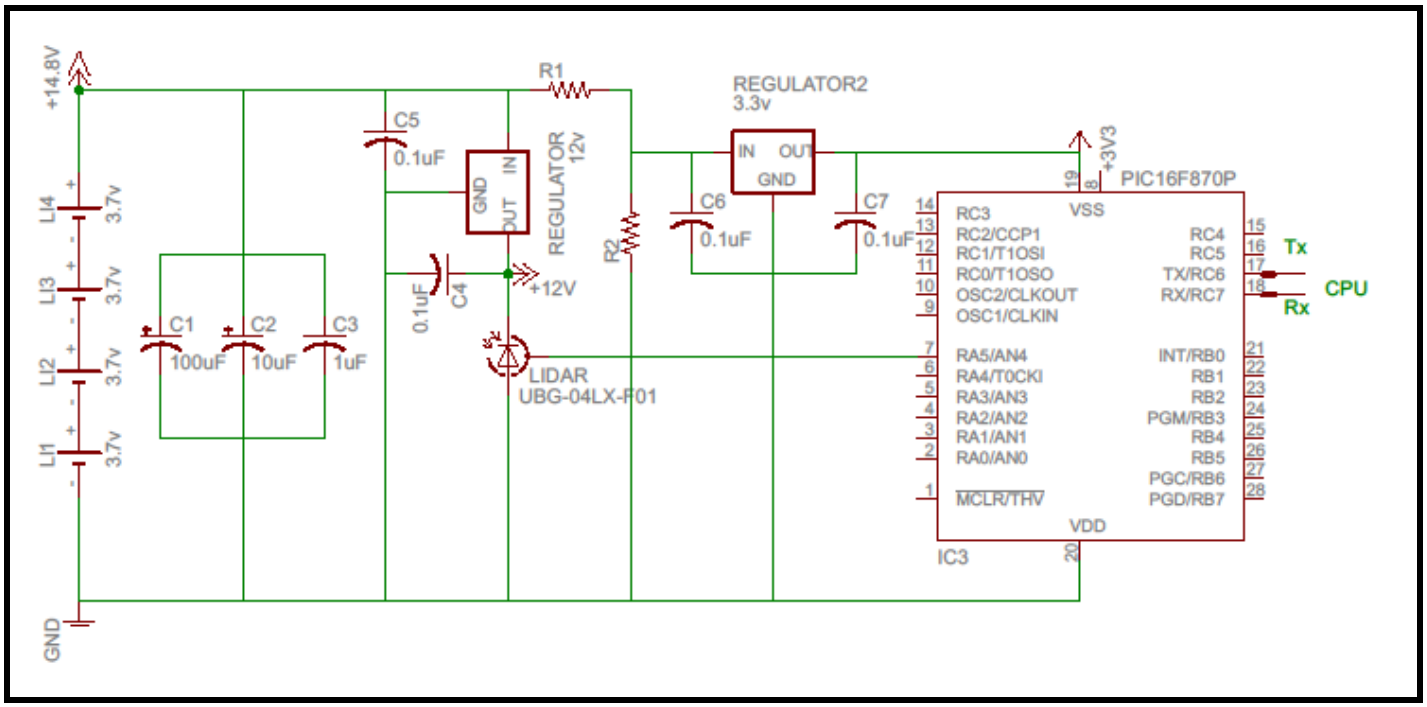

Figure 37. Circuit diagram for LiDAR Power circuit

4.1.4. Data Acquisition from LiDAR

In order to relay the LiDAR sensor's data back to the main computer the sensor's USB connection is used. The USB connection with an independent data tether to the computer was selected over the Serial connection due to the much higher data transfer rate. The maximum rate of data transfer for serial communication ports on a PC is 115 Kbit/s while the maximum rate of data transfer for USB 2.0 is 480 Mbit/s. The use of a 64 foot USB extension from the test vehicle to the computer reduces the actual data transfer rates for the USB to USB 1.1 speeds of 12Mbit/s. With the LiDAR producing 726 data points per scan and 35 scans per second it is not possible to transfer the data in real time via a serial connection but the data is easily passed via USB.

The data sent over the USB connection is in an encrypted format to decrease the amount of data that is passed in each scan. Information regarding the encryption and C code libraries needed to retrieve data from the sensor can be found online.

4.1.5. IMU and Wheel Encoders

The Sparkfun 6-DOF IMU which existed from the work of the previous two groups is now used solely to determine the roll rate of the vehicle. All other data that was collected from the IMU has been replaced with data collected using the LiDAR sensor.

The wheel encoders are used to estimate the velocity of the vehicle but do not account for wheel slip or the effects of cornering in the approximation.

The IMU and wheel encoders pass data to the slave PIC board which then passes the data to the master PIC board. The master PIC board then transmits the serial data via the main data tether to the computer. For a more detailed description of the PIC communication protocol please see "A MODEL PREDICTIVE CONTROL APPROACH TO ROLL STABILITY OF A SCALED CRASH AVOIDANCE VEHICLE" by Nikola Noxon.

4.1.6. Power Supply

The power supply underwent further revision for the final design. The final power supply offers more features such as a wider range of DC supply rails (+3.3V, +5V,+12V) that use high efficiency DC-DC switching voltage regulators, a low-battery indicator LED, an overload protection fuse, and an enable pin to selectively toggle the output of each switching regulator with external hardware; this ideal for implementing an emergency shut-down. It is vital that the batteries be changed once the low-battery indicator LED (yellow) comes on; this indicates that the voltage provided by the cells has dropped below the threshold of +14.7 volts. If the supplied voltage drops too low the boards that control the steering and throttle behavior of the car will start to send and receive bad data that usually results in erratic behavior. In addition, changing the batteries at the appropriate time helps to prevent from deep-discharge.

Please refer to the DC-DC switching power supply datasheets for the circuit and passive components used with each regulator. The low battery indicator circuit consists of two NPN transistors, a trimmer, and a resistor & LED. The trimmer can used to set the threshold voltage at which the LED comes on, currently

set to +14.7 volts. In stand-by this circuit draws less than 5 mA and when activated draws around 25 mA. Each rail of the power supply is rated to a one amp capacity. Currently, the power supply powers the IMU, the PIC microcontroller board, the LiDAR sensor, and the camera and draws about 600 mA offering about a two hours of continuous operation.

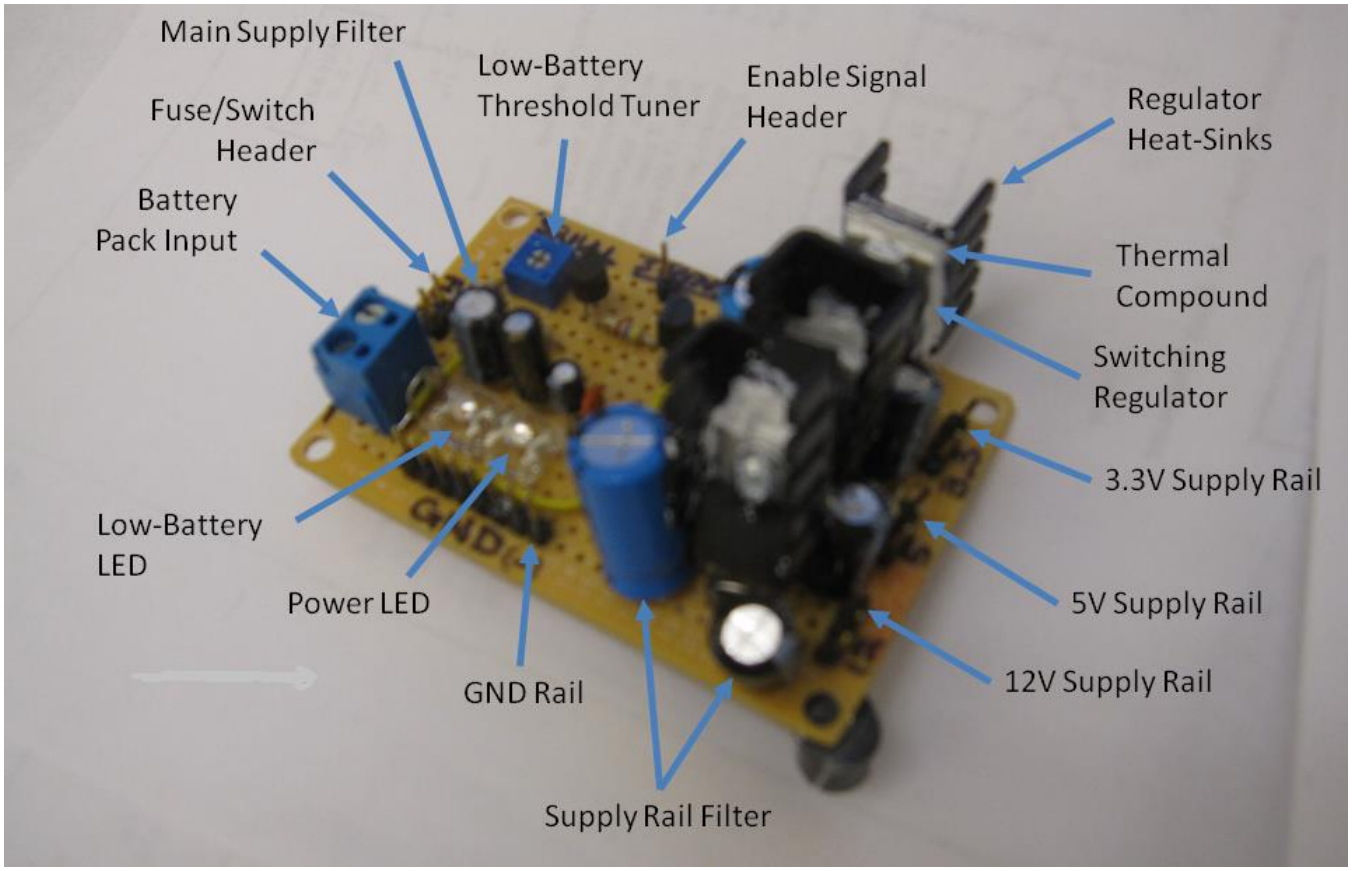

Figure 38. Power supply board with component description

4.1.7. Key Switch Box

The key switch box is where all the connections from the computer and the car interface. The data from the PIC microcontroller board, responsible for relaying steering and throttle data, IMU data, and wheel encoder data as well as camera signal from the car is connected to the box thru the cat5e cable.

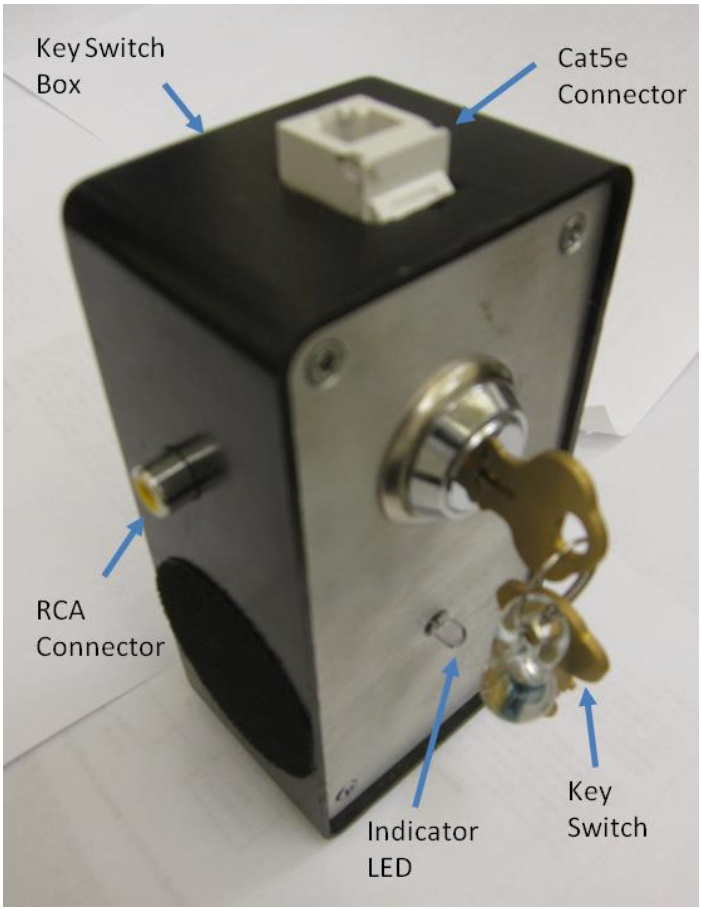

Figure 39. Key box with component labels

Upon coming into the box the cat5e cable connections are broken out with the video signal going to an RCA connector, the toggle signal going to an Atmel microcontroller, and the other signals going to a serial converter. An RS232 to USB serial converter FTDI board located within the switch box provides the required voltage level and protocol conversions to enable the computer to communicate with the microcontrollers. The Atmel microcontroller monitors the key position and provides a signal to the toggle pin of the switching regulator that powers the PIC microcontroller board. The key provides an on/off control to the boards that rely the steering and throttle data, which simultaneously provides an emergency shut-down method; an LED light, located below the key, indicates the on/off status of the PIC board.

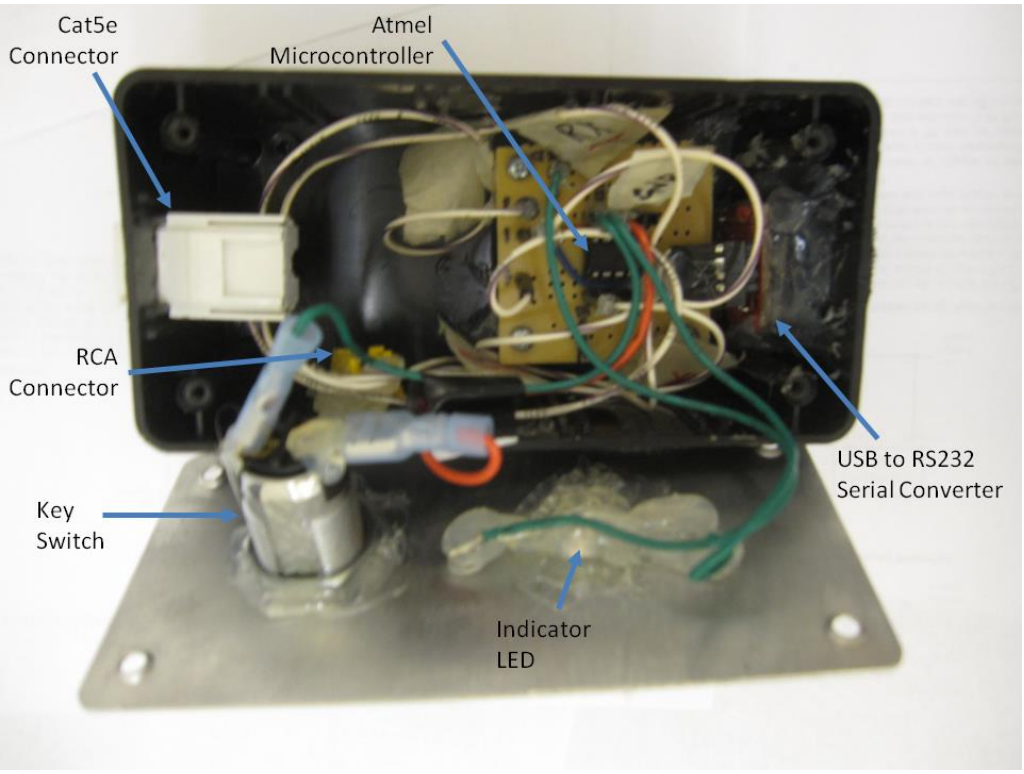

Figure 40. Inner wiring of Key box with component descriptions

4.1.8. User control

User control of the test vehicle is accomplished by use of a Logitec steering wheel and pedal controls. The signal from the steering and pedal commands is interpreted by the Simulink code and passed through the main data tether to the test vehicle.

Figure 41. Logitec steering wheel and pedal controls

4.1.9. Video Feedback

In order to create a more realistic driving experience the CMOS Camera Module Color Camera was used to give a driver point-of-view. The camera is mounted to the top of the test vehicle on a polycarbonate stand and is powered using the existing 12V source. The video feed is returned using a free strand in the CAT 5 cable that connects the test vehicle to the computer.

4.2. Software Development

The top level Simulink block diagram for this system is shown in Figure 42. The primary segments of the code include data collection from the LiDAR using Matlab's C-MEX compiler, data parsing using Java, and RRT path planning using Matlab. The MPC controller is not implemented in this version of the code.

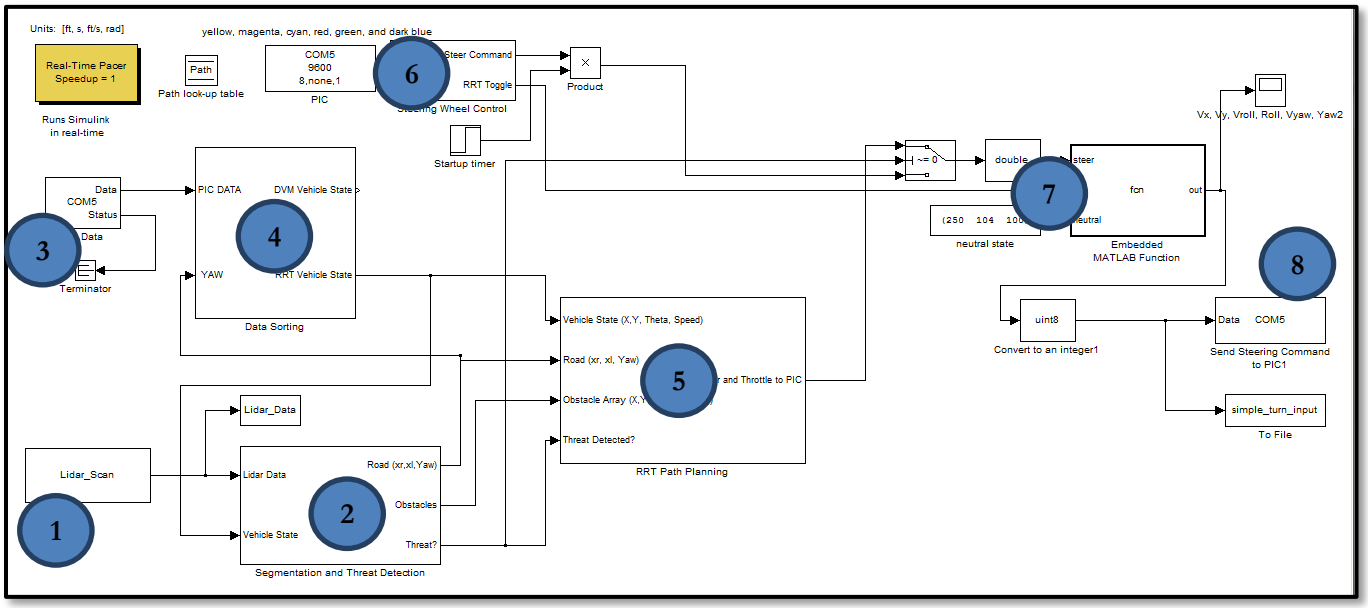

Figure 42. System Simulink high level block diagram

Data is collected from the LiDAR Sensor (1) and is passed into the segmentation and threat determination block (2) where it is parsed into obstacles and road boundaries. Simultaneously the IMU and Wheel Encoder data is retrieved from the serial bus (3) and parsed to determine the vehicle speed. With the data from all of the vehicle sensors the threat coefficient is determined (2) at set high if there is an imminent collision detected. If no threat is detected the user's steer and throttle commands (6) are passed to the vehicle. If a threat is detected a safe path around the obstacle is developed by the RRT Algorithm (5). The toggle between user and computer control is managed by a switch block with a built in function (7) acting as an emergency kill if the "O" button on the steering wheel is pressed. The steer and throttle commands are then sent across the data bus to the car using the COM port block (8)

4.2.1. LiDAR Data collection

The code used to retrieve data from the LiDAR sensor is based on the C libraries provided by Hokuyo and available for download at http://www.hokuyo-aut.jp/02sensor/07scanner/download/products/ubg-04lx-f01/. In order to integrate the C code into the Simulink environment Matlab's MEX capabilities were used. MEX allows C code to be compiled and run in the Matlab environment. For a detailed discussion of MEX operation please see the User Manual in Appendix M. Construction of a custom Simulink S-function allows the compiled C code to be run in Simulink.

The highest level function for the URG Library is GD_Scan. This file contains the C main() function as well as the MEX gateway function. The file has three modes: Initialization, Data Collection, and Shutdown.

In the Initialization routine the code initializes a serial connection with the lidar using the pre-defined commands

```
urg_initialize(&urg); ret = urg_connect(&urg, device, 115200);
```

A data structure that contains all of the connection information, data pointers and handle for the serial connection is defined and set as persistent using the MEXmakememorypersistant() command. The pointer to this data structure (URG_PTR) will be available for subsequent calls to the MEX file and allows the serial connection to remain open even though the MEX file closes. The laser is also turned on during initialization.

In the data collection routine, the persistent URG_PTR is utilized to call the LiDAR's "GD" routine, retrieving the most recent data scan from the buffer. This can result in scan times anywhere between .005 and .05 seconds depending on where in the scan the laser is when the routine is called. The command

```
urg_requestData(URG_ptr, URG_GD, URG_FIRST, URG_LAST)
```

Returns a 726x1 array of long data types representing the distance data collected by each beam. For a more detailed discussion of the function parameters please see the Hokuyo communication protocol on the manufacturer site

In the Shutdown routine all data other than the URG_PTR created in the initialization routine is freed, the laser is set to idle, and the serial connection is terminated. The persistent URG_PTR will remain in memory until "clear mex" is called or Matlab is shutdown.

4.2.2. Segmentation

Once the data is attained from the LiDAR sensor via serial communication, the data is passed to the segmentation algorithm in order to identify obstacles within the point-cloud and to determine their state. The segmentation of detected obstacles within the point-cloud happens in three steps that occur in tandem: point clustering, parsing each point cluster to obtain geometric properties, and obstacle tracking & velocity estimation. In the first step, the segmentation algorithm first identifies obstacles by clustering adjacent points in the point-cloud together to form discrete sets of ordered points, which make up each obstacle's definition. When to begin and when to end an obstacle definition, or cluster of ordered points, is controlled by various parameters, which subsequently control the size and location of the bounding boxes (detected obstacles). To generate bounding boxes around obstacles detected within the point-cloud, the clustered points making up each obstacle definition are parsed using the cluster-method algorithm. The output of the segmentation process is the state of each detected obstacle, including its position, size, and velocity. Parameters control the aspects of how points are clustered; these parameters include the max number of points, max step size, min area, and a scaling factor. A description of each parameter is as follows:

Threshold distance: This parameter controls how far to look for obstacles surrounding the car.

Max Number of Points: This parameter controls the maximum number of points that can be clustered together for each obstacle definition.

Max Step Size: This parameter controls when to end an obstacle definition. If adjacent points within the point-cloud are greater than the *max step size* and are both within the *threshold distance* while the *max number of points* has not yet been reached the definition ends. This allows for obstacles placed near each other or near to walls can be identified and segmented separately.

Min Length: This parameter, determined dynamically as the detected distance multiplied by the angular resolution, controls the minimum width and/or length each detected obstacle may possess. This will avoid any plane surface obstacle detected from having an infinitesimal length or width value.

Scaling Factor: This parameter controls how much each detected object is to be scaled by and is used to slightly buffer each detected obstacle's geometry before path-planning.

Max Velocity: This parameter filters any obstacle velocity estimations that are not feasible, typically occurring with points that fall off either side of the obstacle's definition over time.

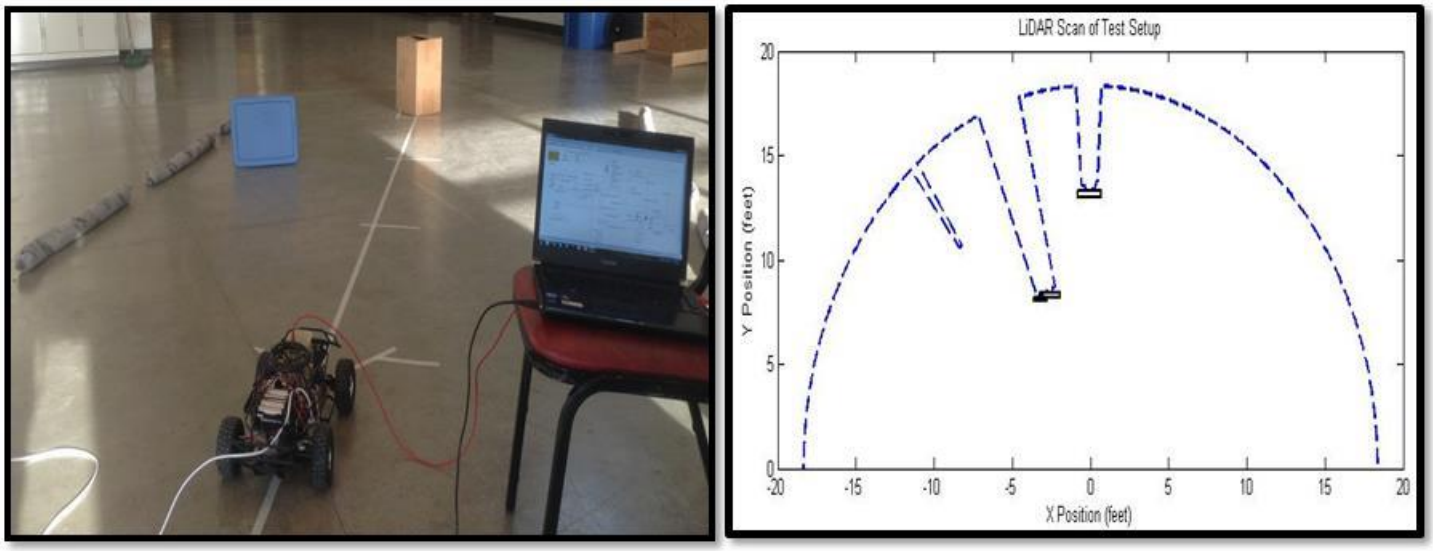

Figure 43. egmented Point-Cloud Results and the Actual Test Layout

To cluster points within the point-cloud, the algorithm iterates through the data starting at the first index and moving the last while a temporary buffer holds the current obstacle definition. Upon iteration, if the current point is at a distance less than the *threshold distance* it is added to the current obstacle definition. If either the *max number of points* or the *step difference* is exceeded then the current obstacle definition is ended, processed, and a new detected obstacle is added to a set holding all detected obstacles. Finally, the buffer is cleared. In addition, if the current point is outside the threshold, but the previous point was inside the threshold the same occurs; the obstacle is also processed, added, and cleared.

Every time the end of an obstacle definition is identified, the points within the definition are processed and the result contains the state of the detected obstacle, which is added to a large set of all detected obstacles. The cluster-method algorithm processes each obstacle definition, or set of points, to attain the geometric information (location and size) of each detected obstacle; by simply using the maximum and minimum x and y values in the each cluster of points within the definition, the bounding box and centroid can be determined.

In order to estimate the velocity of each obstacle they must be tracked through time or the points making up each obstacle definition must be tracked through time. This algorithm estimates each detected obstacle's velocity by calculating the change in position of each point making up the obstacle definition over time, between iterations. Since the number of points in each obstacle definition change through time this method allows it so the same obstacle with different definitions to be compared easily at different times. Keeping the points ordered in the point-cloud allow for easy obstacle tracking as each has a unique index and will always be adjacent to other points within the obstacle definition. A velocity accumulator calculates each point's change in position over time within the obstacle definition and divides by the total number of points to estimate each obstacle's velocity. The first and last points of the obstacle definition are ignored as these are fall off points; these points fall off the obstacle definition over time and are ignored because they produce impossibly large velocity estimations. In addition, the contribution of each point to the velocity estimation is checked against the *max velocity* expected to filter out any other fall off points. Due to the change in position, namely translation and rotation, of the car over time, the previous point-cloud must be brought to the current reference frame in order for this estimation to work. This means that the previous point-cloud must be translated and rotated in order to line up the points to the current point-cloud and match the beam indices. Once the road is detected and the yaw rate is determined the number of indices to rotate the previous point-cloud by can be calculated; the distance to translate is calculated by the speed of the car, given by the wheel encoders, multiplied by the time between iterations. The previous point-cloud cloud is translated point-by-point and rotated point-by-point using a rotation transformation matrix allowing to check the change in position of each point in the obstacle definition by referencing the index number (beam number). It can be noted that obstacles with a smaller number of points in their obstacle definition with which to estimate their velocity will have greater error.

4.2.3. Road Detection

Currently, accurately and reliably identifying the road bounds is a critical facet in determining system performance. The car's yaw is currently calculated by determining the slope of the road using the LiDAR sensor alone. In addition, the path-planning algorithm requires roadway input parameters in order to function properly. As of now, the algorithm determines the road bounds by identifying the location of two traffic cones, both on the same side, in order to calculate the slope intercept of the road line characterizing that side of the roadway. The other side of the roadway can be calculating by offsetting the road line by the known road width in the proper direction. This means for the road to be detected two traffic cones must be identified out of the detected obstacle array, while ensuring they are on the same side of the car.

After the point-cloud data is segmented, a set of detected obstacles exists that contains each obstacle's location as well as the width, length, and velocity components. This set of obstacles is further segmented in

order to differentiate traffic cone obstacles from other obstacles and to identify the road bounds. Once the all the traffic cones are identified in the detected obstacle list, a new list containing the road bound obstacles is created and the original list is trimmed of the road cone obstacles. The road cone obstacle list is then parsed to obtain the actual road boundaries. These boundaries are used to threatening obstacles within the roadway, whether traveling off the roadway is imminent, as well as dictating the bounds the car must stay within during an avoidance maneuver. A description of each parameter controlling the road detection algorithm is as follows:

Road Width: This parameter should reflect the actual road width of the test track and controls the offset when calculating the unknown road line.

Cone Spacing: This parameter should reflect the actual cone spacing used on the test track and controls what spacing to look for when identifying cone obstacles within the set of detected obstacles.

Spacing Buffer: This parameter controls the buffer on the detected *cone spacing* when comparing it to the expected cone spacing when differentiating between obstacles.

Area Threshold: This parameter controls the area expected to be detected by a traffic cone obstacle (from segmentation) and is used to differentiate road cones obstacles and other obstacles.

Minimum Area: This parameter controls the minimum area expected to be detected during segmentation by a traffic cone obstacle.

Area Buffer: This parameter controls the buffer on the detected area of an obstacle when comparing it to the *area threshold* for road cone identification.

Round Bound Offset: This parameter controls the inwards offset of the road lines from the detected road bounds acts as a road detection buffer.

Max Slope Change: This parameter filters out any falsely identified road bounds, which occurs when the previous slope and the new of the road bounds difference is greater than the max slope change conceivable.

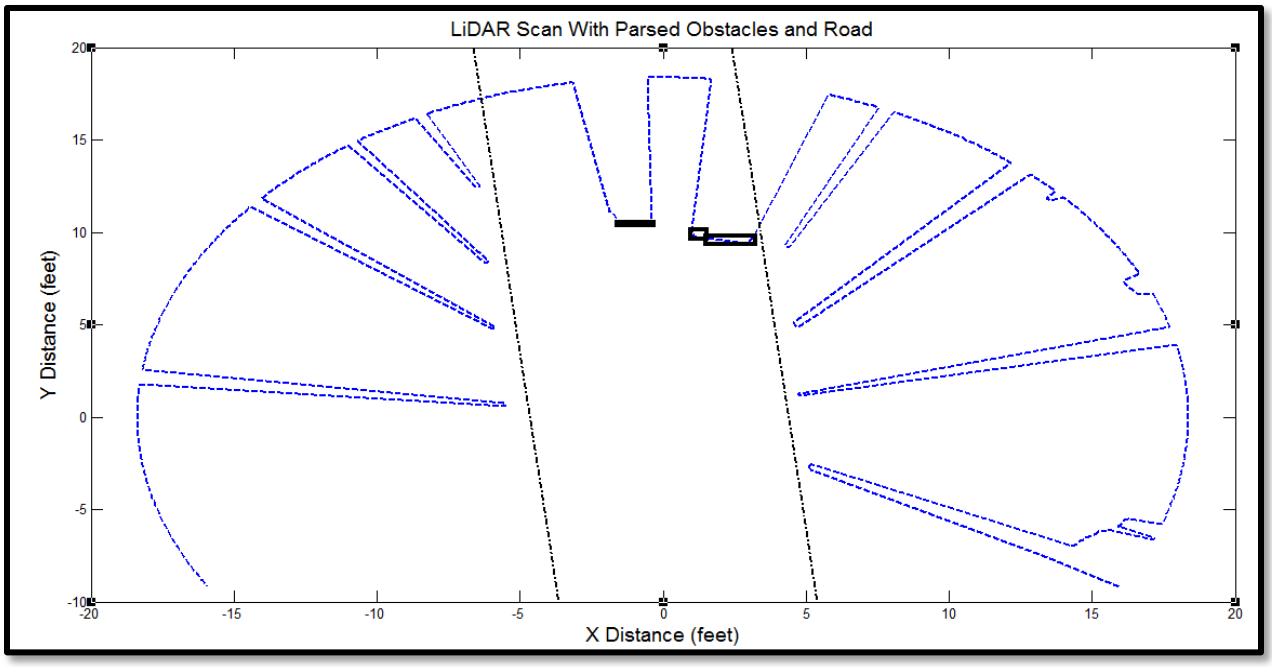

Figure 44. Road detection. Note detected obstacles within the roadway and the inwards from of road lines from the line of cones within the point-cloud.

Once the LiDAR point-cloud is segmented, the set containing the detected obstacles is further processed to parse out road cone obstacles and to identify the road roads. A first pass iterates through the set of detected obstacles and calculates the detected area, searching for areas that match the *area threshold* with respect to the *area buffer*; if there is a match the obstacle is added to a set of possible road cones for further consideration.

After the possible traffic cones are identified the spacing between each possible cone obstacle is compared to the actual *cone spacing* used on the test track. If the spacing between the possible cones matches the *cone spacing* within the *spacing buffer,* two cones are identified; each cone is added to a set containing all the identified traffic cones that define the road bounds. After all cones within the set of possible cone obstacles have been identified and added to the set of identified traffic cones, any duplicates are removed. In addition, all the detected cones are removed from the original set containing all the detected obstacles that is output after segmentation.

Once all the traffic cones have been identified, the set containing them is analyzed to calculate the road bounds and to build the array that will be passed to the path-planning algorithm. This set is iterated through until two cones can be identified on the right or left side of the car, which is done by checking whether the x coordinate has a positive or negative value. When two cones have been identified on either side, the iterations cease and the line's properties describing the road boundaries are calculated (slope, intercept). To ensure that the cones are identified on the same side of the car the detected cone spacing is once again compared to the actual *cone spacing* to check the *max slope change*. With the orientation of the road lines known, the car's yaw angle with the respect to the road is calculated. Due to the trig functions that appear in these calculations the car's yaw angle is never allowed to be zero and rather is set to infinitesimal value when

appropriate. Finally, all the detected obstacles, in the detected obstacle set, that are located outside the road bounds are removed.

If the road bounds cannot be found successfully, either because not enough cones could be identified or the road slope changed dramatically, the previous road bounds are used. When the road cannot successfully be identified a numerous times, successively the system will trigger a flag that sets the car to neutral. This acts as a stop routine for when the car reaches the end of the test track. Even if this routine is mistakenly triggered during a system maneuver there exists a chance to correct upon the next iteration when obstacles, road bounds, and the threat to the car is reevaluated. Implementing more complex solvers may also allow road detection by detecting only one cone on each side.

4.2.4. Threat Determination & User to Autonomous Toggle

Once a set of obstacles are identified that are within the road bounds, they are processed to deem if they pose a threat of an imminent collision. If any obstacle within the set is deemed to be a threat to the car, it is added to a set of threatening obstacles, which is used in the path-planning subsystem. If any threatening obstacle is detected the toggle between user and autonomous control is enabled by setting the toggle high. To determine whether each detected obstacle is to be deemed a threat or not, several parameters and strategies are implemented; however, these are not by any means exhaustive. A description of each parameter is as follows:

Minimum Speed: This parameter controls the minimum speed of the car below which no detected obstacle is deemed threatening and hence the user will remain in control. This parameter aims to prevent the system from engaging in scaled low-speed situations often encountered while driving such as in a car park.

Minimum Distance: This parameter controls the minimum distance of the car to an obstacle which within no threat is considered threatening and the reasoning mirrors that of the minimum speed parameter. Note this parameter may be disabled by setting it equal to zero.

Threshold Distance: This parameter controls the minimum distance of the car to a detected obstacle within the roadway and aids in determining if detected obstacles within the roadway are to be deemed threatening.

Threat Cone Angle: This parameter controls the angle (+/-) of a cone projected in front of the car and aids in determining if detected obstacles within the roadway are to be deemed threatening.

Previous Toggle: This parameter is always set to the previous toggle to help ensure that the system the switch back to user control occurs in a safe manner, after a maneuver has been executed.

Threat Threshold: This parameter controls the threshold value of the threat coefficient that will trigger autonomous control. The value is calculated as the inverse of the time to collision for each detected obstacle within the roadway

Allowable Distance to Road Bound & Threshold Maneuver Angle: This parameter controls the *allowable distance to the road bounds* at the *threshold maneuver angle* that will trigger autonomous control to prevent traveling off of the roadway.

After segmentation and road detection has occurred, the set of detected obstacles that are within the roadway can be processed according to these parameters to build a set of threatening obstacles to pass to the path-planning subsystem and to determine whether the car is under user-control or autonomous control. If the vehicle is not traveling at least the *minimum speed* no obstacles will be deemed threatening and the toggle will not engage the system. However, if the car exceeds the *minimum speed* the threat of each obstacle within the detected obstacle set will be determined. A detected obstacle is deemed threatening and added to the set of threatening obstacles if: it is further than the m*inimum distance,* it is within plus or minus the *threat cone angle,* and the threat coefficient is greater than the *threat threshold* or the obstacle is within the t*hreshold distance*. While an obstacle is added to the threatening obstacle set, the toggle will be triggered if not already. After all detected obstacles have been deemed a threat or not, the distance to each road bound is calculated and compared to the *allowable distance to road bounds* and the *threshold maneuver angle* to determine the danger of leaving the roadway. Outside of this loop the toggle can also be triggered independently depending on the previous toggle state to prevent giving user back control while executing an avoidance maneuver.

4.2.5. Simulation of Data Parsing and Road detection

In order to test the algorithms developed for the segmentation of the LiDAR's point-cloud data and road detection, a simulation was written in the java programming language to graphically show the results in real-time. The user can use the keyboard arrow keys to command the car to move and turn while rectangular obstacles pass by. While the user drives the car, a point-cloud of data is generated, to simulate the LiDAR sensor's data, every couple of milliseconds by casting out lines and detecting the intersection points with the rectangular obstacles. Slight noise was added to the simulated data with a pseudo-random number generator. Circular cone obstacles are drawn on the sides of the road to provide testing of the road detection algorithm. An animation loop keeps the graphics up to date providing the motion of the car and obstacles as well as the visual feedback of how well the segmentation algorithms are performing. In particular, the current and previous point-cloud is shown as well as the detected obstacles and their velocity vectors. The green circle surrounding the car represents the threshold distance, under which obstacles will be segmented and a line for each beam of the LiDAR is drawn for visualization.

This simulation not only helped to verify the algorithm while simultaneously writing the code to be implemented, but it helped to identify issues that were not foreseen and saved time when compared to testing each sub-system on the real car with actual hardware. Not to mention this helped protect the hardware from damage from the testing process. For example, initially it was believed that the difference of circle and rectangles could be detected with the LiDAR sensor and then used to identify the road boundaries. However, the LiDAR data is not ideal and even with the relatively high resolution the difference between the two shapes could not reliably be identified. This was verified by the simulation, see Figure 45 when no noise was present the two shapes could be differentiated, however, simulating a small amount of noise in the data showed this method would not work for road detection. Another observation is that the estimated velocity vectors always point radially towards or away from the car using this algorithm and

obstacles defined with smaller number of points will produce greater error in the estimations of their velocity, see Figure 45.

The java programming language was used due to the numerous data types and data handling APIs offered. In addition, Matlab and Simlink allow direct implementation and use of java objects and classes that can be packaged into Matlab S-functions. During testing, certain files written in the Matlab programming language were found to run too slowly, namely the threat determination code, and were ported to the java language; the code with the exact same function ran several orders of magnitude faster once ported. This is believed to be because Matlab is a higher level programming language with more processing overhead than java.

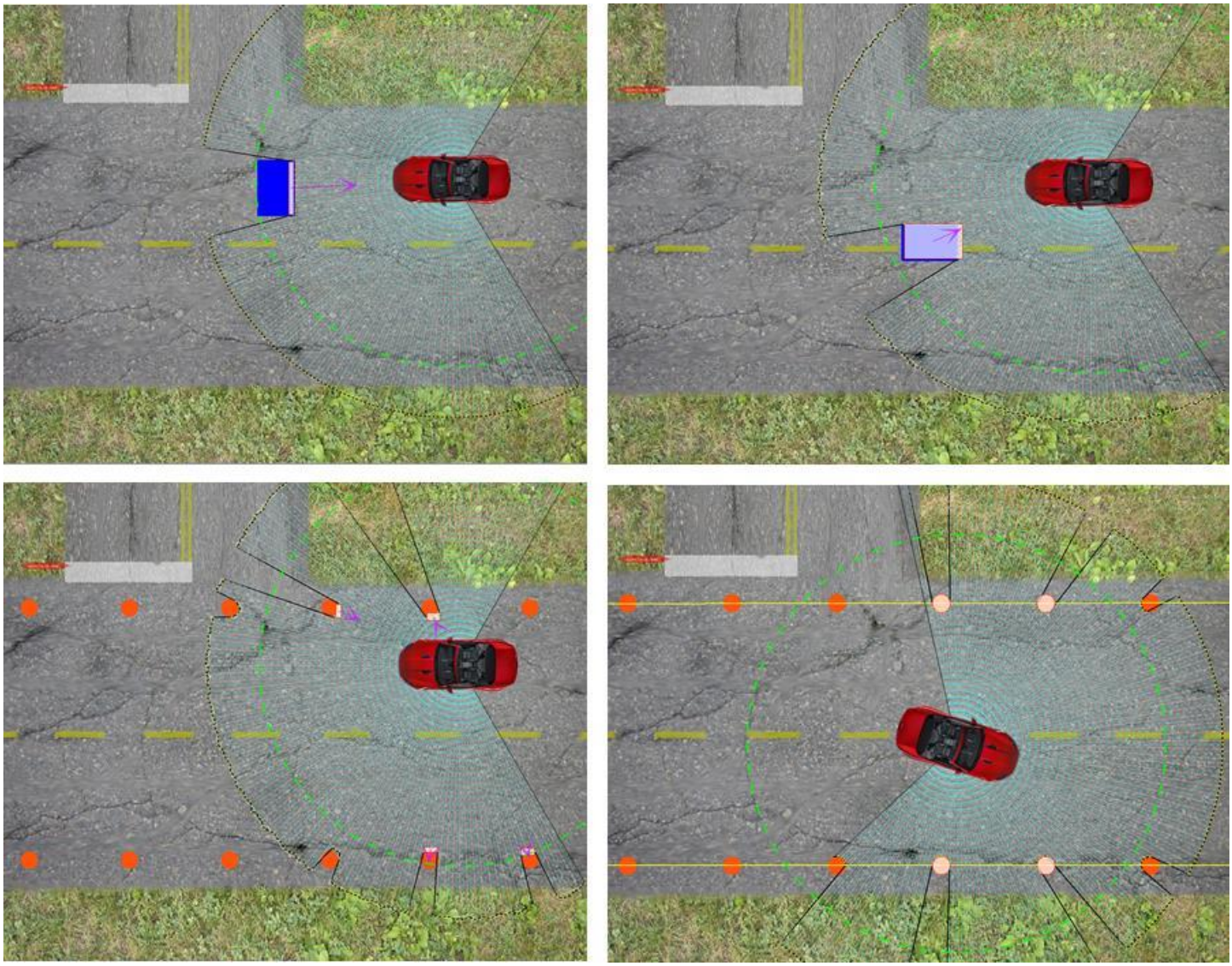

Figure 45. Segmentation simulation screen shots

4.2.6. Rapidly Exploring Random Tree (RRT)

The following section describes the overall functionality of this implementation of the RRT algorithm as well as highlighting changes from the previous group's work

4.2.6.1. Coordinate System

With the addition of the sensor, it is advantageous for the system's coordinate system to be attached to the front of the car at the LiDAR. This new coordinate system is shown in Figure 46. The LiDAR based coordinate system makes much more sense as the car doesn't need to keep track of where it is relative to a fixed global coordinate system. The car only needs to keep track of where the obstacles and road are relative to the car. A comparison between the two coordinate systems is shown in Table 5. In order to convert the system to a LiDAR based coordinate system many updates are needed to the RRT code. The largest changes stem from how the road, goal, and vehicle state are handled. The road and goal in the global coordinate system do not change as the car moves. However, with the LiDAR coordinate system these values will change as the car moves down the road. Also, with this change in coordinate system the x,y position of the car is not necessary as the car always lies at (0,0) relative to the LiDAR. Thus, with this new coordinate system the vehicle position data gathered from the IMU is not needed for path planning. The changes made to the RRT to switch from the global to LiDAR based coordinate system are outlined in more detail in the following sections.

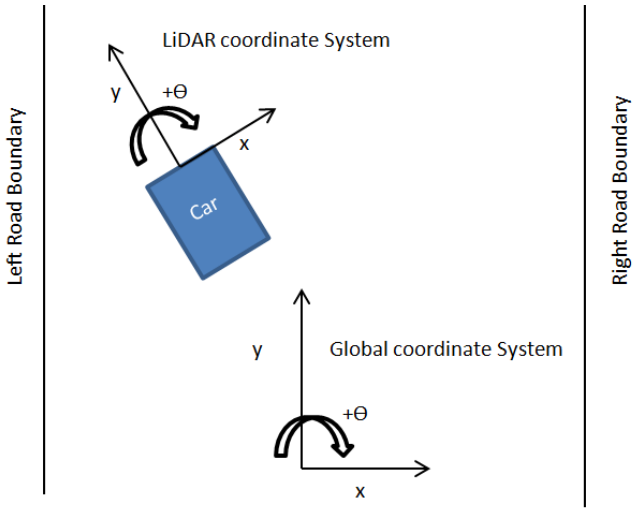

Figure 46. LiDAR and Global Coordinate System

Table 5. Coordinate Comparison

	LiDAR Coordinates	Global Coordinates
Advantages	+ Accurate Obstacle Information + Vehicle position not needed	+ Constant Road state + Constant Goal
Disadvantages	- Road detection required and critical - Variable Goal	- Inaccurate vehicle position - Obstacle state requires coordinate conversion

4.2.6.2. Road Bound Determination

The detection and use of the road is very important in the LiDAR coordinate system. By knowing where the car is relative to the road you essentially know the x-position of the car and the heading of the car. You do not however know the y- position of the car, but this is no longer necessary. The road is described in the code in two arrays. ROAD is an array with the values [xl,xr,yaw], that is the perpendicular distance to the left side of the road, perpendicular distance to the right side of the road, and the angle of the road relative to the y-axis. ROADLINES is another way of describing the road, using the format [m, bl, br], that is the slope of the road, the left road boundaries y-intercept, and the right road boundaries y-intercept respectively. The values that constitute ROAD and ROADLINES are shown in Figure 47. The segmentation code determines the road based on the detected cones and sends the RRT the ROAD variable. ROADLINES is calculated by the function GET_ROADLINES. ROAD and ROADLINES both fully define the road and are used extensively throughout the RRT.

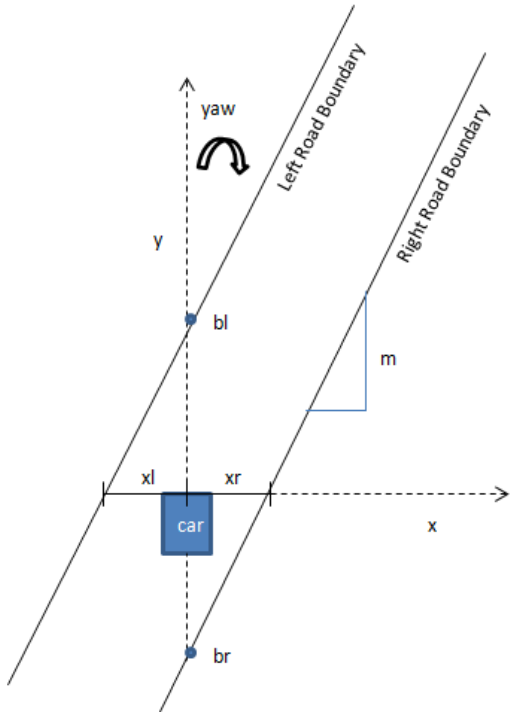

Figure 47 ROAD and ROADLINES variables

4.2.6.3. Goal Determination

In the global coordinate system defining the goal was relatively easy. The goal was just defined as a distance, Y, down the road and in the middle of the road (0,Y). With the LiDAR coordinate system the goal must be defined differently. It is still a point some distance down the road, however since the road is not always straight, the point will have an x-position other than zero. The goal is determined in the function GET_GOAL which requires ROAD and ROADLINES as inputs. The new goal is calculated by finding the equation of the line down the center of the road. Then using a user defined distance, GOAL_DIST, as the hypotenuse to a right triangle, a Y-value for the goal is determined. This value is plugged into the center line equation of the road and a X-value is found. The goal is then (X.Y). In this new method each time the RRT runs a new goal is calculated.

4.2.6.4. Select Random Node

RAND_NODE is a random node that is cast out in front of the car and is used in the path planning. The area in which this random point is cast should be within the road bounds. Thus, this new search space is in the shape of a parallelogram, see Figure 48. To find this new RAND_NODE value, a line parallel to the road, but within the road boundaries is found. Then a random point along that line is found and this becomes the coordinates of RAND_NODE. This method guarantees that RAND_NODE is within the road boundaries and is randomly found. To calculate this value, first a lower and upper limit on the y-

distance are set. This creates the top horizontal lines of a parallelogram. The road boundaries create the the other sides to the parallelogram. A random value is selected using the "rand" function in MATLAB, on the x-axis with the road bounds as the upper and lower limits. A random point is then selected on the y-axis in-between the range specified by the max and min y-values, this will be used as the Y value of RAND_NODE. Then using the random x-value as the x-intercept, a line is generated having the same slope as the road. Plugging in Y into this equation and solving for the x-value, yields the x-coordinate of RAND_NODE.

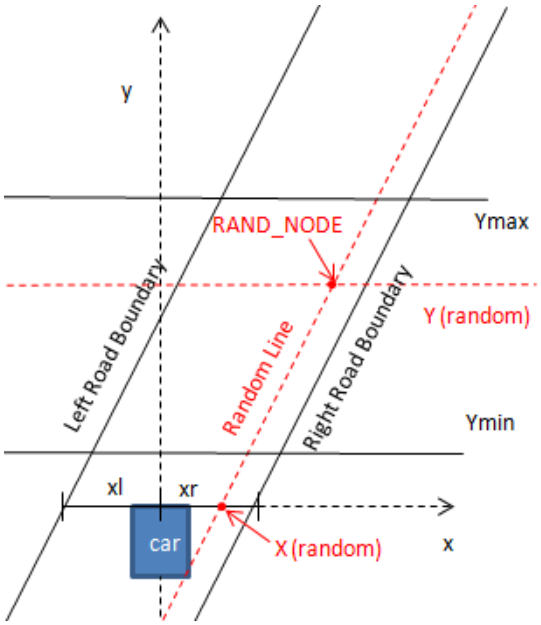

Figure 48 Geometry of RAND_NODE

4.2.6.5. Check for Collision

The CHECK_COLLSION function determines whether the RRT planned path violates the road boundaries or hits an obstacle. With variable road boundaries the code was updated such that it checks the vertices of the car against an angled road. This is accomplished by finding the y-values of the road at the x-coordinates of all the vertices of the car. These eight points are kept in the array Y_max and Y_min. Then the y-values of the vertices of the car are checked against Y_max and Y_min. If they are not between their respective Y_max and Y_min values the road bounds the NOGOGO flag is triggered and the path is terminated. A visual of the geometry is shown below in Figure 49.

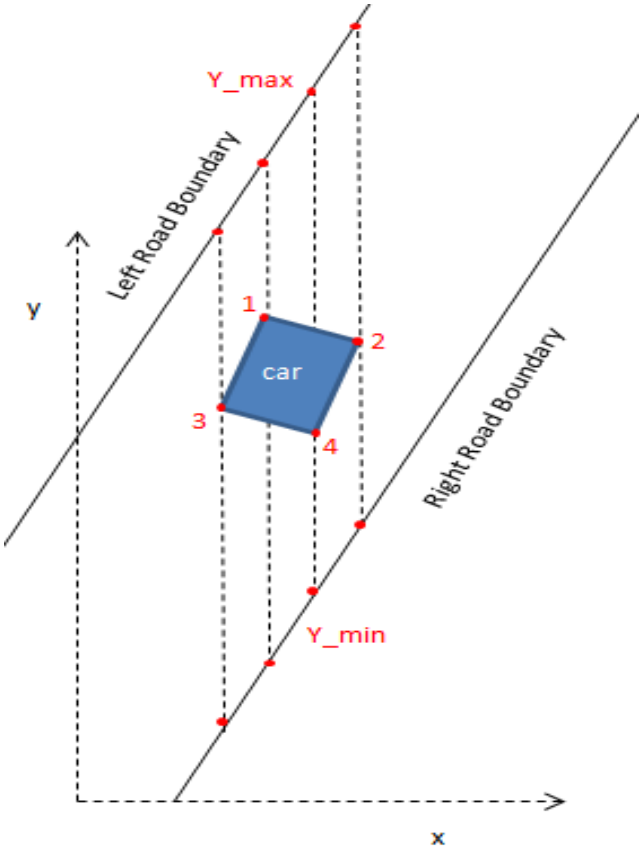

Figure 49 CHECK_COLLISION visual

4.2.6.6. Multiple Obstacle Behavior

It is also important to note that with a LiDAR sensor multiple objects can be detected. This allows for path planning around more than one obstacle. With this new feature the code needed to be updated to allow for multiple obstacle detection. A simple while loop was placed around the CHECK_COLLISION function. Allowing the code to run CHECK_COLLISION for each detected obstacle. If the planned path hits one of the obstacles then the while loop is immediately terminated and a new path is planned.

4.2.7. MPC

For a discussion of the MPC's implementation throughout this project please see "A MODEL PREDICTIVE CONTROL APPROACH TO ROLL STABILITY OF A SCALED CRASH AVOIDANCE VEHICLE" by Nikola Noxon

4.3. Cost Analysis

The following section gives a detailed description of the system cost as well as the expected costs and cost savings if implemented fleet wide.

4.3.1. System Costs

A complete bill of materials for the current system is shown below in Table 6. Most of this equipment was purchased by the previous groups that worked on the project. The items added by the Avoidtronics team are Bold. The total system cost adds up to around $3500, the majority of that being the price of the sensor at $2730.

Table 6. Bill Of Materials

Component	Qty.	Cost per Unit (USD)	Subtotal (USD)
Traxxas Slash RC Truck	1	279.00	279.00
Hokuyo LiDAR	1	2730.00	2730.00
6 DOF IMU	1	87.14	87.14
Slash Roll Cage	1	33.00	33.00
Pickit3	1	57.43	57.43
dsPIC33FJ64MC202	3	2.00	6.00
Misc. Electronic parts	1	15.00	15.00
Stripboard	1	3.00	3.00
Acrylic sheet	1	8.99	8.99
USB Breakout Board	1	22.14	22.14
RS232 Shift Register	2	18.36	36.72
Breakaway Headers	4	2.50	10.00
Telephone Wire	1	25.00	25.00
3.7 Volt Batteries	4	8.00	32.00
Miscellaneous Hardware	1	25.00	25.00
		Total	**3520.42**

4.3.2. Cost Benefit Analysis

This section presents an analysis of the expected costs and benefits of full scale, fleet wide implementation of this this technology. Much of the following analysis relies on the assumption that the cost of this technology will behave similarly to Electronic Stability Control when scaled from a prototype to mass production. All dollar values presented are in undiscounted dollars for the year 2005 and estimates of accidents prevented are for the MY 2010 vehicle fleet in the United States.

If we assume that the target market for implementation of this technology is similar to that of Electronic stability Control, i.e. passenger cars (PC) and light trucks (LTV) we can calculate the yearly cost benefit of implementing this technology as:

$$Benefit = \frac{Incremental\ Cost}{Vehicle} * Vehicles\ Produced - \frac{Damages}{Accident} * Accidents\ Prevented$$

4.3.2.1. Incremental Costs

In scaling this project to a full scale vehicle, many of the components presented in Table 6 could be integrated into existing vehicle systems. The primary cost consideration would continue to be the LiDAR sensor. If it is assumed that the same sensor were implemented in the full scale vehicle and that mass production of and advances in LiDAR technology reduce the cost of the sensor by 80% (this is a conservative assumption as the cost of an entry level LiDAR sensor has decreased by approximately 75% in the last 3 years) then the incremental cost per vehicle in the fleet would be approximately $550. The number of vehicles produced in 2011 in the United States was approximately 3 million.

4.3.2.2. Accidents Prevented

Estimates of the number and type of accidents preventable by this system are based on the "NTHSA 2010 Highway safety facts." In order to accurately assess the cost benefits of this system, the 54 million police reported accidents in 2010 must be limited to frontal collisions that could have been prevented by autonomous steering. Table 7 shows the number of crashes in 2010 by crash type.

Table 7. Crashes by first Harmful Event, Manner of Collision and Crash Severity

Crashes by First Harmful Event, Manner of Collision, and Crash Severity

	Crash Severity							
	Fatal		Injury		Property Damage Only		Total	
First Harmful Event	Number	Percent	Number	Percent	Number	Percent	Number	Percent
Collision with Motor Vehicle in Transport:								
Angle	5,624	18.6	423,000	27.4	906,000	23.6	**1,335,000**	**24.6**
Rear End	1,694	5.6	476,000	30.9	1,267,000	32.9	**1,745,000**	**32.2**
Sideswipe	858	2.8	63,000	4.1	398,000	10.3	**462,000**	**8.5**
Head On	2,848	9.4	66,000	4.3	66,000	1.7	**135,000**	**2.5**
Other/Unknown	76	0.3	2,000	0.1	22,000	0.6	**24,000**	**0.4**
Subtotal	*11,100*	*36.8*	*1,030,000*	*66.8*	*2,659,000*	*69.1*	***3,700,000***	***68.3***
Collision with Fixed Object:								
Pole/Post	1,441	4.8	49,000	3.2	121,000	3.1	**171,000**	**3.2**
Culvert/Curb/Ditch	2,485	8.2	55,000	3.6	105,000	2.7	**163,000**	**3.0**
Shrubbery/Tree	2,432	8.1	46,000	3.0	61,000	1.6	**109,000**	**2.0**
Guard Rail	972	3.2	28,000	1.8	70,000	1.8	**100,000**	**1.8**
Embankment	1,010	3.3	20,000	1.3	29,000	0.8	**50,000**	**0.9**
Bridge	214	0.7	3,000	0.2	11,000	0.3	**15,000**	**0.3**
Other/Unknown	1,644	5.4	61,000	4.0	155,000	4.0	**218,000**	**4.0**
Subtotal	*10,198*	*33.8*	*263,000*	*17.1*	*553,000*	*14.4*	***827,000***	***15.3***
Collision with Object Not Fixed:								
Parked Motor Vehicle	327	1.1	41,000	2.7	275,000	7.1	**316,000**	**5.8**
Animal	203	0.7	14,000	0.9	254,000	6.6	**268,000**	**5.0**
Pedestrian	3,936	13.0	64,000	4.2	1,000	*	**70,000**	**1.3**
Pedalcyclist	610	2.0	51,000	3.3	3,000	0.1	**55,000**	**1.0**
Train	118	0.4	*	*	1,000	*	**1,000**	*
Other/Unknown	321	1.1	10,000	0.6	46,000	1.2	**56,000**	**1.0**
Subtotal	*5,515*	*18.3*	*181,000*	*11.7*	*581,000*	*15.1*	***767,000***	***14.2***
Noncollision:								
Rollover	2,987	9.9	65,000	4.2	38,000	1.0	**106,000**	**2.0**
Other/Unknown	360	1.2	4,000	0.3	16,000	0.4	**20,000**	**0.4**
Subtotal	*3,347*	*11.1*	*69,000*	*4.5*	*54,000*	*1.4*	***126,000***	***2.3***
Total	****30,196**	**100.0**	**1,542,000**	**100.0**	**3,847,000**	**100.0**	**5,419,000**	**100.0**

*Less than 500 or less than 0.05 percent.

**Includes 36 fatal crashes with an unknown first harmful event.

Exclusion of rear end collisions, all non-collision accidents, and all "collisions with fixed objects" -as they occur most often off the roadway- yields the correct target population of accidents for all vehicles. The results of this simplification are given in Table 8

Table 8 Preventable Crashes by first Harmful Event, Manner of Collision and Crash Severity

First Harmfull Event	Crash Severity						Total	
	Fatal		Injury		Property Damage Only			
	Number	Percent	Number	Percent	Number	Percent	Number	Percent
Collision with motor vehicle in transport	9,406	63	554,000	75	1,392,000	71	1,955,406	72
Collision with object not fixed	5,515	37	181,000	25	581,000	29	767,515	28
Total	14,921	1	735,000	27	1,973,000	72	2,722,921	100

The analysis must be further limited by vehicle type to include only Passenger Cars and Light trucks.

Table 9. Vehicles involved in Crashes by vehicle type and crash severity

Vehicles Involved in Crashes by Vehicle Type and Crash Severity

Vehicle Type	Crash Severity						Total	
	Fatal		Injury		Property Damage Only			
	Number	Percent	Number	Percent	Number	Percent	Number	Percent
Passenger Car	17,718	39.6	1,579,000	56.7	3,754,000	55.7	**5,350,000**	**55.9**
Light Truck	17,428	39.0	1,053,000	37.8	2,704,000	40.1	**3,775,000**	**39.5**
Large Truck	3,484	7.8	58,000	2.1	214,000	3.2	**276,000**	**2.9**
Motorcycle	4,633	10.4	78,000	2.8	14,000	0.2	**96,000**	**1.0**
Bus	249	0.6	12,000	0.4	42,000	0.6	**54,000**	**0.6**
Other	546	1.2	5,000	0.2	9,000	0.1	**15,000**	**0.2**
Total	***44,713**	**100.0**	**2,785,000**	**100.0**	**6,737,000**	**100.0**	**9,567,000**	**100.0**

*Includes 655 vehicles of unknown type involved in fatal crashes.

Table 9 gives the vehicles involved in each crash type by vehicle type and can be used as a basis for further analysis. If we make the assumption that the percentage of passenger cars and light trucks involved in each accident type applied uniformly to the accidents presented in Table 8 we can fully develop the target population of accidents using

$$Target\ Population = Target\ Accidents * \frac{Accidents_{Passenger\ Cars} + Accidents_{Light\ Truck}}{Total\ Accidents}$$

The results of the above calculation are shown in Table 10

Table 10 Preventable Crashes by first Harmful Event, Manner of Collision and Crash Severity For Passenger cars and Light Trucks

First Harmfull Event	Crash Severity						Total	
	Fatal		Injury		Property Damage Only			
	Number	Percent	Number	Percent	Number	Percent	Number	Percent
Collision with motor vehicle in transport	7,393	63	523,530	75	1,333,536	71	1,864,459	72
Collision with object not fixed	4,335	37	171,045	25	556,598	29	731,978	28
Total	11,728	0	694,575	27	1,890,134	73	2,596,437	100

The table presented above represents a system effectiveness of 100% which is not a realistic assumption. Further analysis will be conducted with an effectiveness rate of 50%, similar to that of Electronic Stability Control.

4.3.2.3. Damages per accident

In order to fully define a monetary cost benefit for the implementation of the system it is necessary to calculate not only the savings from property damages and travel delay, but also to ascertain the financial implications of an injury or fatality. Table 11 gives the National Highway Traffic and Safety Administration's definition of the financial loss due to travel delay and property damage by MAIS injury severity.

Table 11 Financial loss due to travel delay and property damage by MAIS injury level

	Unit Cost	
MAIS	Travel Delay	Property Damage
1	$871	$4,309
2	$948	$4,432
3	$1,054	$7,622
4	$1,120	$11,023
5	$10,255	$10,589
Fatal	$10,255	$11,516
PDO**	$900	$1,664
Total		

Table 12 gives the estimated comprehensive cost savings from reducing fatalities as published by the National Highway Traffic and Safety Administration

Table 12. Calculation of Fatla Equivalents NHTSA Values

Calculation of Fatal Equivalents

Injury Severity	Comprehensive Cost (2000 $)	Comprehensive Cost* (2005 $)	Relative Fatality Ratio
MAIS 1	$10,396	$11,654	0.00311
MAIS 2	$153,157	$171,689	0.04576
MAIS 3	$306,465	$343,547	0.09156
MAIS 4	$720,747	$807,957	0.21534
MAIS 5	$2,384,403	$2,672,916	0.71241
Fatality	$3,346,966	$3,751,949	1.00000

Source: Table VIII-9 of "The Economic Impact of Motor Vehicle Crashes 2000"
* Adjusted from 2000 $ by a factor of 1.121

Due to a lack of published data it must be assumed that the accidents causing injury in Table 10 are evenly divided amongst the MAIS 1-5 injuries. This assumption could be greatly improved by finding a correlation between the number of injuries and the percentage of injuries in each MAIS severity level. On the basis of this assumption we find that, combined with the number of accidents prevented the savings due to implementation of this system is in the hundreds of billions of dollars.

Table 13 Total Savings of fleet wide system integration

		50% System Effectiveness		Distracted Drivers Only	
Accident Classification	Comprehensive Cost	Crash Type Population	Total Savings	Crash Type Population	Total Savings
MAIS 1	$ 11,654	406,320	$ 4,735,247,453	40,632	$ 473,524,745
MAIS 2	$ 171,689	90,294	$ 15,502,400,722	9,029	$ 1,550,240,072
MAIS 3	$ 343,547	60,196	$ 20,679,983,439	6,020	$ 2,067,998,344
MAIS 4	$ 807,957	30,098	$ 24,317,889,786	3,010	$ 2,431,788,979
MAIS 5	$ 2,672,916	15,049	$ 40,224,712,884	1,505	$ 4,022,471,288
Fatal	$ 3,751,949	7,222	$ 27,094,699,704	722	$ 2,709,469,970
Property Damage only	$ 2,564	1,204,000	$ 3,087,056,000	120,400	$ 308,705,600
Total	-	-	**$ 132,554,933,987**	-	**$ 13,255,493,399**
Cost Per Unit	-	-	**$ 559**	-	**$ 56**

Chapter 5. Design Verification

The following section describes the testing procedure used to validate the design as well as the results of said testing. Autonomous

5.1. Testing Procedures

To ensure the system functions suitably the specifications outlined in Table 1 must be tested. A complete test plan can be found in Appendix N. The test plan was developed to test the most important aspects of the system and to verify that the project meets the specifications that were agreed upon with the sponsor. Below is a more complete description of the tests in the test plan.

Battery Swap Time: This test will be performed to ensure that if a battery runs out of power it will be able to be replaced in a reasonable time. The tester will time how long it takes to replace all the batteries on the car. Required Equipment: stop watch

Battery Lifetime: During the ESV convention, the system may need to be running for long periods of time. It is important that the lifetime of each battery pack be known, so that appropriate replacement batteries can be purchased. The tester will run the system from fully charged and record the time it takes for the battery to completely discharge. Required Equipment: stop watch

Sensor Range: One of the important specifications of the LiDAR is its range. The range is how far away and how close the sensor can detect. The test will be performed by putting different objects at different distances away from the LiDAR and seeing which it senses and which are out of its range. Required Equipment: measuring tape.

Sensor Viewing Angle: It is essential that the LiDAR has a viewing angle of at least 54 degrees from the front of the car. This is to ensure that it sees all objects that could cause frontal collisions. To find the viewing angle objects will be placed around the sensor at different angles and a maximum viewing angle will be recorded. Required Equipment: protractor

Sensor Scan Speed: The LiDAR must have a frequency of at least 20 Hz to match the frequency of the Matlab code. This will be tested by collecting data from the LiDAR in real time then recording the frequency of the acquisition.

Detected Obstacle Size: An obstacle will be placed in the sensing range of the car. The sensor will detect the object then run the data through the code. The obstacle size that is determined from the sensor and sensor processing code will then be compared to the actual size of the object. The two areas must be within 20% of each other for a passing test. Three different obstacles with different sizes will be tested at three different locations. Required Equipment: measuring tape

Detected Obstacle Location: An obstacle will be placed 3ft and 7ft away from the car. The obstacle location will be determined from the sensor. Then the distance between the detected obstacle and actual obstacle will be

determined. This distance must be less than 2 inch at 3ft away and less than 4 inches at 7ft away. Required Equipment: measuring tape

Detected Obstacle Velocity: A moving obstacle will be placed in front of the sensor. The sensor will detect the object then run the data through the code; the code will determine the obstacles velocity. This velocity will be compared to the actual velocity which will be found by knowing the distance the obstacle travels in a certain time. Required Equipment: measuring tape, stopwatch

Maneuver Speed: The car is supposed to simulate crash avoidance at freeway type speeds. Therefore at a 1/10 scale the car should be able to perform its maneuvers at a speed of 6.81 mph, which scaled is 68.1 mph. To test this, a maneuver will be performed at the systems max speed. The tester will record the distance the car travels and the time of the maneuver to determine the maneuver speed. Required Equipment: measuring tape, stopwatch

Repeatability: With the implemented sensor the car should successfully avoid the three collision scenarios completed by the previous group. They are avoiding a stationary car, a car that starts stationary then moves away, and lastly a moving car. The car should be able to avoid collision in all three of these scenarios with a 95% success rate. Required Equipment: obstacle car, road barriers

Driver Satisfaction Survey: The purpose of this test is to quantify the public's reaction to an autonomous crash avoidance system. The test will have participants drive the car towards an imminent collision then have the car's systems take over and avoid the obstacle. A survey will be provided to the driver after the test and the driver will indicate whether they were satisfied with the technology or if it was unsatisfactory. Eighty percent of the participants must be satisfied to for a passing test and at least 30 participants must be surveyed.

Avoid Two Static Obstacles: The purpose of this test is evaluating the system behavior with multiple obstacles in the roadway. Two boxes will be placed in the roadway and the car will be driven directly at one of the boxes, activating the avoidance system. The system should be able to avoid collisions with an 80% success rate.

5.1.1. Testing Results

The results of the tests described in the Design Validation section of this report are presented below as well as pictures of the test setup and additional descriptions where applicable.

Table 14. Final Subsystem testing results

Specification	Requirement	Result	Pass
Battery Swap Time (min)	10	3	✓
Battery Lifetime (min)	50	60	✓
Sensor Range (ft)	1 - 10	.1 - 15	✓
Sensor Viewing Angle (deg)	54	240	✓
Sensor Scan Speed (Hz)	20	~35	✓
Detected Obstacle Size	±20%	±30%	X
Detected Obstacle Location	±6%	±2%	✓
Detected Obstacle Velocity	±10%	±50%	X
Maneuver Speed (ft/s)	10	10	✓

The results of the initial sub-system testing are presented in Table 14 above. The detected obstacle size and detected obstacle velocity were outside of the specifications range.

The detected obstacle size being out of range is due to the fact that with a single, 2D scanner it is impossible to estimate the size of a box oriented so that the sensor can only see a planar face of the box. If the box is oriented so that a corner and two sides can be seen the algorithm approximates the size of the obstacle within 10%. Figure 50 below shows a scan of two boxes and the detected obstacles. In this setup the two boxes were oriented so that the lidar could only see the planar surface of the boxes.

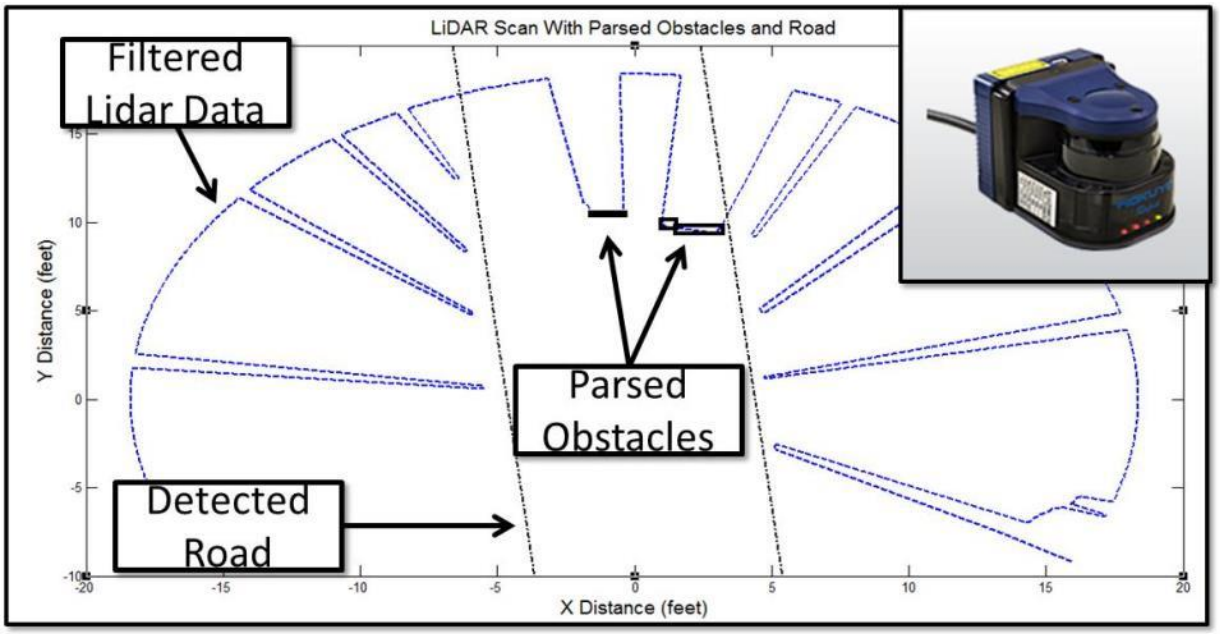

Figure 50. Lidar scan with filtered data. Obstacles and road bounds are parsed from the data

As a result the detected obstacles have a depth that is much less than the depth of the actual obstacle. Though the specification was written as the detected obstacle size, it was later determined that the important property is the detected frontal area rather than the detected size. If the algorithm accurately detects the frontal area of the obstacle it will plan a path around the obstacle. The danger of not knowing the depth of the obstacle is that the path may attempt to return to the center of the road before the end of the obstacle, causing the test vehicle to collide with the rear section of the obstacle. It was determined through testing that this was not a concern. As soon as the test vehicle starts to drive along the initial path around the front of the detected obstacle, it is no longer directly aligned with the obstacle and is able to get depth information for the next planned path. As a result the detected obstacle size being out of range does not adversely affect the system performance.

The detected Obstacle Velocity was also out of the acceptable range during testing. The algorithm being used to determine the change in position of the detected obstacle between two sequential scans was not robust enough to handle all of the possible cases of vehicle motion. Though the estimation of the vehicle velocity is simple, determining which two of the LiDAR beams to compare to each other to determine the change in distance is extremely challenging. The test vehicle during a maneuver is both rotating and translating as it scans. This means that the change in position of the obstacle is a function of the change in position of the test vehicle. The rotation of the test vehicle can be accounted for by applying a coordinate transform matrix to the distance data from the previous scan to bring it into the frame of reference of the current scan. Accounting for the translational motion of the test vehicle is much more challenging as there is no global reference of how far the test vehicle has moved between scans. As the test vehicle drives in a straight line, Objects on the left and right of the center of the test vehicle will experience "beam falloff"

where a beam that was initially on the object may fall off the edge of the object due to the forward motion of the test vehicle. This results in the object in that beam having an apparent velocity even if the object is not moving. Due to inaccurate velocity estimates it was predicted that the test vehicle would not be able to consistently avoid moving obstacles. Due to time restraints it was decided that full system testing should be conducted even though the velocity estimation was inaccurate. This effectively limits the scope of the system to static obstacles or obstacles that are moving very slowly. In the case of an obstacle that is moving very slowly the high frequency with which new paths are planned is sufficient to avoid the obstacle. Potential solutions to this problem are presented in the Future Work section of this report.

It was determined that full system testing could be conducted, even though the Detected Obstacle Size and Detected Obstacle Velocity were not within the specified ranges. The testing for the Repeatability criteria was conducted by setting up a test track and testing the system twenty times for each of the three scenarios. The same test setup was used for the driver satisfaction survey and is shown in the figure below. In the single static obstacle test, a single box was placed in the center of the test track. In the static obstacle moves away at the last second test a single obstacle was placed in the center of the road and then moved off of the road to the right when it was 5 feet from the test vehicle. In the moving obstacle test as single obstacle was driven across the road from right to left across the path of the test vehicle. The two static obstacle test was similar to the single static obstacle test with an obstacle in the center of the road, but with a second obstacle 5 ft behind and to the left of the first obstacle. The two static obstacle test and the test setup for all of the other scenarios is shown in Figure 51

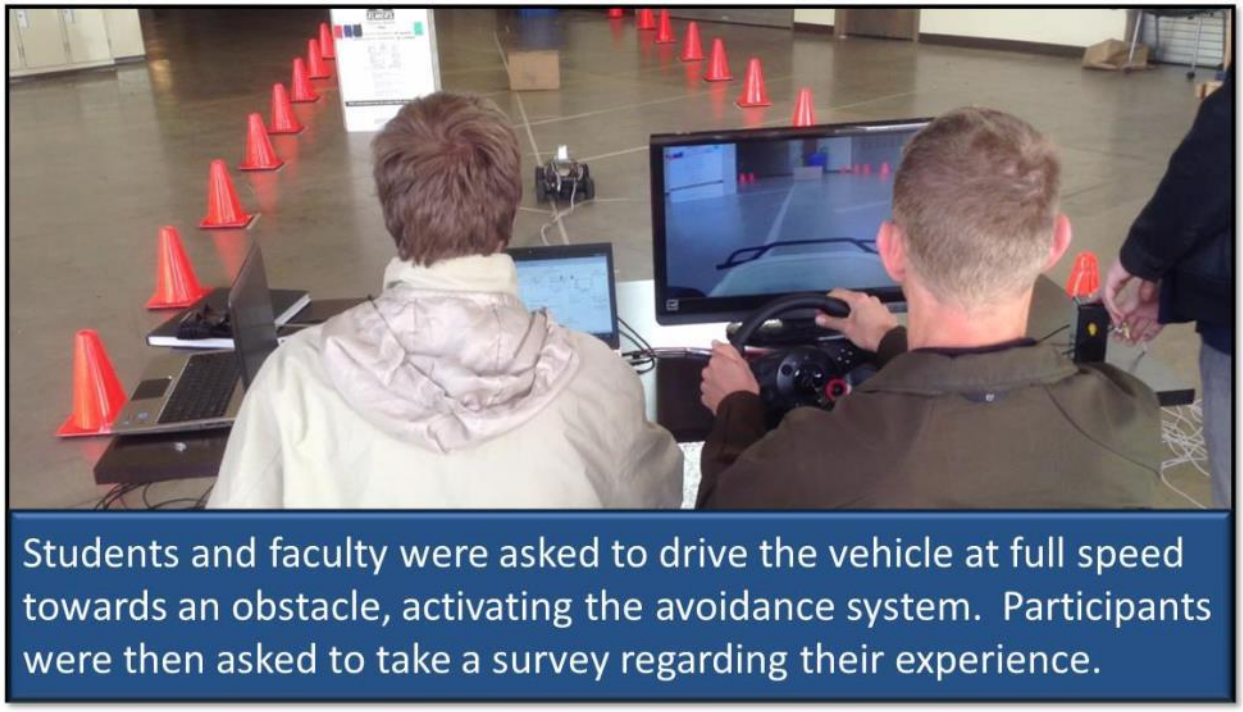

Figure 51. Experimental setup for reliability test and driver satisfaction survey

The results of the Repeatability testing are shown in Table 15.

Table 15. Results from repeatability testing as well as the two obstacle test

Test Scenario	Requirement	Result (20 Runs)	Pass
Single Static Obstacle	95%	80%	
Static Obstacle Moves Away at Last Second	95%	90%	
Moving Obstacle	95%	50%	
Two Static Obstacles	80%	95%	

The results of the full system testing did not meet the specifications set out at the onset of this project except for the system's ability to avoid two static obstacles.

The requirement for the Single Static Obstacle avoidance was set at 95% in the project specifications. During testing the system was actually able to avoid collisions in 80% of the test runs. The test setup for the single obstacle avoidance case was similar to the test setup described above, however only one obstacle was place in the center of the road. It would seem that the single obstacle test is the simplest case of all; however an analysis of the system architecture showed that this is not the case. In each of the failed runs the data from the LiDAR, the segmentation, the RRT and all other subsystems were stored and analyzed. It was discovered that the primary reason that the system failed was due to the random nature of the RRT algorithm. With the obstacle placed in the center of the road, there is the same number of viable paths on the left hand side of the obstacle as there are on the right hand side of the obstacle. This results in successive paths being planned, one to the right and one to the left. While both left and right are valid paths, the steer commands issued by the first path were counteracted by the steer commands for the second path. This resulted in the test vehicle driving almost perfectly straight down the road until a collision was unavoidable and the RRT Algorithm failed. When the RRT failed, the system continues to read the steer commands previously issued and attempts to follow the last path set out by the RRT. If the RRT failed far enough obstacle, the car would none the less avoid the obstacle. If the RRT failed too close to the obstacle, or did not fail at all, the car would continue straight towards the obstacle with perhaps one desperate maneuver at the last second.

The requirement for the Static Obstacle Moves Away at Last Second test was set at 95% in the project specifications. During testing the system was actually able to avoid collisions in 90% of the test runs. The test setup for the static obstacle moves away at last second test is identical to the single static obstacle test with the exception that the obstacle drives out of the path of the vehicle. When the test vehicle is 5 feet away from the obstacle the obstacle begins to drive off the road to the right. Surprisingly, the system was able to more consistently avoid the obstacle in this test than in the static obstacle test. A review of the data showed that when the system initially engaged these tests were subject to the same left-right toggling as the single static obstacle test. As the obstacle moved off of the road, it reduced the number of viable paths on the right side of the obstacle while increasing the number of viable paths on the left side of the obstacle. As

a result, after the first 2-3 iterations the RRT would tend to plan paths to the left of the obstacle. With multiple consecutive paths being planned to the left of the obstacle the test vehicle would more consistently avoid the obstacle. The cases where the test vehicle did not successfully avoid the obstacle were caused either by the system being unable to identify the road boundaries during a maneuver or from the RRT planning a path in the direction of the moving obstacle before failing. In the case were the system was unable to properly identify the road boundaries it was noticed that in some runs the RRT would never-the-less produce a path. This path would attempt to drive the vehicle along a road that could be 90 degrees rotated from the actual orientation of the road. As a result the RRT would produce steer commands that caused the test vehicle to drive erratically. Subsequent scans may have produced correct road boundaries and valid paths; however the interjection of near random steer commands would often cause the system to fail. Updates to the code needed to fix the issues causing erratic road behavior are discussed in the future work section of this report.

The requirement for the moving obstacle avoidance was set at 95% in the project specifications. During testing the system was actually able to avoid collisions in 50% of the test runs. After testing of the velocity estimation algorithm, it was not expected that the system would be able to avoid moving obstacles consistently. With the moving obstacle going from left to right, the system was able to avoid a collision only in situations where the first 2-3 paths were planned to the left of the vehicle. Without accurate velocity estimation, the system would plan paths into the way of the moving obstacle as often as it would plan paths away from the moving obstacle. With a system frequency of 20Hz it was anticipated that the test vehicle would be able to avoid a moving obstacle in more than 50% of the cases, however this was not the case. Updates to the code required improving the velocity estimation and therefore the ability to avoid moving obstacles is discussed in the future work section of this report.

5.1.2. Driver Satisfaction Survey

A copy of the driver satisfaction survey with the result from testing is presented in Appendix I . The result of a small selection of the questions and their interpretation are discussed in this section. It should be noted that the demographic of people who were involved in the system testing is Mechanical Engineering students and faculty at Cal Poly and my not accurately represent the opinion of the general public.

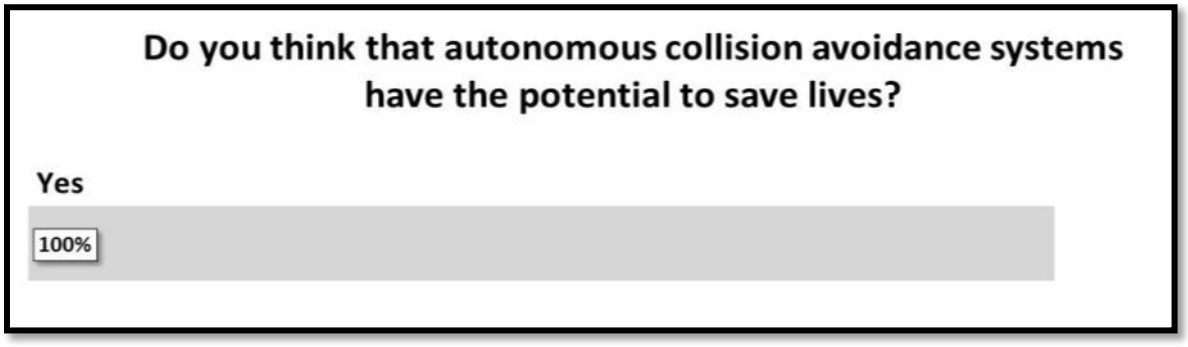

Figure 52. Question from driver satisfaction survey with results

Every participant was asked if they thought that autonomous collision avoidance systems have the potential to save lives. 100% of the people asked agreed that this technology has the potential to save lives. This indicates that when the technology is mature people will be more likely to consider it on their vehicle if they think that it could save their life someday

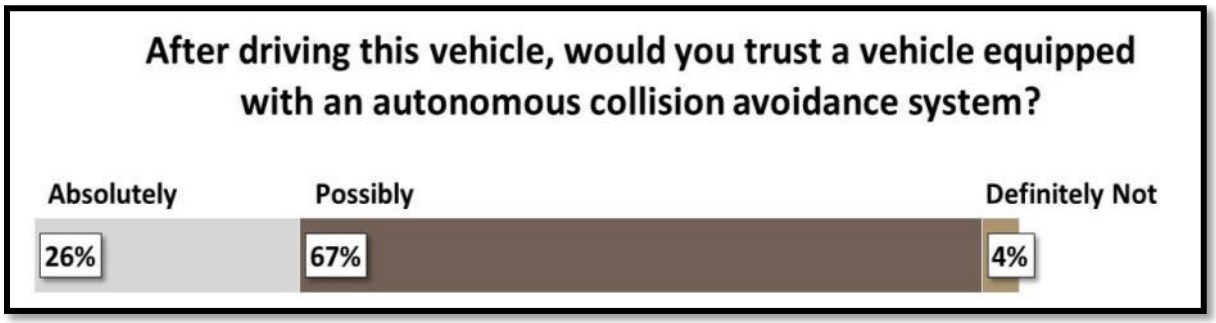

Figure 53. Question from driver satisfaction survey with results

26% of the survey participants said that they would absolutely trust a vehicle with autonomous collision avoidance technologies and 67% of the participants said that they would possibly trust this technology. This was an interesting contradiction to the fact that the majority of participants thought that the largest roadblock to implementation of this technology is driver's perceptions of the technology.

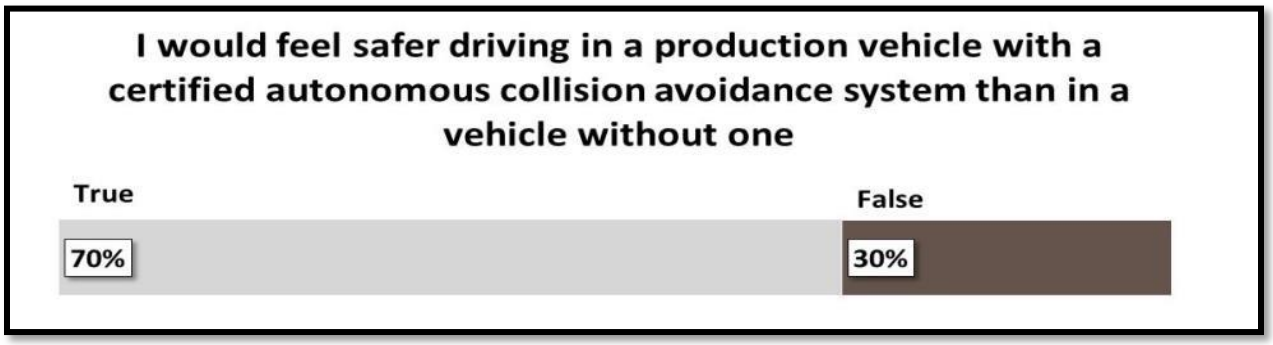

Figure 54. Question from driver satisfaction survey with results

This question shows that, for our test demographic, the overwhelming majority of the participants would feel safer driving a vehicle with an autonomous collision avoidance technology than a similar vehicle without.

It was discovered after reviewing the survey data that very few conclusions could be drawn regarding a change in perception caused by the test. The survey questions asked did not align such that a distinct change in opinion could be measured. As a result the data was used primarily as information regarding the survey participant's inclinations regarding autonomous vehicle technology in general.

Chapter 6. Conclusions and Future Work

In this section the conclusions will be presented with the future work needed to fix known issue or improve system performance.

6.1. Conclusion

After the national level presentation the team was selected to compete at the Enhanced Safety of Vehicles international student design competition in Seoul, South Korea. The team placed first at the international competition. Despite winning the international competition, the system did not perform to the specifications set up at the start of the project. Many of the major issues that led to substandard system performance have been documented and are discussed in the future work section of the report. The system was unable to avoid moving obstacle consistently due to the inaccuracies in the velocity estimation. There were also issues associated with running the RRT algorithm at a high frequency such as the system oscillating between paths to the left and then to the right of the obstacle. The LiDAR based obstacle detection and segmentation of the detected obstacles works very well and will continue to be an integral part of this project throughout further development. Issues involving the consistent detection of the road boundaries led to some system failures and will need to be improved in future iterations of the project.

6.2. Future Work/Recommendations

- *Obstacle Identification*– Implementing another sensor, using the existing camera, and or implementing a more robust algorithm, possibly utilizing edge detection or color detection, can not only allow for obstacle differentiation, which can be used to bias and more accurately determine the threat to the system improving user perception and avoiding false user to autonomous toggle while also dramatically increasing the road detection performance.

- *Update and Improve Velocity Estimation & Obstacle Tracking* – As of now the velocity vectors produced from the segmentation and tracking algorithm are always radially pointed towards or away from the vehicle. This makes them useless for path-planning, but adequate for conservative threat coefficient determination. Once this issue is addressed, the system should avoid moving obstacles significantly better.

- *Implement Camera for Road Detection* - Use of the existing camera in tandem with the LiDAR data will make road detection easier. This update alone should allow for near perfect static obstacle avoidance.

- *Optimized Path-Planning Algorithm* - Would eliminate the pitfall of the current system, which has extreme difficulty committing to a direction when faced with a sole obstacle centered in the roadway; so much so that the system often fails. This update would include checking the previously planned path and determining if a new path is needed. If the old path is still a valid path an new

path should not be planned and the test vehicle should be allowed to continue following the previously issued steer commands.

- *User To Autonomous Control Toggle* - As of now, when the system is turned on the toggle is initialized to user control. Upon detection of any threatening obstacles the system engages and the toggle turns on. Once the threat are safely avoided and passed the system toggle is set to neutral and will remain so until the system is turned off and restarted, It is trivial to have the system return to user control once the threats are safely passed, however, the test track was not long enough to justify this. In addition, the threat determination and toggle to autonomous control was sensitive during testing, but improvements are expected if obstacle road detection is improved and obstacle identification is implemented.

- *Throttle/Brake Control* - Implement throttle/brake control in the control loop in addition to steering control. This would allow for determining whether the safest maneuver is steering control, braking, or a combination of the two.

- *On-board Processing* – Doing the processing onboard will increase the frequency at which the system can operate. It will also remove the physical tether to the computer which will make the system more aesthetically pleasing

- *C Code Memory Leak* – In its current implementation the MEX code that connects to the LiDAR and collects data leaks memory. A memory leak is when memory is set aside for a variable and is never cleared. This results in Matlab bogging down the computer after 2-3 runs of the system and needing to be restarted. Updating this memory leak should help improve system performance as the machine operating the code will have more available RAM.

- *IMU Data Filtering* - Implement a Kalman filter to be able to detect the yaw of the car accurately and either use alone or compare to yaw determined from the road detected with the LiDAR sensor. It would be most beneficial, in terms of processing, accuracy, and reliability, to use the IMU for yaw determination instead of the LiDAR. This would allow the road detection using the LiDAR alone to not be as critical, which currently is a major pitfall.

- *Simulation* – Can be extended to simulate the path-planning, threat determination, and autonomous control of the actual system and may serve as a stepping stone for on-board processing. This could also save time testing the system in simulation to catch some errors that may otherwise take longer to identify running sub-system or full-system tests on the actual system. More realistic acceleration and turning algorithm could also be implemented to better simulate the car and obstacle dynamics.

Appendix A Quality Function Deployment

	Presentation Driver	Dr. Charles Birdsong	Cal Poly Graduate Students	ESV Competition	Cost ($)	Number of Sensors (#)	Horizontal Range (ft.)	Sensor (Sampling) Frequency (Hz.)	Horizontal Sensor Viewing Angle (Degrees)	Vertical Sensor Viewing Angle (Degrees)	Wireless Communication Frequency (Hz.)	Max. Manuvering Speed (mph)	Repeatability (%)	Weight (lbf)	Sensor Weight (lbf)
System Requirements															
Avoid Frontal Collisions	1	1	3	1		9	9	1	3	3		1			
Return Car to Original Course (Collision Permitting)	11	21	13	8								1	3		
f	5	4	5	5					3			1	1		
Imminent Collision Avoidance Only	12	22	19	15											
Effective Response to Mutilple Crash Senarios	13	13	18	14									3		
Emergency Braking	14	7	20	7											
Durability	15	20	7	16	3	1									
No Rollover While Executing Evasive Manuvers	2	3	6	4								3			
Human Factors															
Driver Feels In Control	6	27	21	12											
Safe	9	8	17	9								1	3		
Reliability	10	9	9	11	1	3							9		
Repeatability	7	23	8	10	1	3							9		
Miscellaneous															
Modular Design	28	14	1	22											
Well-Documented and Annotated	27	2	2	13											
Integratable System	26	15	4	21									1		
Equipment Preservation	25	17	10	20	1							1			
Presentation Requirements															
Lightweight	17	24	22	18										9	1
Shippable	18	16	23	17	1									9	1
Asthetically Pleasing (Presentation and Car)	8	6	25	2	3										
Interactive, Informative, and Fun	4	5	24	3	3										
Steering Wheel Controls	3	18	11	6	1										
Sensor Requirements															
Cost	21	19	28	28	9	3	1		1	1					
Small Size/Low Profile	19	10	27	27		3									1
Detects Objects Close and Far	22	11	14	26		1	9		3	3		1	1		
Continuously Scan and Detect Objects	23	12	15	24		3		9				1	1		
Wireless Communication	20	26	12	19				1			9				
Power Efficiency	24	28	26	25										3	1
Varied Obstacle Dectection & Avoidance	16	25	16	23		3									
Google Autonomous Cars					190000	4*	230		360		100			3200	
Mercedes Early Detection Systems						1	600					n/a			
Mercedes Pre-safe Breaking System						2**	90		80			120			
MIT Autonomous Airplane					8000	2	98	40	270			25		4.4	0.66
Microsoft Kinect Controller					100	2	2.3-20	30	57	47	30				
Target					2500	2	25	20	60	60	>20	25	99		

● = 9	Srong Correlation	*	LIDAR, Image analyzation, position sensor, radar (4), IMU, Wheel encoder
○ = 3	Medium Correlation	**	Short range and long range radar
Δ = 1	Small Correlation	***	40% braking applied/Full braking
Blank	No Correlation		

Sensor Size (in.^3)	Cost of Repairs ($)	Driver Satisfaction Index (%)	Battery Lifetime (hrs.)	Time to Collision (s)	Manuver Acceleration Limit (g's)	Collision Speed (mph)	Controlled Manuver Time (s)	Required RRT Processing Time (s)	Delta angle before and after manuever (°)	Able to port sensor code to other system (days)	Emergency shut-down time (ms)	Setup Time (mins)	Resolution (HxW)	Successful Test Scenarios	Google Autonomous Cars	Early Detection Systems	Automatic Braking System	MIT Autonomous Airplane
															5	2	2	4
							3		9						5	1	1	
								1						9	5	1	5	
		1		9				3							1	5	5	1
														9	5	1	1	3
				3		9									5	1	5	
	9														4	5	5	1
					9									3	4		5	
		9		3	1											5	4	
					1						9			3	4	4	4	4
		3												3	4	5	5	5
														9	5	5	5	5
										9								
												9						
	9											3		9				
3																		
		9										1			1	5	5	3
		9	1															
		9																
1															1	3	3	2
9															1	2	2	5
				1											5	3	3	4
															5	3	3	5
																		5
			9															4
														9	5	1	1	3
				2.6														
				1.6/0.6***	0.4	20			0									
19									0									
													640x480					
1	0	100	4	5	2	0	2	0.01	<2	2	100	10	1080x720	10				

Appendix B Specifications Sample Calculations

Horizontal Viewing Angle

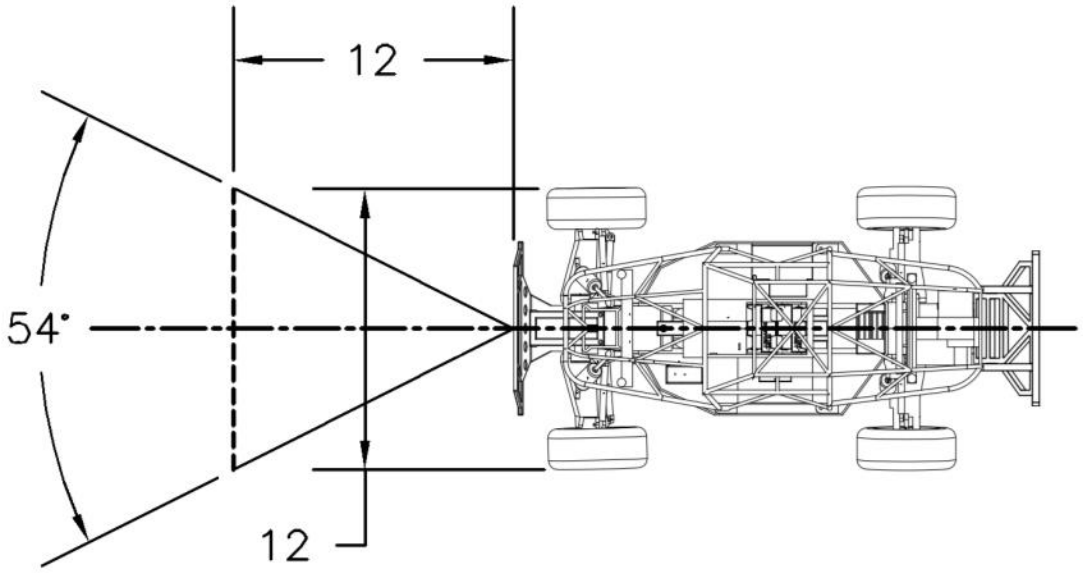

Figure 55 Required Viewing Angle for Full View of Wheel-Base 12 inches from Front Bumper

Sensor Size

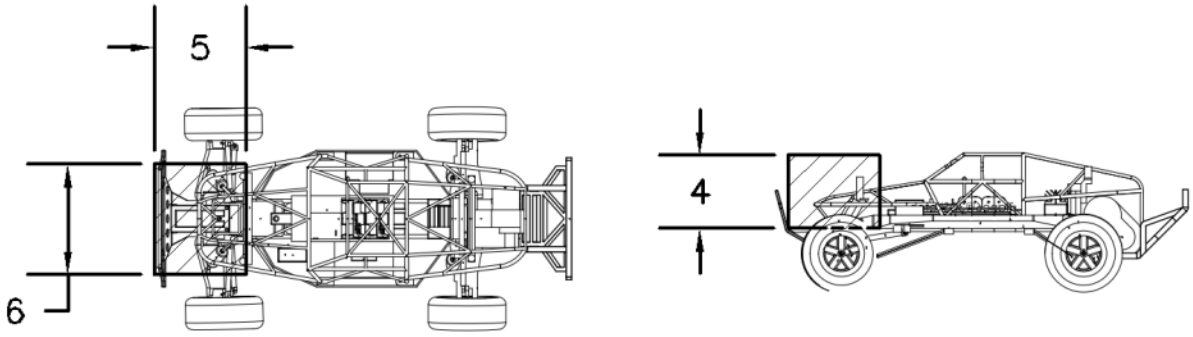

Figure 56 Sensor Size and Available Space Comparison

Appendix C Prototype Car Code

This code was used to sample and process Ultrasonic, IR, and LiDAR data during testing. The code was developed for an Arduino board.

```
// Graphing sketch


// This program takes ASCII-encoded strings
// from the serial port at 9600 baud and graphs them. It expects values in the
// range 0 to 1023, followed by a newline, or newline and carriage return

// This example code is in the public domain.

import processing.serial.*;

Serial myPort;        // The serial port
PrintWriter output;  // text file writer
int xPos = 1;         // horizontal position of the graph
long time = 0;    // program run time - timestap

void setup () {
// set the window size:
size(400, 300);

// List all the available serial ports
println(Serial.list());
// I know that the first port in the serial list on my mac
// is always my  Arduino, so I open Serial.list()[0].
// Open whatever port is the one you're using.
myPort = new Serial(this, Serial.list()[0], 9600);
// don't generate a serialEvent() unless you get a newline character:
myPort.bufferUntil('\n');
output = createWriter("sensordata.txt"); // create txt file stream
// set inital background:
background(0);
}
void draw () {
// everything happens in the serialEvent()
}

void exit() {
   output.close();
}
void serialEvent (Serial myPort) {
// get the ASCII string:
String inString = myPort.readStringUntil('\n');
if (inString != null) {
// trim off any whitespace:
inString = trim(inString);
// convert to an int and map to the
float inByte = float(inString);
time = millis();                          // get current program run-time in milliseconds
output.println(time+" "+inString);        // print data with a timestamp to a text file f
inByte = map(inByte, 0, 1024, 0, height);  // map incoming value to screen height
```

```
 // plot data in real-time for viewing during experiment
 // draw the line:
 stroke(127,34,255);
 line(xPos, height, xPos, height - inByte);

 // at the edge of the screen, go back to the beginning:
 if (xPos >= width) {
 xPos = 0;
 background(0); // clear background
 }
 else {
 // increment the horizontal position:
 xPos++;
 }
 }
 }
```

Arduino (Atmega32) Sketch

```
/*
  CarSensorData
  Reads an analog input on pin 0, converts it to voltage, and prints the result to the ser
  Attach the center pin of a potentiometer to pin A0, and the outside pins to +5V and grou

 This example code is in the public domain.
 */
#include <DistanceSRF04.h>
//Transistor controlled power enable
int Enable = 7;
//Front mounted bumper LED for photocell line marker detection"
int LED = 5;
DistanceSRF04 Dist;
// the setup routine runs once when you press reset:
void setup() {
  Serial.begin(9600);      // initialize serial communication at 9600 bits per second
  pinMode(Enable, OUTPUT); // initialize power enable pin as output
  pinMode(LED, OUTPUT);    // initialize LED pin as output
  digitalWrite(Enable, HIGH); // enable power to sensors
  digitalWrite(LED, HIGH);  // turn on LED
  Dist.begin(2,3);         // initialize ping unltrasonic sensor on digital pin 2 and 3
}

// the loop routine runs over and over again forever:
void loop() {
  int sensorValue = analogRead(A0);  // read the input on analog pin 0
  Serial.println(sensorValue);  // transmit the value over serial communication
  delay(50);  // delay for 50 ms (sample @ 20 Hz)
}
```

Appendix D Hokuyo UBG-04LX-F01 Scanning Laser Rangefinder

Date:2008.2.01

Scanning Laser Range Finder
UBG-04LX-F01
-Rapid-URG-
Specifications
CODE:U07K001

③× 1	Mistakes Correction	4	2010/05/05	Uotani	PR-5788
②× 1	Mistakes Correction	5	2007/07/30	Maeda	PR-5681
①	Revision	All	2007/01/19	Yamamoto	PR-5394
Symbol	Amended Reason	Pages	Date	Corrector	Amendment No

Approved by	Checked by	Drawn by	Designed by	Title	Scanning Laser Range Finder UBG-04LX-F01 Specifications	
MAEJIMA	MAEDA	YAMAMOTO	MAEDA	Drawing No.	C-42-3539	1/6

HOKUYO AUTOMATIC CO.,LTD.

1. General

UBG-04LX-F01 is a laser sensor for area scanning. The light source of the sensor is infrared laser of wavelength 785nm with laser class 1 safety. Scan area is 240° semicircle with maximum radius 4000mm. Pitch angle is 0.36° and sensor outputs the distance measured at every point (682 steps). Laser beam diameter is less than 20mm at 2000mm with maximum divergence 40mm at 4000mm.

Principle of distance measurement is based on calculation of the phase difference, due to which it is possible to obtain stable measurement with minimum influence from object's color and reflectance.

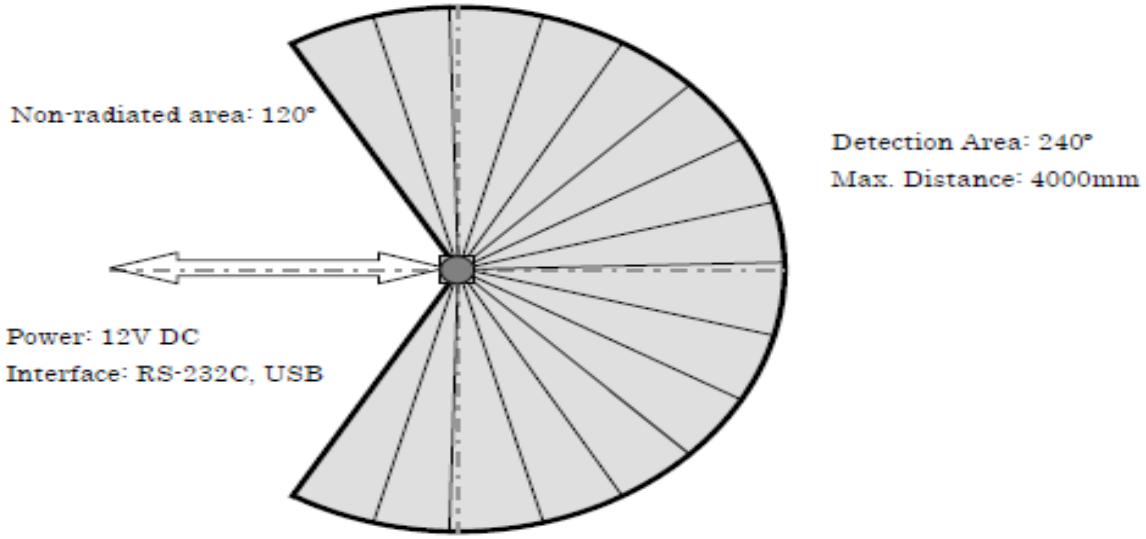

Figure 1

Note
Figure 1 shows the detectable area for white Kent sheet (80mm×80mm). Detection distance may vary with size and object.

2. Important Notice

This sensor is designed for indoor use only.
This sensor is not a safety device/tool
This sensor is not for use in military applications
Read specifications carefully before use.

3. Specifications

Product Name	**Scanning Laser Range Finder**
Model	**UBG-04LX-F01**
Light source	Semiconductor laser diode (λ =785nm), Laser safety Class 1 (FDA) Laser Power: Less than0.67mW (Class 1 is satisfied by rotating scanner)
Power source	12V DC ±10%
Current consumption	370mA or less (Rush current 700mA)
Detection Distance Standard Object	Accuracy Range: 60～4,095mm Square Kent Sheet 80mm*
Accuracy	Refer Attached Data Sheet with the Product (Nominal Range 0.06～1m : ±10mm*, 1～4m : 1% of Distance)*
Resolution	1 mm
Scan Angle	240°
Angular Resolution	0.36° (360° /1024 steps)
Scan Time	28msec/scan
Interface	RS-232C (19.2, 57.6, 115.2,500,750kbps) USB 2.0 (Full Speed) OUTPUT 2 (Synchronous, Malfunction)
Ambient (Temperature/Humidity)	- 10 ~ +50°C, 85% or less (without dew and frost)
Preservation temperature	-25 ~ +75°C
Ambient Light Resistance	10000Lx or less
Vibration Resistance	Double amplitude 1.5mm 10 ~ 55Hz, 2 hours each in X, Y and Z direction, and 98m/s² 55Hz ~ 150Hz in 2 minutes sweep, 1 hours each in X, Y and Z direction
Impact Resistance	196 m/s², 10 times each in X, Y and Z direction
Protective Structure	IP40
Insulation Resistance	10MΩ for DC 500Vmegger
Weight	Approx. 185 g (260g with 1m cable)
Case	Front Case: Polycarbonate, Back: PBT
External dimension (W×D×H)	60×60×75mm (Reference design sheet No. MC-40-3150)

*Under standard test conditions

4. Quality reference value

Operating Vibration resistance	19.6m/s², 10Hz ~ 150Hz with 2 minutes sweep, 0.5 hours each in X, Y and Z direction
Operating Impact resistance	49 m/s², 10 times each in X, Y and Z direction
Angular Speed	360 deg/s
Angular Acceleration	π/2 rad/s²
Sound level	25db or less (at 300mm)
FDA	This product complies with 21 CFR parts 1040.10 and 1040.11. (Scheduled)

5. Interface

CN1 (8 Pins)

	Lead Color	UBG-04LX-F01
1	RED	OUTPUT COM-
2	WHITE	ERR OUTPUT (Malfunction)
3	BLACK	OUTPUT (SYNCHRONOUS)
4	PURPLE	GND (9pin Dsub 5p)
5	YELLOW	RxD (9pin Dsub 3p)
6	GREEN	TxD (9pin Dsub 2p)
7	BLUE	0V
8	BROWN	DC 12V

Note
1. GND and 0V are connected inside the sensor
2. OV and OUTPUT COM- are isolated.
3. Attachment connector PHR-8 (JST Mfg. Company) is for test purpose only. Do not use it for any other purposes.

CN1 USB-mini (5 Pin)
Cable is not included. Use commercially available compatible unit.

Note:
Communication Protocol: Refer document C-42-3320B

6. Signals
1. Synchronous signal:
Output one pulse in every scan for 4msec. See the figure below for the output timing.

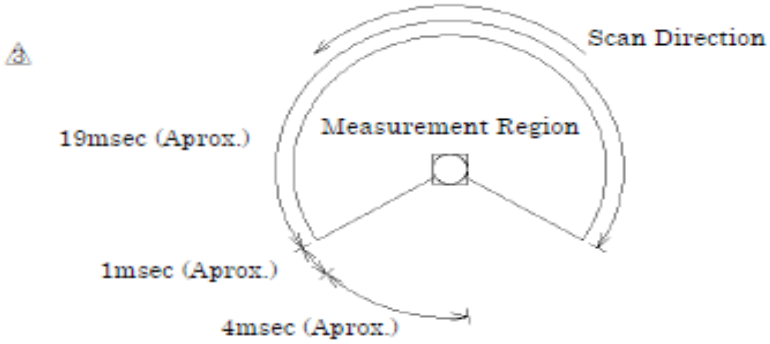

SYNC OUTPUT ON Duration

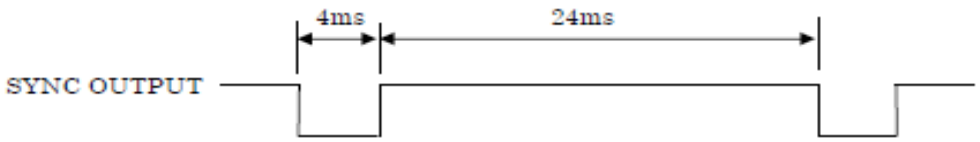

2. Error Signal:
All output signals are switched off in case of malfunction. Malfunction details can be checked with communication.

7. Output Circuit: ⚠2
Open collector output (DC 30V, 50mA Max.)

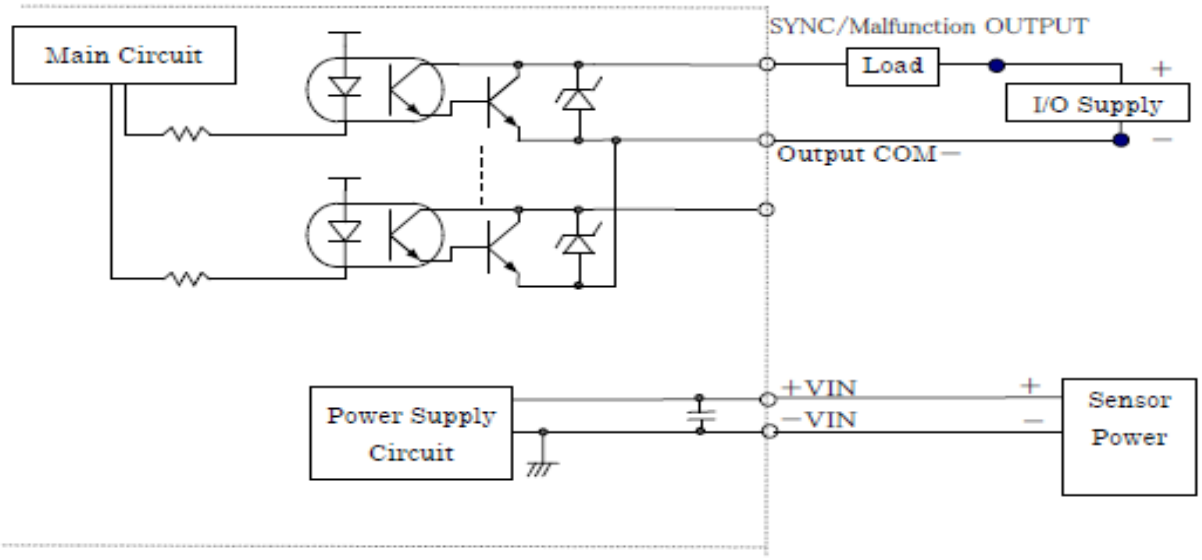

Title	UBG-04LX-F01 Specifications	Drawing No	C-42-3539	5/6

8. Notice:

- Supply voltage is DC 12Volts. Sensor will damage if high voltage is supplied.
- The maximum data step is 682points. Sensor's angular resolution is 0.3515625° (360° /1024 steps) and angular range is 239.765625° ((682-1)×360/1024)
- Angular range and resolution can be specified form the host. Read communication protocol specification for details.
- Sensor scans anticlockwise from top view.
- When RS232S connection is used, communication may not establish due to circuit or host incompatibility if baud rate is setting is more than 500Kbps.
- USB driver is communication device class (CDC) supported by standard operating system. The device is connected as a RS232C port with the same utility.

9. Firmware Update History

Firmware Version	Details

Appendix E CMOS Camera Module Color Camera Spec Sheet

Product Specification

CUSTOMER'S APPROVAL

COMPANY _____

SIGNATURE _____

DATE _____

This product specification is subject to change without noice.
Please return one copy with your signature on this page for approval.

Product Specification

1. SPECIFICATION

Model	32KM NTSC	32KM PAL
Image device	1/3" PIXEL CMOS SENSOR PC1089K	
TV Type	NTSC	PAL
Effective Pixels	728(H) x 488(V) 380K	
Cell Size	6.35㎛(H) x 7.40㎛(V)	
Horizontal Resolution	More than 520 TV Lines	
Sync. Type	Internal	
Scanning System	2:1 Interlace 2:1 Interlace	
Scanning System	15.735KHz	15.625KHz
Scanning Frequency (H)		
Scanning Frequency (V)	60Hz	50Hz
Video Output	1.0 vp-p Composite (75Ω)	
Gamma Correction	0.45 typ.	
Sensitivity	0.2 Lux @ F2.0	
S/N Ratio	More than 42Db (AGC OFF)	
Gain Control Gain Control	Automatic Automatic	
Electronic Shutter	1/60 ~ 1/100,000sec Auto	1/50 ~ 1/100,000sec Auto
Power Supply	Regulated DC12.0V (6V ~ 20V)	
Consumption Current	Max 50mA	
Reverse Polarity	Yes	
Lens Mount	Fixed Lens Mount	
Operation Temp	10 50℃ (H idit 10%RH 60%RH) -10 ~ 50℃ (Humidity: 10%RH ~ 60% RH)	
Operation Temp	-20 ~ 70℃ (Humidity: 10% RH ~ 60%RH)	
Preservation Temp	32mm(H) x 32mm(W)	
Dimensions		
Weight	Approx. 26g	
Lens Options	Board	
	Pinhole	
	Varifocal	f=3.6(Standard) / 2.2 / 2.9 /

RoHS	Varifocal Compliant	4.3 / 6 / 8 / 12mm Flat/Cone Pinhole: f=3.7(Standard) / 2.8 / 4.3mm
	Varifocal Compliant	Manual Varifocal: 4~8mm, 28~12mm
	Varifocal Compliant	Manual Varifocal: 4~8mm, 28~12mm

Product Specification

2. DIMENSION (mm)

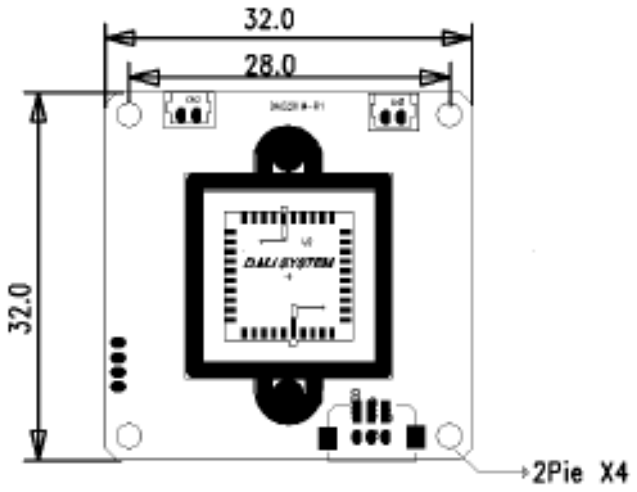

Product Specification

3. INTERFACE SPECIFICATION

3.1) Picture Status

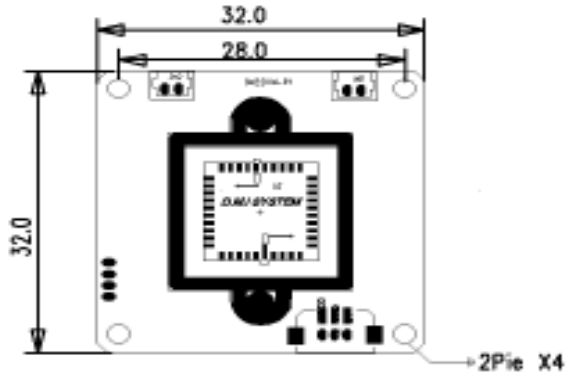

3.2) I/O CONNECTOR FUNCTION

DC12.0V (RED)	DC POWER INPUT(DC12V)
GND(BLACK)	GROUND
VIDEO OUT(YELLOW)	VIDEO SIGNAL OUTPU

3.3) I/O Harness

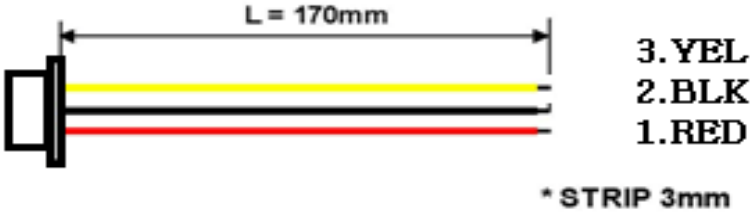

Appendix F LM 2592HV SIMPLE SWITCHER specification Sheet

For a complete specification sheet please see the Manufacturer site or the Dropbox/Data Sheets

National Semiconductor

August 2001

LM2592HV
SIMPLE SWITCHER®Power Converter 150 kHz 2A Step-Down Voltage Regulator

General Description

The LM2592HV series of regulators are monolithic integrated circuits that provide all the active functions for a step-down (buck) switching regulator, capable of driving a 2A load with excellent line and load regulation. These devices are available in fixed output voltages of 3.3V, 5V, and an adjustable output version.

This series of switching regulators is similar to the LM2593HV, but without some of the supervisory and performance features of the latter.

Requiring a minimum number of external components, these regulators are simple to use and include internal frequency compensation†, improved line and load specifications and a fixed-frequency oscillator.

The LM2592HV operates at a switching frequency of 150 kHz thus allowing smaller sized filter components than what would be needed with lower frequency switching regulators. Available in a standard 5-lead TO-220 package with several different lead bend options, and a 5-lead TO-263 Surface mount package.

Other features include a guaranteed ±4% tolerance on output voltage under all conditions of input voltage and output load conditions, and ±15% on the oscillator frequency. External shutdown is included, featuring typically 90 µA standby current. Self protection features include a two stage current limit for the output switch and an over temperature shutdown for complete protection under fault conditions.

Features

- 3.3V, 5V, and adjustable output versions
- Adjustable version output voltage range, 1.2V to 57V ±4% max over line and load conditions
- Guaranteed 2A output load current
- Available in 5-pin TO-220 and TO-263 (surface mount) Package
- Input voltage range up to 60V
- 150 kHz fixed frequency internal oscillator
- On/Off control
- Low power standby mode, I_Q typically 90 µA
- High Efficiency
- Thermal shutdown and current limit protection

Applications

- Simple high-efficiency step-down (buck) regulator
- Efficient pre-regulator for linear regulators
- On-card switching regulators
- Positive to Negative converter

Note: † Patent Number 5,382,918.

Typical Application (Fixed Output Voltage Versions)

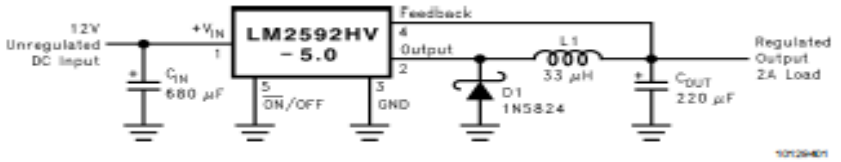

SIMPLE SWITCHER® and Switchers Made Simple® are registered trademarks of National Semiconductor Corporation.

 DS101294 www.national.com

LM2592HV SIMPLE SWITCHER Power Converter 150 kHz 2A Step-Down Voltage Regulator

Appendix G Gannt Chart

See Dropbox/Administrative/Schedule

Appendix H ATMEL ATtiny 13A Micro controller specification sheet

For Complete Data Sheet please see Dropbox/Data Sheets

Features

- High Performance, Low Power AVR® 8-Bit Microcontroller
- Advanced RISC Architecture
  - 120 Powerful Instructions – Most Single Clock Cycle Execution
  - 32 x 8 General Purpose Working Registers
  - Fully Static Operation
  - Up to 20 MIPS Througput at 20 MHz
- High Endurance Non-volatile Memory segments
  - 1K Bytes of In-System Self-programmable Flash program memory
  - 64 Bytes EEPROM
  - 64 Bytes Internal SRAM
  - Write/Erase Cycles: 10,000 Flash/100,000 EEPROM
  - Data retention: 20 Years at 85°C/100 Years at 25°C (see page 6)
  - Programming Lock for Self-Programming Flash & EEPROM Data Security
- Peripheral Features
  - One 8-bit Timer/Counter with Prescaler and Two PWM Channels
  - 4-channel, 10-bit ADC with Internal Voltage Reference
  - Programmable Watchdog Timer with Separate On-chip Oscillator
  - On-chip Analog Comparator
- Special Microcontroller Features
  - debugWIRE On-chip Debug System
  - In-System Programmable via SPI Port
  - External and Internal Interrupt Sources
  - Low Power Idle, ADC Noise Reduction, and Power-down Modes
  - Enhanced Power-on Reset Circuit
  - Programmable Brown-out Detection Circuit with Software Disable Function
  - Internal Calibrated Oscillator
- I/O and Packages
  - 8-pin PDIP/SOIC: Six Programmable I/O Lines
  - 10-pad MLF: Six Programmable I/O Lines
  - 20-pad MLF: Six Programmable I/O Lines
- Operating Voltage:
  - 1.8 – 5.5V
- Speed Grade:
  - 0 – 4 MHz @ 1.8 – 5.5V
  - 0 – 10 MHz @ 2.7 – 5.5V
  - 0 – 20 MHz @ 4.5 – 5.5V
- Industrial Temperature Range
- Low Power Consumption
  - Active Mode:
    - 190 µA at 1.8 V and 1 MHz
  - Idle Mode:
    - 24 µA at 1.8 V and 1 MHz

ATMEL

8-bit AVR® Microcontroller with 1K Bytes In-System Programmable Flash

ATtiny13A

Summary

Rev. 8126FS–AVR–05/12

Appendix I Driver satisfaction survey and results

Thank you for participating in the Autonomous Vehicle Technology Survey being conducted by California Polytechnic State University's Advanced Vehicle Collision Avoidance team. The survey is a combination of multiple-choice and short-answer questions and takes approximately 10-15 minutes to complete.

Definition of Autonomous Vehicle:
For the purposes of this survey, we define an autonomous vehicle as one that can self-navigate and pilot without human intervention using advanced technologies such as sensors, actuators, vehicle-to-vehicle and vehicle-to-infrastructure communication, etc. We also recognize that autonomy may come in varying degrees, from selective use (e.g., parking assist) to continuous autonomous operation.

---

1. In your view, how soon will fully autonomous vehicles be capable of reliable operation on public streets?
   a. The technology is ready now (11%)
   b. Less than 5 years (19%)
   c. In 5 to 10 years (22%)
   d. In 10 to 25 years (37%)
   e. More than 25 years (7%)
   f. Never (4%)

2. Do you think that autonomous collision avoidance systems have the potential to save lives?
   a. Yes (100%)
   b. No (0%)

3. Would you trust a production vehicle equipped with an autonomous collision avoidance system?
   a. Absolutely (26%)
   b. Marginally (67%)
   c. Definitely not (7%)
   (please explain) _____

4. Would you consider purchasing a vehicle with a certified autonomous collision avoidance system?
   a. Definitely would (22%)
   b. Probably would (52%)
   c. Definitely would not (11%)
   d. Depends (please explain)_____(15%)_____

5. I would feel safer driving in a production vehicle with a certified autonomous collision avoidance system than in a vehicle without one.
   a. True (70%)
   b. False (30%)

6. In your opinion, how much would a consumer buying a luxury vehicle be willing to pay for an autonomous collision avoidance system?
    a. Less than $500 (0%)
    b. Between $500 and $1000 (0%)
    c. Between $1000 and $2000 (37%)
    d. More than $2000 (59%)
    e. No one would ever buy it (0%)

7. Would you be more likely to buy a vehicle with an autonomous collision avoidance system if the initial cost was offset by savings on your insurance rates?
    a. Yes (78%)
    b. No (0%)
    c. Maybe (22%)

8. Which of the following would most likely make you think that a vehicle with an autonomous collision avoidance system is safer than a vehicle without one?
    a. Acceptance and implementation by a large car manufacturer (15%)
    b. Certification by the National Traffic Highway and Safety Administration (26%)
    c. A live demonstration of the technology (33%)
    d. A recommendation from a friend (0%)
    e. I already think that these vehicles are safer (11%)
    f. Other(Please explain) _____ (0%)

9. Do you think people would drive more recklessly if their vehicle had a collision avoidance system?
    a. Definitely (22%)
    b. Probably (19%)
    c. Possibly (37%)
    d. Unlikely (22%)
    e. No (0%)

10. While driving on the freeway a driver initiates a lane change into an unsafe situation where they may or may not have been able to avoid a collision. During the lane change their Certified autonomous collision avoidance system activates and steers them out of the unsafe situation, but during the maneuver side-swipes a nearby vehicle. Who should be liable for the property damage?

    (select all that apply)
    a. The vehicle manufacturer (4%)
    b. The supplier that provided the component hardware or software (11%)
    c. The driver (30%)
    d. federal government (0%)
    e. The entity that certified the vehicle for autonomous driving mode (if one exists) (4%)
    f. The driver's insurance (7%)
    g. Other (please specify)_____

STOP Do not complete this until after the demonstration

1. Did the car avoid the obstacles?
    a. Yes (95%)
    b. No (5%)

2. During the avoidance maneuver did you feel: (select all that apply)
    a. Surprised (37%)
    b. Comfortable (4%)
    c. Scared (0%)
    d. Confused (11%)
    e. Relieved (7%)
    f. No Feeling (4%)
    g. Other (please explain) _ _____(7%)_____

3. After driving this vehicle you _____ purchase a vehicle with autonomous technology (as compared during the first portion of the survey)
    a. Definitely would (15%)
    b. Probably would (48%)
    c. Probably would not (11%)
    d. Depends (Please explain)_____(19%)_____

4. Do you think that autonomous collision avoidance systems have the potential to save lives?
    a. Yes (100%)
    b. No (0%)

5. After driving this vehicle, would you trust a vehicle equipped with an autonomous collision avoidance system?
    a. Absolutely (26%)
    b. Marginally (67%)
    c. Definitely not (4%)
    (please explain)_____

6. After driving this vehicle, how comfortable would you feel riding in a vehicle with an autonomous collision avoidance system?
    a. Very Comfortable (19%)
    b. Comfortable (63%)
    c. Not Comfortable (15%)
    d. I would never ride in one of these vehicles (0%)

7. Do you think a fully autonomous vehicles will ever be safer and more reliable than human drivers? If so by what year.
    a. Yes (15%)
    b. No (30%)
    Year_____ (2030 average)

8. What do you think the biggest hurdle car manufacturer's face in trying to create and implement autonomous vehicles?
    a. Consumer perceptions/bias (30%)
    b. Technological capabilities (4%)
    c. Financial reasons (15%)
    d. Government regulations (0%)
    e. Liability issues (22%)
    f. Other (Please Explain) _____

9. Imagine you are a CEO of a large car manufacturer how much of your R&D budget would you allocate towards autonomous vehicle systems?
    a. <5% (15%)
    b. 5-10% (48%)
    c. 10-25% (30%)
    d. 25-40% (4%)
    e. >40% (0%)

10. What improvements could be made to the system you drove today to make the experience more enjoyable:

Appendix J GD_Scan code (abbreviated)

For a complete version of the code please see dropbox/Working System/URG

```
  \example md_scan.c

  \brief Sample of MD scan

  Get the distance data of specified number of times using MD command.

  \author Satofumi KAMIMURA

  $Id: md_scan.c 1989 2012-05-18 00:32:36Z satofumi $
*/
#include "urg_ctrl.h"
#include <stdio.h>
#include <stdlib.h>
#include <assert.h>
#include <math.h>
#include "mex.h"

struct coords {
    double* yptr;
    double* xptr;
};

/* declared global to allow for the use of the mexmakepersistant command*/
static urg_t *URG_ptr = NULL;

void exitFcn()
{
  if (URG_ptr != NULL)
    urg_laserOff(URG_ptr);
    urg_disconnect(URG_ptr);
       mxFree(URG_ptr);}

/* Handles exiting in case of an error state while connecting */
static void urg_exit(urg_t *urg, const char *message)
{
  printf("%s: %s\n", message, urg_error(urg));
  urg_disconnect(urg);
  free(URG_ptr);

#ifdef MSC
  getchar();
#endif
  exit(1);}

/* Start of the initialization routine, Urg data structure is stored for
 *later calls to the function*/
void main(void)
{
  enum {
    CaptureTimes = 1,
  };

  /* Define COM port, should be dynamic in future development */
  const char device[] = "COM12"; /* For Windows */
```

Appendix K Java Segmentation Code (abbreviated)

For a complete version of the code please see dropbox/Working System/LiDar processing Class

```
import java.util.ArrayList;                                          // Import data collection
handling library for datatype arraylist
import java.util.*;                                                        // Import data
collection handling library for datatype hashset
import static java.lang.Math.*;                                      // Import library for
common math functions

public class ClusterMethodWithFinal {
       // Global Variable Initialization
       private ArrayList<double[]> AllObstacles = new ArrayList<double[]>();       // Store all
current obstacles
       private ArrayList<double[]> ThreateningObstacles = new ArrayList<double[]>();      //
Store all current threatening obstacles
       private ArrayList<double[]> Obstacle = new ArrayList<double[]>();           // Discrete
group obstacle constructor
       private ArrayList<double[]> VelocityObstacleChk = new ArrayList<double[]>();
       private ArrayList<double[]> RoadPts = new ArrayList<double[]>();            // Road
bounds
       private ArrayList<Integer> PossibleRoadPts = new ArrayList<Integer>();      // Possible
road bound indexes from detected obstacles
       private ArrayList<Integer> toRemove = new ArrayList<Integer>();                    //
Remove identified road bounds from detected obstacles
       private int   Threshold = 50;                                               // Threshold
distance value in feet (Obstacles and road boundaries determined within this range)

       // Note: can rewrite to identify and determine road boundaries even outside of this
threshold (max sensor range)
       private int   maxNumPts = 10;                                               // Max points
allowed for point clustering when forming discrete groups representative of obstacles and
boundaries
       private double      MaxVelocity = 10.0;                                     // Twice the
max anticipated velocity in ft/s (relative terms - max velocity possible)
       private double      ScalingFactor = 1;                                      // Scaling
factor, % (Buffer)
       private double      angularRes_rad = 0.36*(PI/180);                 // LiDAR sensor's
angular resolution in radians
       private int   beamnumber = 726;                                     // Default value -
set dynamically to the length of the point-cloud array (below)
       private double      areamin = 0.001;                                        // Cone area
min. for road detection
       private int         noRoadCount = 0;                                        // Current #
of successive no road bounds
       private boolean noRoadFlag = false;                                         // Current no
road bound flag -  set ea. iteration
       private double[] roadBounds = {0,0,0,0,0,0};                 // Road bounds [-
d_l,d_r,yaw,m,b_l,b_r]
       private double[] prevRoadBounds = {0,0,0,0,0,0};       // Previous road bounds [-
d_l,d_r,yaw,m,b_l,b_r]
       private double      prevRoadSlope= 0;                                       // Previous
slope of road bounds
       private double      deltaYaw = 0;                                           // Change in
yaw (determines if car has turned)
```

Appendix L RUN_RRT code (abbreviated)

For a complete version of the code please see dropbox/Working System/RRT

```
function FINAL_PATH = RUN_RRT(VEHICLE, OBSTACLE_ARRAY, ROAD)

%BEGINNING OF SIMULINK BLOCK*******************************

TEMP_NODE= zeros(3);     %[x,y,cn]
TREE=zeros(500, 3);     %[x,y,cn]
ROUTE_TREE=zeros(400,2);%[x,y]
PATH=zeros(50,5);       %[x,y,theta,delta,t,r]
NODE_DIST=5;
DONE=0;
NODES=1;
RAND_GO=0;
TREE=zeros(500,3);
FINAL_TREE=zeros(20,2);
%EC: Don't need this TREE(1,1:2)=VEHICLE(1:2);
%EC: Don't need this TREE(1,3)=0;
FAIL=0;
ITERATIONS=0;
VEHICLE_GEO_ACTUAL = [22/12 1];
BUFFER = .5;
VEHICLE_GEO=VEHICLE_GEO_ACTUAL+BUFFER; %[length,width]
FINAL_PATH=zeros(50,5); %arbitrary size

%Trimming Function
index = find(OBSTACLE_ARRAY(:,1),1,'last'); % Find the first 0 in array
OBSTACLE_ARRAY = OBSTACLE_ARRAY(1:index+1,:); % Trim array to that index
SIZE=size(OBSTACLE_ARRAY); %OBSTACLE array size
ONumber = SIZE(1); %Number of Obstacles

% no road detected
if ~any(ROAD)
    FAIL = 1;
end

% Road aligned along car axis
 if ROAD(3) == 0
    ROAD(3) = 0.00000001;
 end

%GET LINES OF ROAD BOUNDARIES
ROADLINES = GET_ROADLINES(ROAD);  %ROADLINES = [slope,left y-intercept, right y-
intercept]

%GET GOAL
GOAL = GET_GOAL(ROAD,ROADLINES);



while (DONE==0 && FAIL==0)
    NOGOGO=0;
    %ADD A TEMPORARY NODE TO [TREE]
```

Appendix M System Operation Manual

Setting up The System

Setting up the Software

Computer with Matlab 2010b or higher

Microsoft Visual C++ Redistributable 2008 or higher with Windows SDK 6.1

a. Windows SDK 7.1

- OR

b. Microsoft Visual C++ Redistributable 2008 or higher with Windows SDK 6.1

- AND

c. Install the latest java runtime environment (JRE), however, it is recommended that you install the latest java development kit (JDK) should you need to update the segmentation code and recompile it. See oracle's website for more details.

    - http://www.oracle.com/technetwork/java/javase/downloads/index.html

The exact software required depends on which version of MATLAB you have, and if you are running a 32bit or 64bit computer. You must set the MATLAB compiler to C++ using the MATLAB command "mex –setup". Select the C++ 2008 or 2010 compiler form the list of available options. See the following for more details:

http://www.mathworks.com/support/compilers/R2012a/win64.html
http://www.mathworks.com/help/techdoc/ref/mex.html

To run the RSC/RRT program, see the "MATLAB Documentation for Roll Stability Control" in the MATLAB sub-folder.

Onboard Control Unit Programming

The following is required to program the onboard control unit

1. Onboard control unit
2. PICkit3 with USB cable

3. MPLAB IDE

MPLAB IDE can be found for free on their website at:

http://www.microchip.com/stellent/idcplg?IdcService=SS_GET_PAGE&nodeId=1406&dDocName=en019469&part=SW007002

To program using the PICKit3, see the following documentation:

http://www.sparkfun.com/datasheets/Programmers/PICkit_3_User_Guide_51795A.pdf

There are three folders containing the full code for each MCU. "picware" is an old file, which assumes that one MCU runs the onboard control unit (OCU). This could be used in the future if a new control unit using a larger, faster dsPIC, was installed. "picware 2" contains the code for MCU1 that communicates with the computer and controls the throttle/steering. "picware 3" contains the code for MCU2 that gathers the IMU data, and sends it back to MCU1. The MCUs split responsibility for gathering encoder data.

Setting up the Hardware

To setup the hardware:

- Begin by turning on and opening a computer equipped with the proper version of Matlab and with the proper compilers and supporting software installed.
- Setup the steering wheel and foot pedals by plugging them into both power and a free USB port on the computer.
- Next plug in the TV monitor to the key switch box to the RCA connector and power.
- Take the 100' cat5e cable and connect one end to the car and the other to the key box.
- Attach the LiDAR sensor with the 65' USB cable to the computer.
- Attach the key box to the computer with an USB A-to-micro cable.

Replacing the Li-Battery Pack Cells:

- The Li-Battery has a PCB protection board as a safety feature and requires that the board be reset each time the batteries are replaced. No voltage will appear across the battery pack's terminals after replacing the batteries until the PCB board is reset. To reset the PCB board apply a voltage of around 12-16VDC with another source, connecting the ground signals and power signals together for a brief time; just a few seconds is sufficient:
    - Disconnect the fuse and master switch jumper wire from the header marked FUSE on the power supply.

- Replace the dead Li-cells with newly charged Li-cells.
- Obtain a voltage source of around 12-16 VDC.
- Connect the ground of the battery pack to the ground on the source and the power from the source to the positive terminal of the battery pack. This is most easily accessible by touching the wires to the screws of the terminal block itself.
- Test the voltage across the terminal block or battery pack.
- If no voltage appears repeat the above process.

- Reconnect the fuse and switch to the header on the power supply to reconnect all hardware components.

Running the System

To run the full system:

- Ensure that the hardware and software setup has been performed.
- Open the Simulink model MPC_gamecontroller_LiDAR.mdl in the RRT folder.
- Ensure the COM ports for the key box match the hardware reference in the Simulink model with the device manager. Check that the Lidar COM port matches the COM port in the gd_scan file (see updating LiDAR code below)
- Verify all connections and battery conditions.
- Turn the key on the switch box to the OFF position.
- Turn on the master switch on the front of the car and make sure the LiDAR sensor turns on and blinks green and the camera view is visible on the TV monitor.
- Next turn on switch on the PIC microcontroller boards to the on position. Nothing will happen if the key on the key switch box is in the OFF position.
- Now turn the motor controller on by pressing the button, the LED on should be solid green. If not please refer to the troubleshooting portion below.
- Now turn the key on the switch box to the ON position. The LED on the switch box and the LED on the motor controller should be solid red.
- The system is ready to start: press the play button in the Simulink model. If not started soon after turning all the hardware on the motor controller may go idle in which case refer to the troubleshooting section below.
- After initialization and calibration routines are done the user will be in control and able to drive down the test track with autonomous control taking over once a threat is detected until after the obstacles are passed, when the system will turn to neutral.

To run the LiDAR sensor sub-system:

To run the segmentation sub-system:

- After running the LiDAR subsystem or loading previously saved data, open any of the road testing Simulink models such as RoadTestingFinalVersionWitThreat.mdl
- Change model parameters in the start-up callback method
- Click RUN

To run the path-planning sub-system:

- open MAIN_BLOCK_V1 in the RRT folder
- change the road, obstacle, and vehicle speed to desired values
- Click RUN
- NOTE: this will only run one iteration of the RRT and plan only one path

Plotting Data outputs from a run:
After the run open "RoadBounds and Obstacle Plotter.m" and run this file

To run the LiDAR from the command line:

- Make sure that it is powered on and connected to the computer
- Check that the COM Port is set correctly
- Type "gd_scan(0)" in the command line to connect
- Type "[x y] = gd_scan(1)" to collect data
- Type "gd_scan(2)" to disconnect

Updating the Software

LiDAR C Code:
The LiDAR Code will need to be updated to match the COM port that the LiDAR is plugged into on the computer. This will be different for each machine that it is plugged into, so it will be good practice to do this before running the system. To Update the COM port in the code or to make any other changes:

- Make sure that the C compiler is installed and set up as described above
- From Matlab Open the file titled gd_scan (in the URG folder)
- Check the COM port in the device manager (Control Panel)
- Update the name of the COM port in the code (line 57 if nothing has changed)

```
/* Define COM port, should be dynamic in future development */
const char device[] = "COM12"; /* For Windows */
```

- Save the file
- Make sure that the Current folder is URG in matlab
- In the matlab command line compile the code using the following command:
  - mex -output gd_scan -v *.c
- Find the compiled MEX file (gd_scan.mex) and copy it into the RRT file
-

Java Segmentation Code

Ensure that the latest version of the java development kit (JDK) from Oracle is installed. To compile the java code into classes that are usable within Matlab and Simulink, files must be compiled with the correct version of java, version 1.6. The command to perform this compilation can be issued from the command line with a computer, installed with the java development kit (JDK), located in the same folder. The command line can be located and opened by finding an application called 'command prompt.' The compilation command will produce a (.class) file that can be implemented in Matlab and Simulink by placing the file in the appropriate place, or the RRT folder. There is a callback function in the Simulink model that constructs the class for use while running at every model start time; the end callback function also clears the java class at model end time. Note when java objects are initialized/constructed they clear the objects in the workspace so they must be initialized prior to initializing any other object, such as the object used to communicate with the LiDAR (gd_scan). See start-up and end functions from the Simulink model callbacks.

To compile:

- Open Command Prompt (Windows) or Terminal Application (Mac and Linux)
- Navigate the command line to the folder containing the java file to be compiled. Note you will start in the root directory.
- The command 'dir' (Windows) or 'ls' (Mac and Linux) lists the contents of the current directory. The command 'cd' stands for change directory.
-
- Keep using the 'dir' (Windows) or 'ls' (Mac and Linux) to list the contents of the current directory and then use 'cd directoryToNavigate2' until you are in the directory with the (.java) file to be compiled. Note if you need to go back a directory in the directory tree type 'cd ..' into the command line.
- Once in the correct folder compile by typing the following into the command line.
    - **'javac –source 1.6 –target 1.6 NameofJavaFileToCompile.java'**

Note that if you are recompiling any files for the java segmentation simulation the –source 1.6 –target 1.6 is not required.

    - **'javac NameofJavaFileToCompile.java'**
-
- If no errors appear, place the file now with (.class) into the dRRT folder so the Simulink model start-up callback method can find the class.

Updating the Hardware

Power Supply

The power supply was designed to be somewhat future-proof by offering multiple high-efficiency supply rails each boosting a 1 A current draw capacity and powered by a pack of Li-cells to provide long life and

hopefully will need minimal modifications. It should be noted that the 5V switching regulator was disconnected and disabled because, during testing, the feedback loop of regulator was shorted causing damage that resulted in strange behavior in the output power when under load. If the 5V rail is desired to be used in the future a replacement switching regulator should be installed, as well as the supporting passive components. Please refer to regulator datasheets for further information.

Switch Key Box

The emergency switch, while cutting throttle to the car will also lock the wheels in one direction as the

It may be desired to update the switch key box wiring, for example, splicing the video signal to provide both a connection to a TV monitor and the computer for image processing. These updates can be performed by opening the box, gently, by removing the faceplate attached with four machine screws. The Amtel ATtiny 13A microcontroller that monitors the position of the switch can also be updated or expanded to include features, such as a remote controlled shut-down via a TV remote and an IR sensor. See datasheet, existing AVR and Arduino code folder, as well as well-supported online community resources.

Troubleshooting

- If the motor controller LED is blinking green turn off the master switch and restart the system from the start of the running the system portion above. Another option is to turn off the motor controller and PIC microcontroller board and reset them in the order specified in the running the system portion above.
- If Matlab crashes due to a error referencing an unknown state check the LiDAR sensor connections and try to establish connection from the Matlab command line by typing gd_scan(0). If no errors are reported the connection is successful, disconnect with gd_scan(2). Note gd_scan(1) will return a single scan's data from the LiDAR sensor
- If Matlab gives an error referencing a COM communication problem, check the COM ports in the device manager and ensure that they match the ports referenced in the Simulink model for each piece of hardware.
- If the toggle never engages the system when there is an apparent threat ensure that wheel encoder data is being received. If not, check the wheel encoders' continuity.

Report Date		Sponsor						Component/

TEST PLAN

Item No	Specification or Clause Reference	Test Description	Acceptance Criteria	Test Responsi	Test Stage	SAMPLES		TIMING	
						Quantity	Type	Start date	Finish date
1	Battery Swap time	Replace all batteries on car, record time	<10 min	All	PV	1	C	2/5/2013	2/5/2013
2	Battery Lifetime	Discharge fully charged battery record time until the battery is dead	>50 min	All	PV	2	C	2/5/2013	2/5/2013
3	Lidar Range	Place objects in front of lidar and see at which point the Lidar does not sense the object	1-10ft	All	PV	1	C	2/5/2013	2/5/2013
4	Lidar Viewing Angle	Place objects around the Lidar at different angles, record maximum viewing angle	> 54 degrees	All	PV	1	C	2/5/2013	2/5/2013
5	Lidar Scan Speed	Collect Data from Lidar in Real time. Record frequency of acquisition	20Hz	All	PV	1	C	2/17/2013	2/17/2013
6	Manuever Speed	Perform system test, record time of manuever and distance the car travels, caclulate manuever speed	> 6.81mph	All	PV	1	B	3/5/2013	3/5/2013
7	Repeatability	Perform 3 tests outlined by previous group	>95%	All	CV	6	B	3/9/2013	3/9/2013
8	Detected Obstacle Size	Compare detected obstacles two-deminsional projected area with actual obstacles area	Error < 20%	All	DV	3	B	3/4/2013	3/4/2013
9	Detected Obstacle Location	Calculate distance between detected obstacle location with actual obstacle location	<2 inch at 3ft away <4 inches at 7ft away	All	DV	3	B	3/4/2013	3/4/2013
10	Detected Obstacle Velocity	Calculate obstacle's sensed velocity compare to obstacles actual velocity	<15% difference	All	DV	3	B	3/4/2013	3/4/2013
11	Driver Satisfaction Survey	Participants drive the car and experience the automated manuever. Driver feedback is recorded through survey. Numerical satisifaction Index is calculated.	>80%	All	CV	10	A	5/1/2013	5/1/2013
12									

Appendix O LiDAR Mounting Bracket Technical Drawings

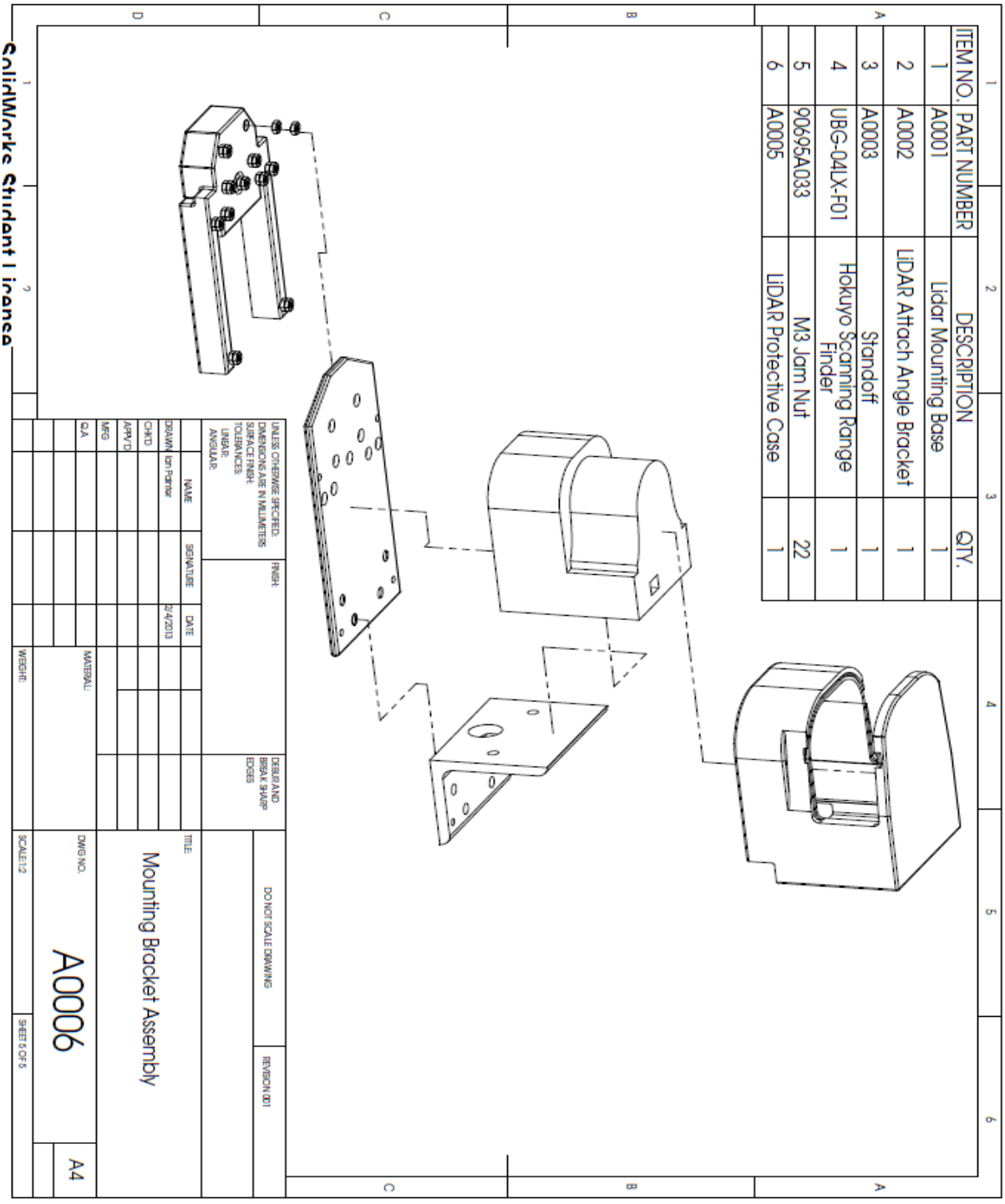

ITEM NO.	PART NUMBER	DESCRIPTION	QTY.
1	A0001	Lidar Mounting Base	1
2	A0002	LiDAR Attach Angle Bracket	1
3	A0003	Standoff	1
4	UBG-04LX-F01	Hokuyo Scanning Range Finder	1
5	90695A033	M3 Jam Nut	22
6	A0005	LiDAR Protective Case	1

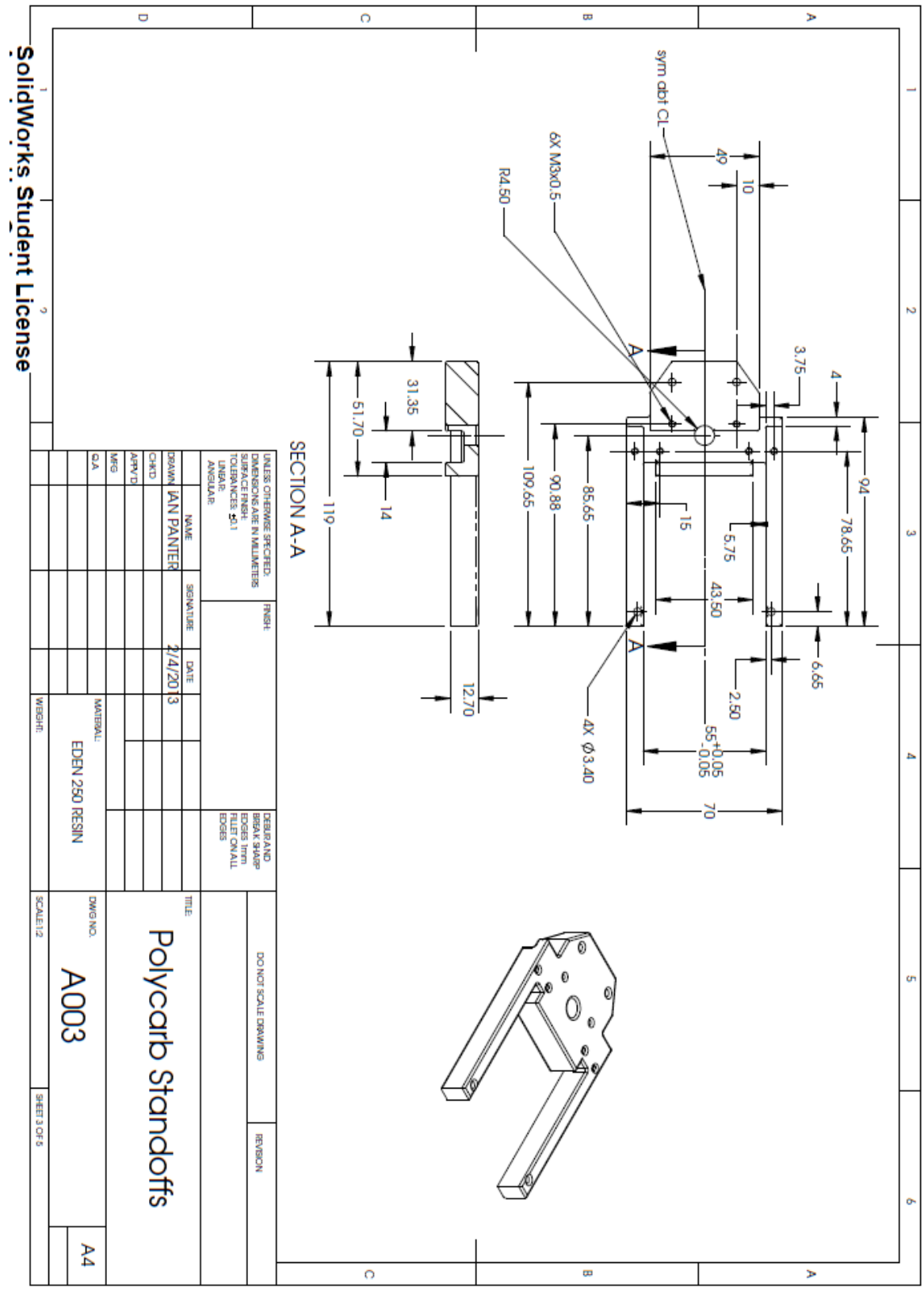
sym abt CL
6X M3x0.5
R4.50
49
10
3.75
4
94
78.65
6.65
2.50
4X Ø3.40
70
55 +0.05 -0.05
43.50
5.75
15
85.65
90.88
109.65
31.35
51.70
14
119
12.70
SECTION A-A
A
A
SolidWorks Student License
UNLESS OTHERWISE SPECIFIED:
DIMENSIONS ARE IN MILLIMETERS
SURFACE FINISH:
TOLERANCES: ±0.1
LINEAR:
ANGULAR:
FINISH:
DEBUR AND BREAK SHARP EDGES 1mm FILLET ON ALL EDGES
NAME
SIGNATURE
DATE
DRAWN
IAN PAINTER
2/4/2013
CHK'D
APV'D
MFG
Q.A
MATERIAL:
EDEN 250 RESIN
WEIGHT:
DO NOT SCALE DRAWING
REVISION
TITLE:
Polycarb Standoffs
DWG NO.
A003
A4
SCALE:1:2
SHEET 3 OF 5

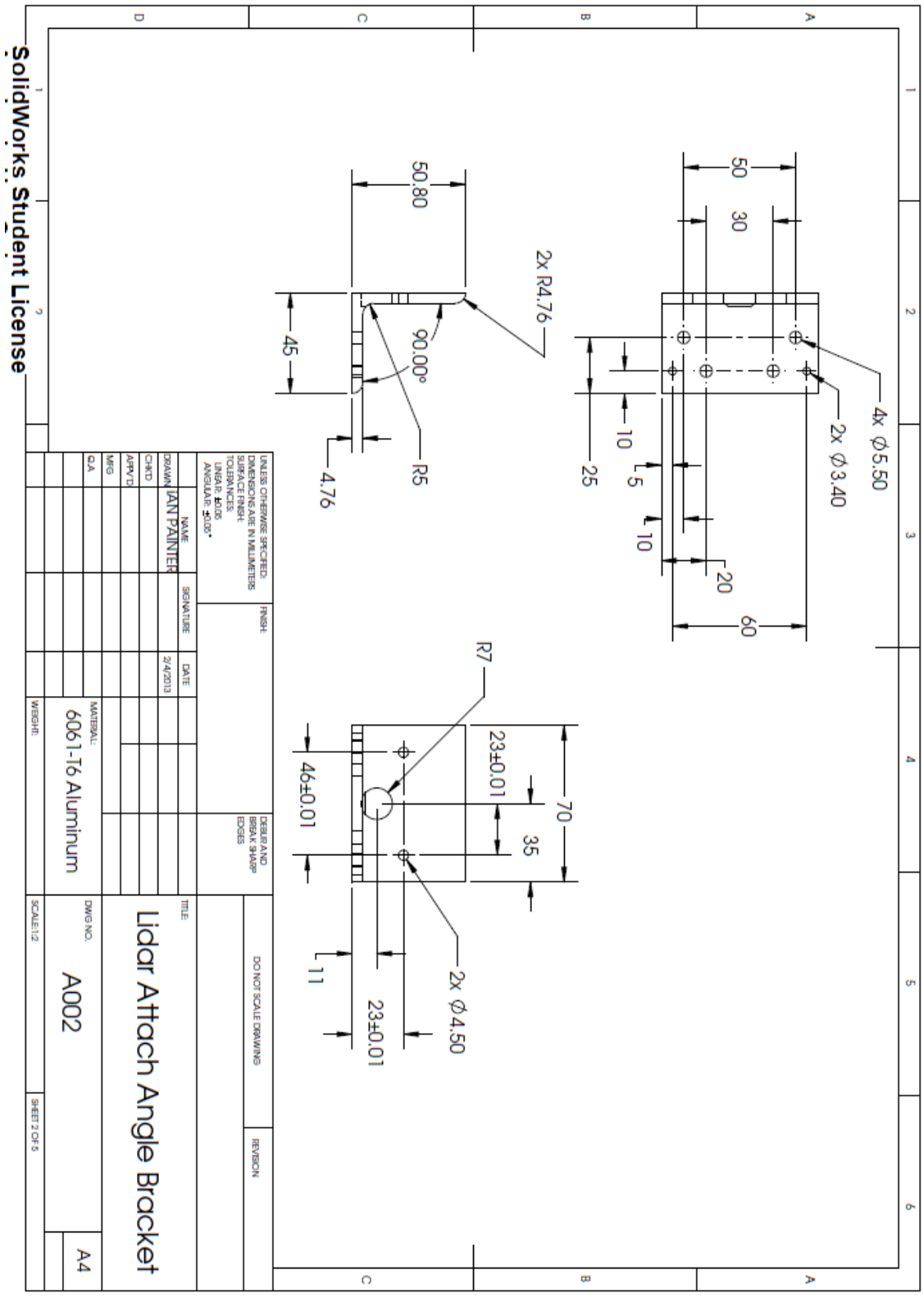

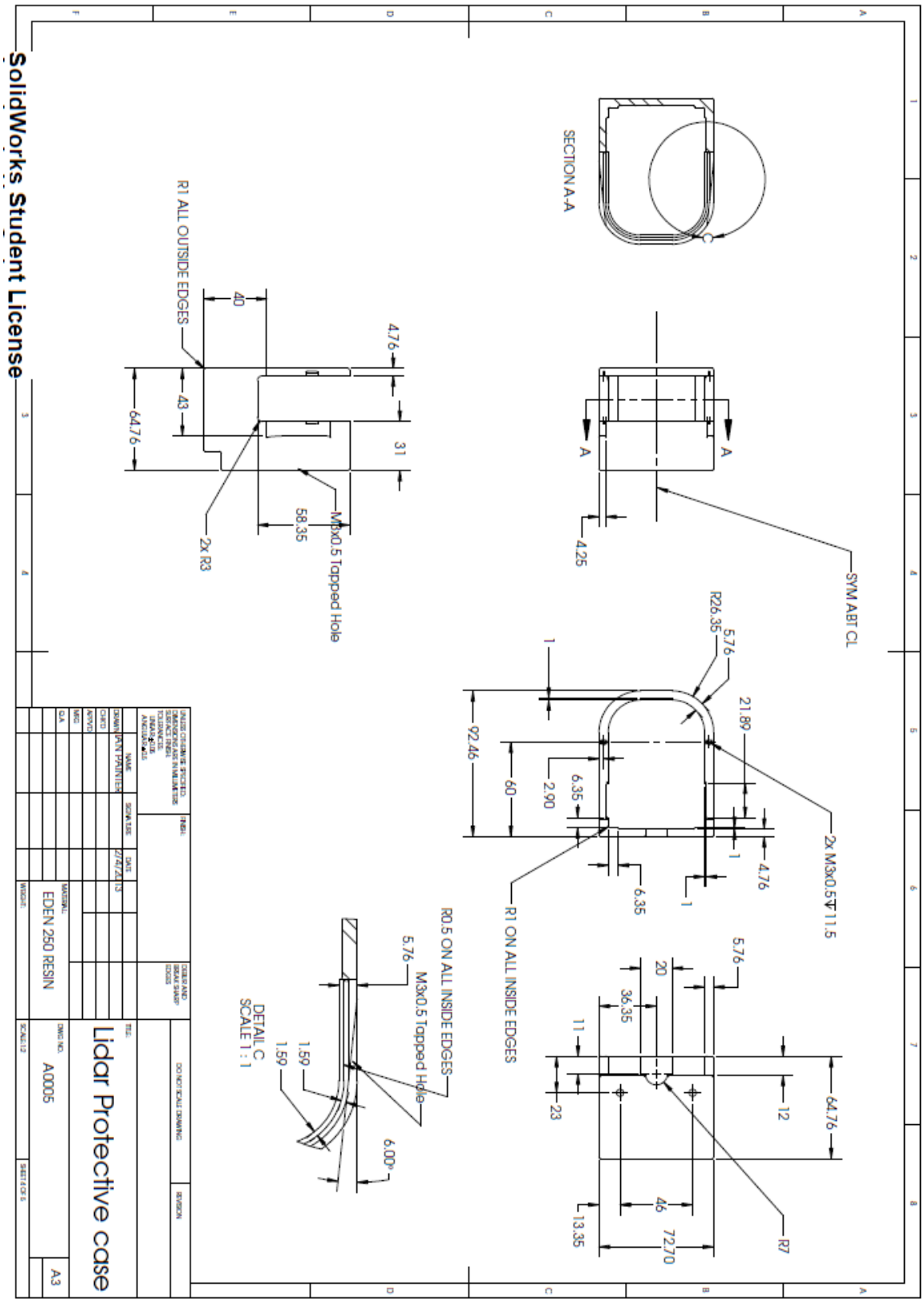

SolidWorks Student License

AVOIDTRONICS

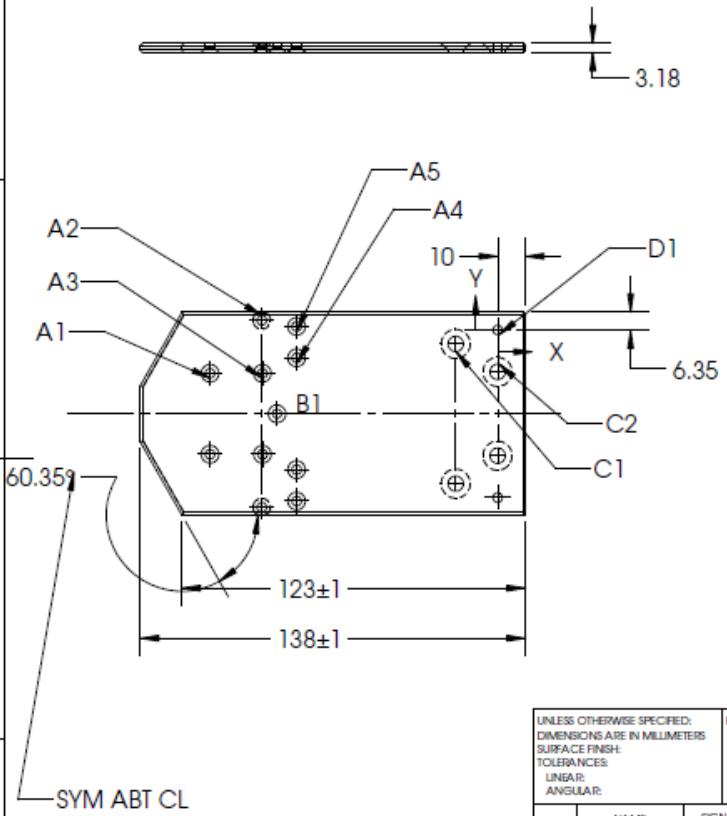

TAG	X LOC	Y LOC	SIZE
A1	-103	-15.50	Ø 3.40 THRU ALL ⌵ Ø 6.30 X 90°
A2	-84.48	3.45	Ø 3.40 THRU ALL ⌵ Ø 6.30 X 90°
A3	-84.23	-15.50	Ø 3.40 THRU ALL ⌵ Ø 6.30 X 90°
A4	-72	-10	Ø 3.40 THRU ALL ⌵ Ø 6.30 X 90°
A5	-71.99	1.25	Ø 3.40 THRU ALL ⌵ Ø 6.30 X 90°
B1	-79	-30	Ø 3.20 THRU ALL ⌵ Ø 6.30 X 90°
C1	-15	-5	Ø 5.50 THRU ALL ⌵ Ø 10.40 X 90°
C2	0	-15	Ø 5.50 THRU ALL ⌵ Ø 10.40 X 90°
D1	0	0	Ø 3.40 THRU ALL

UNLESS OTHERWISE SPECIFIED:
DIMENSIONS ARE IN MILLIMETERS
SURFACE FINISH:
TOLERANCES:
LINEAR:
ANGULAR:

FINISH:

DEBUR AND BREAK SHARP EDGES

DO NOT SCALE DRAWING

REVISION

	NAME	SIGNATURE	DATE
DRAWN	IAN PAINTER		2/4/2013
CHK'D			
APPV'D			
MFG			
Q.A			

MATERIAL: 6061-T6

WEIGHT:

TITLE: Lidar Mounting base

DWG NO. A0001

A4

SCALE:1:2

SHEET 1 OF 5

Appendix P Li-Ion Cell Specification Sheet

SANYO

Lithium ion

May. 2007

Cell Type UR18650Y

Specifications

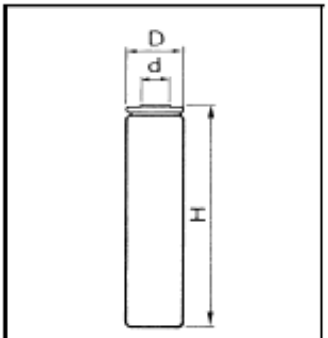

Dimensions(Typ.) of Bare Cell		
	H	64.7 mm
	D	18.05 mm
	d	9.0 mm

Nominal Capacity		Min.1900mAh
Nominal Voltage		3.7V
Charging Method		Constant Current -Constant Voltage
Charging Voltage		4.2V
Charging Current		Std. 1330mA
Charging Time		3hrs.
Ambient Temperature	Charge	0 ~ +40 °C
	Discharge	-20 ~ +60 °C
	Storage	-20 ~ +50 °C
Weight (Max.)		43.3g
Dimensions (Max.)	(D)	18.10mm
	(H)	64.80mm
Volumetric Energy Density		421Wh/l
Gravimetric Energy Density		162Wh/kg

Maximum size without tube

*When designing a battery pack, get the precise information on a cell battery drawing

Typical Characteristics

Discharge rate characteristics

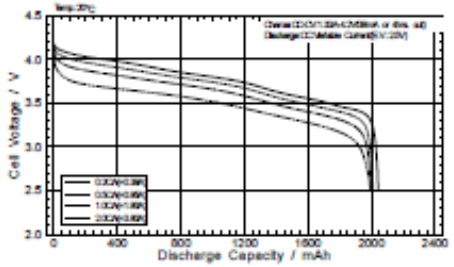

Discharge temperature characteristics

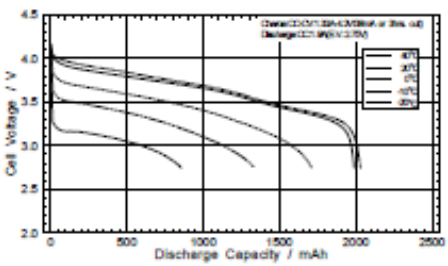

Charge characteristics